APPLYING PHASE CHANGE MATERIALS (PCMS) TO DISASTER-RELIEF PREFABRICATED TEMPORARY HOUSES (PTHS) FOR IMPROVING THEIR INDOOR THERMAL ENVIRONMENTS IN SUMMER TIME

WANG CAIXIA

PhD

The Hong Kong Polytechnic University

This programme is jointly offered by The Hong Kong Polytechnic University and Sichuan University

2021

The Hong Kong Polytechnic University

Department of Building Services Engineering

Sichuan University

Institute for Disaster Management and Reconstruction

Applying Phase Change Materials (PCMs) to Disaster-relief Prefabricated Temporary Houses (PTHs) for Improving Their Indoor Thermal Environments in Summer Time

WANG Caixia

A thesis submitted in partial fulfillment of the requirements for the Degree of Doctor of Philosophy

Feb 2021

Certificate of Originality

I hereby declare that this thesis is my own work and that, to the best of my knowledge and belief, it reproduces no material previously published or written, nor material that has been accepted for the award of any other degree or diploma, except where due acknowledgement has been made in the text.

WANG Caixia

Abstract

Natural disasters endanger the lives and properties of people and their frequent occurrences have left hundreds of thousands of disaster victims homeless. Therefore, providing disaster victims with suitable temporary shelters has been one of the key issues in post-disaster management. It is noted that disaster-relief prefabricated temporary houses (PTHs) have been massively used during disaster relief reconstructions period due to the advantages of convenient transportation, easy installation and short construction period to provide the much-needed shelters. However, previous related field studies have demonstrated that as no energy-consuming environmental control systems such as an air conditioner were normally installed inside PTHs, in summer time, the thermal environment inside PTHs can become intolerably hot, and thus harmful to disaster victims' health both physically and mentally. It has been therefore urgently needed to apply simple and low cost measures to disaster-relief PTHs for improving their indoor thermal environments in summer. On the other hand, phase change materials (PCMs) have been extensively used in various permanent buildings for helping improve indoor thermal environmental control successfully, with however little application to disaster-relief PTHs for enhancing their indoor thermal environmental controls. Consequently, a programmed research work on applying PCMs to disaster-relief PTHs for improving their indoor thermal environment in summer time has been carried out and is reported in this Thesis.

This Thesis begins with, firstly, describing a purposely established experimental setup having two different Designs of applying PCMs to PTHs to facilitate the experimental work required in this programmed research work. For Design 1, two different scaled model houses (MHs) were used and for Design 2, a full-scale experimental PTH was used. Appropriate measuring instrumentations were provided to the setup.

Secondly, an experimental study on applying PCMs to disaster-relief PTHs for improving their internal thermal environment in summer is presented. The experimental setup was used and the two designs examined in the experimental study. In Design 1, PCMs were fixed to the internal surfaces of one of the two MHs and the related experimental results demonstrated that both indoor air temperature and internal surface temperatures of the PCM based MH can be reduced at daytime. However, in Design 2, a movable PCM based energy storage system (PESS) was used and the related experimental results suggested the use of the movable PESS with a total charge of 148.8 kg PCM helped reduce the average indoor air temperature by 3.2 to 3.6 ^oC. The experimental results for both Designs suggested that, due to the nature of disaster relief and since outdoor air at a lower temperature may be the only cooling energy source for charging the PCM, a movable PESS was preferred, so that it can be moved to outdoor at night time for being charged with more cooling energy using lower temperature outdoor air or via sky radiation but not adversely increasing the air temperature inside PTHs.

Thirdly, the Thesis presents a numerical study on optimizing the designs of applying PCMs to a disaster-relief PTH to improve its summer daytime indoor thermal environment. The numerical study followed up the experimental study to numerically examine different designs of applying PCMs to a disaster-relief PTH in order to identify the best design for guiding future practical applications. A numerical model for the full-scale PTH was established using EnergyPlus platform and experimentally validated. The numerical study included two parts. In the first part, a total of 16 different designs were defined and the simulated results demonstrated that the 10th design, or D10, was identified as the most effective design, and could result in the highest number of acceptable hours at 90 hours. In the second part, increasing PCM's thickness to beyond 20 mm would lead to negligible effects on further improving the thermal environment inside the full-scale PTH. Hence, 20 mm thickness for PCM was recommended as a reference design value for future practical applications.

Finally, a further numerical study on applying the movable PESS to disaster-relief PTHs used in 12 selected cities located in different climate regions to improve the thermal environments inside PTHs in July is reported. The previously developed and experimentally validated EnergyPlus based simulation model for a PTH incorporating the movable PESS was deployed. In this further numerical study, in order to quantitatively describe the degree of improvement in the thermal environment inside PTHs after applying PCMs, a number of evaluating indexes including Unacceptable

Degree Hours inside a PTH without incorporating the movable PESS (*UDH*) and after incorporating the movable PESS (*UDH'*) and the absolute difference between *UDH* and *UDH'* (Δ), were proposed. Using the meteorological data in the typical weather year of 1989, the further numerical study showed that, in all the 12 selected cities in July, after introducing the movable PESS to the PTHs, both the monthly maximum and the averaged air temperature inside the PTHs, the daily peak and daily average indoor air temperature on the hottest day were lowered. In all the 12 selected cities, although applying the movable PESS to disaster-relief PTHs in July was functional, it was more effective for the following seven cities including Singapore, Miami, Bangkok, Chengdu, Damascus, Hanoi and Urumqi, with six of the seven cities located in both tropical and temperate climate regions, based on the proposed evaluating indexes.

Publications Arising from the Thesis

Journal Papers

- **Caixia Wang**, Xiao Huang, Shiming Deng, Enshen Long, Jianlei Niu. An experimental study on applying PCMs to disaster-relief prefabricated temporary houses for improving internal thermal environment in summer, Energy and Buildings, 2018, (179): 301-310. (Based on Chapter 5)

- **Caixia Wang**, Shiming Deng, Jianlei Niu, Enshen Long. A numerical study on optimizing the designs of applying PCMs to a disaster-relief prefabricated temporary-house (PTH) to improve its summer daytime indoor thermal environment, Energy, 2019, (181): 239-249. (Based on Chapter 6)

- **Caixia Wang**, Shiming Deng, Enshen Long, Jianlei Niu. A numerical study on applying the movable PESS to disaster-relief prefabricated temporary houses used in different climate regions to improve indoor thermal environments in summer. Journal of Building Engineering, Under review. (Based on Chapter 7)

Acknowledgements

First of all, I must express my grateful thanks to my Chief Supervisor, Prof. Deng Shiming, from the Department of Building Services Engineering (BSE), The Hong Kong Polytechnic University, and my Co-Supervisor, Prof. Long Enshen, from the Institute for Disaster Management and Reconstruction, Sichuan University, and Prof. Niu Jianlei, from the Department of Building Services Engineering (BSE), The Hong Kong Polytechnic University, for their encouragement, valuable suggestions, patient guidance and continuous help throughout the course of my study. It is my fortune to be their student.

My special thanks go to The Hong Kong Polytechnic University, Sichuan University and Hong Kong Jockey Club for financially supporting my study. I would like to also thank all my colleagues and friends at The Hong Kong Polytechnic University and Sichuan University for their assistance, understanding, and support throughout my studies. In addition, I would like to express my gratitude to Mr. Huang Xiao and Mr. Liang Weijie for their support in my experimental work.

Last but not the least, my great thanks to my family members: my grandparents, parents, parents-in-law, husband and daughter, for their love, understanding, encouragement and support in my life.

Table of Contents

List of Figures

Chapter 4

Chapter 5

Chapter 6

Chapter 7

List of Tables

Chapter 6

Chapter 7

Nomenclature

Variable	Description
T_i	The air temperature inside the PTH, ^oC
T_o	The outdoor air temperature, ^oC
TR_3’	The internal surface temperature of the west wall for the reference MH, ^oC
TP_3’	The internal surface temperature of the west wall for the PCM based MH, ^oC
TR_5’	The internal surface temperature of the roof for the reference MH, ^oC
TP_5’	The internal surface temperature of the roof for the PCM based MH, ^oC
TR_6	The air temperature inside the reference MH, ^oC
TP_6	The air temperature inside the PCM based MH, ^oC
TD_{ia}	The temperature difference between the air temperatures inside the PTHs and upper limit of tolerable air temperature, ^oC
TD_{ia_r}	The temperature difference in the reference MH, ^oC
TD_{ia_p}	The temperature difference in the PCM based MH, ^oC
TD_{ia_f} ’	The temperature difference in the full-scale PTH with PESS, ^oC
TD_{ia_f}	The temperature difference in the full-scale PTH without PESS, ^oC
T_E	Internal surface temperature of PTH’s east wall, ^oC
T_W	Internal surface temperature of PTH’s west wall, ^oC
T_S	Internal surface temperature of PTH’s south wall, ^oC
T_N	Internal surface temperature of PTH’s north wall, ^oC

T_R	Internal surface temperature of PTH's roof, ^oC
T_F	Internal surface temperature of PTH's floor, ^oC
T_{Mt}	Measured temperature at each hour, ^oC
T_{St}	Simulated temperature at each hour, ^oC
$\bar{y}$	Average measured temperature during the entire measurement period, ^oC
AVE_{day}	Average air temperature inside the PTH during 8:00 - 20:00, ^oC
T_{top}	Upper limit of tolerable air temperature inside a PTH, ^oC
UDH	Unacceptable degree hours inside a PTH, $^oC \cdot h$
$T_{in,j}$	Hourly average air temperature at j^{th} hour inside the PTH without incorporating the movable PCM design, ^oC
n	Total number of hours in the summer month of July
UDH'	Unacceptable degree hours inside a PTH after incorporating the movable PCM design
$T'_{in,j}$	Hourly average air temperature at j^{th} hour inside a PTH after incorporating the movable PCM design, ^oC
Δ	Absolute difference between *UDH* and *UDH'*, $^oC \cdot h$
Δ'	Relative difference between *UDH* and *UDH'*, %
T_{in}	Daytime hourly average air temperature inside the disaster-relief PTH without incorporating the movable PCM design, ^oC
T_{in}'	Daytime hourly average air temperature inside the disaster-relief PTH after incorporating the movable PCM design, ^oC

List of Abbreviations

PCMs	Phase change materials
PTHs	Prefabricated temporary houses
MHs	Model houses
PESS	Phase change material energy storage system
RMSD	Root Mean Square Deviation
$CV_{(RMSD)}$	Coefficient of Variation of root mean square deviation
UDH	Unacceptable Degree Hour

Chapter 1

Introduction

Following natural disasters that destroy human habitats [Gunawardena et al., 2014], such as earthquakes, tsunamis, floods, typhoons and bushfires, prefabricated temporary houses (PTHs) are massively used in disaster relief reconstructions [Tang et al., 2017; Aye et al., 2012; Tas et al., 2011]. For example, after the 2008 mega-scale Wenchuan Earthquake in China, more than 21 million victims were resettled in PTHs during the post-disaster transitional period of up to 36 months [Wang et al., 2018]. In most cases, such fast-installed PTHs were the only choice for disaster victims during a post-disaster transitional period, which may nonetheless last for up to several years [Felix et al., 2015; Asefi and Sirus, 2012; Dikmen et al., 2012]. However, given their temporary nature, few indoor thermal environmental control systems are usually installed inside PTHs and therefore, their indoor thermal environments are cold in winter and hot in summer [Huang et al., 2015]. Exposed to a poor indoor thermal environment for a long time may result in the physical and mental illness of PTHs' occupants, especially those disaster victims [Zhang et al., 2017a]. Therefore, improving the indoor thermal environments for the occupants in PTHs using simple and low-cost measures, such as passive designs [Wang et al., 2017; Wang et al., 2016a], is urgently needed.

On the other hand, various studies have shown that the use of phase change materials (PCMs) could help improve the indoor thermal comfort in different buildings. Although PCMs have been widely applied to various permanent buildings as passive measures for improving their indoor thermal environments [Saffari et al., 2017], their full-scale applications to temporary disaster-relief PTHs are seldom reported. This may be due to the temporary nature of PTHs since they are not expected for long term use. However, the actual use of PTHs may no longer be temporary following some mega-scale natural disasters, such as the 2008 Wenchuan Earthquake. It becomes therefore highly necessary to investigate the applications of PCMs to PTHs for improving their indoor thermal environments for the well-beings of PTHs' occupants, most of them being disaster victims. To this end, a programmed research work has been carried out and is presented in this Thesis.

This Thesis begins with an extensive literature review in Chapter 2 where firstly a review on the occurrences and the risk assessment and management of natural disasters is reported. Secondly, a review on the previous experimental and numerical studies on the thermal environments inside disaster-relief buildings including disaster-relief PTHs and their improvements is presented. Thirdly, related studies on applying PCMs to buildings are reviewed. Finally, the research gaps identified through reviewing the previous related studies are discussed.

In Chapter 3, the backgrounds, the title, the aims and objectives of, and the research methodologies used, in the programmed research work are presented.

Chapter 4 presents the establishments of two experimental model houses (MHs) and a full-scale experimental PTH for two different designs of applying PCMs and their associated instrumentations. The experimental MHs and full-scale PTH were for carrying out the required experiments of the programmed research work reported in this Thesis. A detailed description of Design 1 was firstly presented, followed by detailing that of Design 2. In Design 1, there were two MHs, one as a reference MH, and the other a PCM based MH where PCMs were fixed to its internal surfaces. However, in Design 2, a movable PCM based energy storage system (PESS) was used in the full-scale experimental PTH. The availability of the experimental MHs and the full-scale experimental PTH in the two designs is expected to be essential in successfully carrying out the programmed research work proposed in Chapter 3.

In Chapter 5, an experimental study on applying PCMs to disaster-relief PTHs using the two experimental MHs and the full-scale experimental PTH of the two different designs is reported. The two different designs of applying PCMs were examined. The related experimental results for Design 1 demonstrated that both indoor air temperature and internal surface temperatures in the PCMs based MH can be reduced at daytime, and those for Design 2 suggested the use of the movable PESS with a total charge of 148.8 kg PCMs helped reduce the average indoor air temperature inside the full-scale PTH by 3.2 ^{o}C to 3.6 ^{o}C. The experimental results from both Designs suggested that, due to the nature of disaster relief and since outdoor air at a lower temperature at nighttime may be the only cooling energy source for charging the PCM, a movable PESS system was preferred, so that it can be moved to outdoor at nighttime for being charged with the cooling energy from the outdoor air at a lower temperature and sky radiation, and not adversely increasing the air temperature inside PTHs.

In Chapter 6, a numerical study on optimizing the designs of applying PCMs to a disaster-relief PTH to improve its indoor thermal environment in summer is reported. A numerical model for the full-scale experimental PTH was established using EnergyPlus platform and experimentally validated. The numerical study included two parts. In the first part, a total of 16 different designs were defined and the simulated results demonstrated that the 10th design, or D10, was identified as the most effective one, and could result in the highest number of acceptable hours at 90 hours. In the second part, it was numerically shown that increasing PCM's thickness to beyond 20 mm would lead to negligible effects on further improving indoor thermal environment in summer. Hence, 20 mm thickness for PCM was recommended as a reference design value for future practical applications.

Chapter 7 presents a further numerical study on applying the movable PESS to the PTHs installed in 12 selected cities in different climate regions around the world to improve their indoor thermal environments in July. The experimentally validated EnergyPlus based simulation model for the experimental PTH incorporating the movable PESS used in Chapter 6 was deployed in the numerical study. Using the meteorological data in the typical weather year of 1989, the numerical study showed that, in all the 12 selected cities in July, after introducing the movable PESS to the PTHs, the maximum temperature, the monthly averaged air temperature inside the PTHs, the daily peak and daily average indoor air temperatures on the hottest day were all lowered. In all the 12 selected cities, although applying the movable PESS to disaster-relief PTHs in July was functional, it was more effective for the following seven cities including Singapore, Miami, Bangkok, Chengdu, Damascus, Hanoi and Urumqi, with six of the seven cities located in both tropical and temperate climate regions, based on the evaluating criteria proposed in this Chapter.

The conclusions of the Thesis and the proposed future work are presented in Chapter 8.

Chapter 2

Literature review

2.1 Introduction

Natural disasters pose threats to the sustainable development of human society and cause losses in human lives and properties. For example, the death toll in the Huaxian Earthquake in the year of 1556 in China exceeded 830000, and that in the 2004 Indian Ocean Earthquake and Tsunami 292000. According to statistics, from 1900 to 2018, there were about 14748 number of natural disasters worldwide, resulting in more than 32.65 million deaths, 8.57 million injuries and 174.16 million homelessness. The total number of people affected was as high as 7.99 billion, leading to enormous economic losses of more than 3.34 trillion US dollars. Natural disasters can occur anywhere in the world, causing lasting and far-reaching harm and bringing huge losses to human society.

Natural disasters occur frequently in China, such as floods, droughts, typhoons, earthquakes, ice and snow disasters and landslides, etc. For example, on May 12, 2008, an earthquake measuring at 8.0 on the Richter scale occurred in Wenchuan County, Aba Qiang Tibetan Autonomous Prefecture, about 90 kilometers northwest of

Chengdu, Sichuan Province. The earthquake affected a large area, covering 852 counties in 8 provinces, and the cumulative number of people affected exceeded 45 million. According to the official data, a total of 69227 people were killed, 17923 missing and 360355 injured in the Wenchuan Earthquake. A total of 2114845 wounded were treated in hospitals. More than 5 million buildings collapsed in the affected area and more than 21 million buildings were severely damaged. Totally, more than 25 million families were affected. The massive destruction of houses and subsequent secondary disasters have led to the emergency relocation of more than 12 million people. How to resolve the problem of the rapid resettlement for mega-scale disaster victims became one of the most important tasks following a major natural disaster.

Disaster-relief PTHs have the characteristics of convenient large-scale mass production, convenient transportation and rapid construction. Therefore, they are widely used in post-disaster resettlement [Wang et al., 2018; Shen et al., 2005]. According to the statistics, following the Wenchuan Earthquake, the number of temporary houses built to resettle the affected people exceeded 625000 [Subasinghe, 2013], including 107000 public resettlement temporary houses such as hospitals and schools, and 71000 and 429000 residential resettlement temporary houses for rural and urban residents, respectively [Ni and Qian, 2017]. Fig. 2.1 shows a photo for disaster-relief temporary houses following the Wenchuan Earthquake. In addition, in

Middle East, disaster-relief temporary houses were also used for emergency resettlement of disaster victims who lost their homes. Fig. 2.2 shows the relief temporary houses donated to war victims by the Khuzaa, an international disaster-relief organization, in a Palestinian town on the eastern Mediterranean coast of the Gaza Strip [Asfour, 2019].

Fig. 2.1 The resettlement site of disaster-relief PTHs-Wenchuan in 2008

Fig. 2.2 The resettlement site of disaster-relief PTHs-Khuzaa [Asfour, 2019]

Although disaster-relief PTHs are only intended to provide transitional or temporary accommodation, it has been widely acknowledged that disaster victims often lived in disaster-relief PTHs for as long as several years [Belcher and Bates, 1983; Alexander, 1984; Gutierrez, 2017]. It has been noted that disaster-relief PTHs were made of light colour steel board, so that they may be rapidly erected in a disaster area, with limited construction materials, limited space requirement but poor ventilation provisions, resulting in severe indoor thermal environment, and impacting negatively on the health of victims [Huang et al., 2015].

Therefore, disaster victims not only had to bear the grief of losing their families and homes, but also suffered the poor living environment in disaster-relief PTHs, which was not beneficial to the physical and mental health of victims [Zhang et al., 2017a; Cao et al., 2014; Fussell and Lowe, 2014; Tsuchiya et al., 2019]. As a result, appropriate and effective measures should be taken to improve the thermal environment inside disaster-relief PTHs [Wang et al., 2017; Wang et al., 2016a; Sodha et al., 1986], so as to provide victims with a more comfortable post-disaster transitional living environment [Davis, 1978].

On the other hand, studies have shown that the use of PCMs [Tyagi et al., 2012; Zhou et al., 2012; Pomianowski et al., 2013] could help improve the thermal comfort in different buildings [Soares et al., 2013; Tyagi et al., 2013]. For examples, Sage-Lauck and Sailor [2014] evaluated the impacts of using PCMs on indoor thermal comfort in an insulated residential building using experimental and numerical approaches. Figueiredo et al. [2017] used different constructive solutions incorporating PCMs for indoor thermal comfort assessments in real case studies in school buildings. Alam et al. [2017] completed a comparative analysis on the effectiveness of different application methods for PCMs to enhance the level of thermal comfort inside residential buildings.

Although a considerable number of studies have been carried out to study the applications of PCMs [Kenisarin and Mahkamov, 2016; Konuklu et al., 2015] to various permanent buildings for enhancing their indoor thermal environmental control

[Saffari et al., 2017; Silva et al., 2016a; Weinläder et al., 2016], full-scale applications of PCMs to disaster-relief PTHs were limited [Lin et al., 2016; Song et al., 2018]. This may be due to the temporary nature of PTHs since they were not expected for long-term use. However, as mentioned before, since the actual use of PTHs may no longer be temporary, it became highly necessary also to study the applications of PCMs to disaster-relief PTHs for improving their indoor thermal environments, for the well-beings of disaster victims.

In this Chapter, an extensive literature review on applying PCMs to improve the thermal environment inside disaster-relief PTHs and some related issues is reported. Firstly, a review on the occurrences and the risk assessment and management of natural disasters is presented. This is followed by reporting a review on the previous studies on the thermal environment inside disaster-relief temporary houses including PTHs. Thirdly, previous experimental and numerical studies applying PCMs to buildings are reviewed. Finally, a conclusion is given, where future required research work on applying PCMs to improve the thermal environment inside PTHs is identified and summarized.

2.2 The occurrence and risk assessment and management of natural disasters

2.2.1 Occurrences of natural disasters

Natural disasters are caused by natural events or forces that cause the death or injury to human lives and the damage to social properties. Since the beginning of the 20th century, the economic losses and the number of people affected by natural disasters have shown an increasing trend. Tables 2.1 to 2.3 detail the top 20 natural disasters from 1900 to 2019, based on the total number of people affected, total death and total economic losses. The flood disasters in China and the droughts in India were widespread, affecting the largest number of people. More than 330 million people were affected by the 2015 drought in India alone (Table 2.1). A severe drought and a severe flood occurred in China in 1931 and 1928, respectively, resulting in a total death of more than 670000 people (Table 2.2). The total economic losses caused by Hurricane Harvey in southern Texas in August 2017 amounted to US $171.1 billion. In 2011, the total economic losses caused by the earthquakes in Japan exceeded US $210 billion. These have demonstrated that natural disasters have brought heavy casualties and economic losses to human beings all over the world and caused catastrophic damages to the entire human society.

Table 2.1 Top 20 natural disasters based on the number of people affected globally from 1900 to 2019

Ranking	Type of disaster	Country	Year	Number of affected people (Million people)
1	Drought	India	2015	330.00
2	Drought	India	1987	300.00
3	Drought	India	2002	300.00
4	Flood	China	1998	225.24
5	Flood	China	1991	206.00
6	Drought	India	1972	200.00
7	Flood	China	2003	154.37
8	Flood	China	1996	150.00
9	Flood	China	2010	140.19
10	Flood	India	1993	128.00
11	Flood	China	1995	125.50
12	Flood	China	2002	113.22
13	Flood	China	2007	111.04
14	Hurricane	China	2002	107.40
15	Flood	China	1994	105.90
16	Flood	China	1999	104.93
17	Flood	China	1989	100.00
18	Drought	India	1965	100.00
19	Drought	India	1982	100.00
20	Flood	China	2011	93.36

Table 2.2 Top 20 natural disasters based on the number of death toll from 1900 to 2019

Ranking	Type of disaster	Country	Year	Number of death (Million people)
1	Flood	China	1931	3.70
2	Drought	China	1928	3.00
3	Infectious disease	India	1920	2.50
4	Infectious disease	Former Soviet Union	1917	2.50
5	Flood	China	1959	2.00
6	Drought	Bangladesh	1943	1.90
7	Drought	India	1942	1.50
8	Drought	India	1965	1.50
9	Infectious disease	China	1909	1.50
10	Infectious disease	India	1907	1.30
11	Drought	India	1900	1.25
12	Drought	Former Soviet Union	1921	1.20
13	Drought	China	1920	0.50
14	Flood	China	1939	0.50
15	Infectious disease	India	1926	0.42
16	Infectious disease	Bangladesh	1918	0.39
17	Hurricane	Bangladesh	1970	0.30
18	Drought	Ethiopia	1983	0.30
19	Infectious disease	India	1924	0.30
20	Earthquake	China	1976	0.24

Table 2.3 Top 20 natural disasters based on the amount of economic loss from 1900 to 2019

Ranking	Type of disaster	Country	Year	Economic loss (Billion US$)
1	Earthquake	Japan	2011	210.00
2	Hurricane	America	2017	171.11
3	Hurricane	America	2005	158.23
4	Earthquake	Japan	1995	100.00
5	Earthquake	China	2008	85.49
6	Hurricane	America	2012	77.50
7	Hurricane	Puerto Rico	2017	68.00
8	Hurricane	America	2004	55.23
9	Hurricane	America	2008	45.76
10	Hurricane	America	2011	43.45
11	Flood	Thailand	2011	40.32
12	Hurricane	America	1992	34.50
13	Flood	China	2016	31.79
14	Flood	China	1998	31.74
15	Earthquake	America	1994	30.00
16	Earthquake	Chile	2010	30.00
17	Earthquake	Japan	2004	28.00
18	Hurricane	America	2016	27.35
19	Extreme weather	China	2008	21.10
20	Earthquake	Turkey	1999	21.00

From these three Tables, it was clear that natural disasters occurred frequently and spreaded widely all over the world [Ward et al., 2020]. Main types of natural disasters included flood [Forero-Ortiz et al., 2020], drought [Ngcamu and Chari, 2020], earthquake [Wang et al., 2020; Stahl et al., 2017], typhoon [Karaca and Aslani, 2016], storm [Weiskerger and Phanikumar, 2020], geological disaster [Wang et al., 2012], forest fire [Burger et al., 2020; Xu et al., 2020] and prairie fire [Bercak et al., 2018; Dou et al., 2018], landslide [Juang et al., 2019], tropical cyclone [Cardona et al., 2014; Hong and Moller, 2012; Trepanier et al., 2017], volcano [de Vallejo et al., 2020; Freire et al., 2019] and tsunami [Iimura et al., 2020]. Furthermore, natural disasters can occur in different parts of the world, included Asia [Ali et al., 2020; Dagher et al., 2020], Europe [Paul, 2002; Radovic et al., 2012], Africa [Edoun et al., 2015; Michellier et al., 2020], America [Alcantara-Ayala, 2010; Ishizawa and Miranda, 2019] and Oceania [Forbes et al., 2018; Wisetjindawat et al., 2017].

Generally, a natural disaster can possess the following six characteristics:

- Potentiality. Prior to disasters, there can be incubation periods with varying lengths, when energy was accumulated or converted to break the original balance and stability;

- Suddenness. Before a disaster occurred, there were often no direct signs or strict rules to be found, so that a disaster was usually not easy to be detected and distinguished by people;
- Periodicity. Disasters of the same nature can occur repeatedly after a certain period of time;
- Simultaneity. Some disasters of the same or different types could often follow one after another or occur concurrently;
- Complexity. The periodicity of disasters was not confined to only one time scale. Certain disasters may often form a disaster chain with other disasters;
- Multiple causes. One cause may lead to multiple disasters, and a single disaster may be the result of multiple causes [Carrasco-Ochoa and Martinez-Trinidad, 2004].

Most natural disasters were regarded as normal events in the evolution of the earth system, but they have become important restrictive factors hindering the development of human society and economy. Various types of natural disasters caused not only direct economic losses and casualties, but also various indirect losses, and may even affect the stability and sustainable development of the whole society [Chan et al., 2019].

2.2.2 Risk assessment and management of natural disasters

One of important issues for managing natural disasters was their risk assessments [Nascimento and Alencar, 2016; Rinaldi and Bergamini, 2020]. This was because the risk assessment for natural disasters can help to determine natural disaster prevention standards, optimize the implementation sequences of disaster prevention system construction, optimize the emergency rescue sequence (by providing a scientific basis for decision-making including the selection of emergency and disaster-relief priorities, the choice of sequence, and the selection of emergency and disaster-relief methods), form scientific land management in natural disaster risk areas and provide a basis for post-disaster loss assessments.

Ward et al. [2020] systematically reviewed risk assessment models of natural disasters at a global scale. According to the nature of different types of disasters, such as hydrological disasters, meteorological disasters and climatological disasters, generally available risk assessment models were also different. However, knowledge sharing and cooperation were encouraged.

Li et al. [2016] compared the existing natural disaster risk assessment frameworks , as shown in Fig. 2.3, and proposed a new framework, Hazard, Vulnerability and Adaptation Capability, as illustrated in Fig. 2.4.

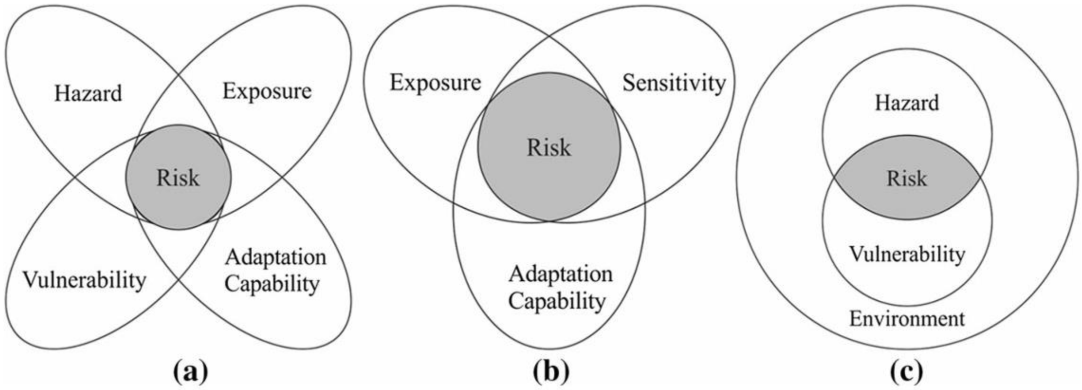

Fig. 2.3 Typical component based risk assessment frameworks [Li et al., 2016]

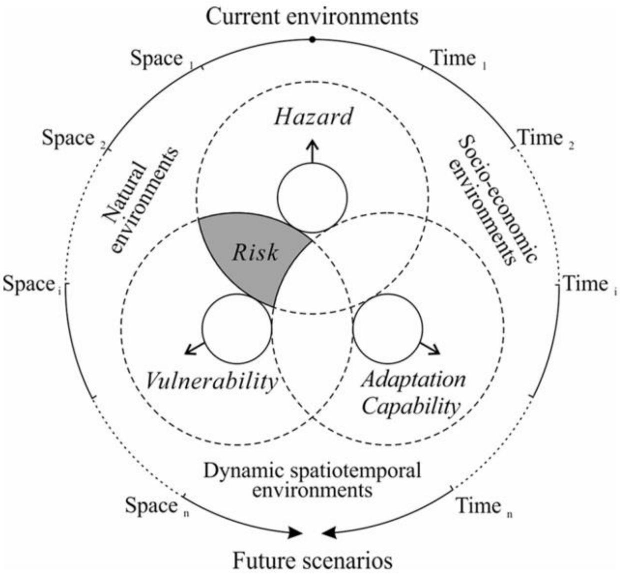

Fig. 2.4 A new scenario based risk assessment framework [Li et al., 2016]

Rus et al. [2018] conducted a systematic study on urban natural disaster assessments and responses. They emphasized the importance of optimizing pre-disaster mitigation measures and rational planning of urban layout, as shown in Fig. 2.5 and Fig. 2.6, respectively.

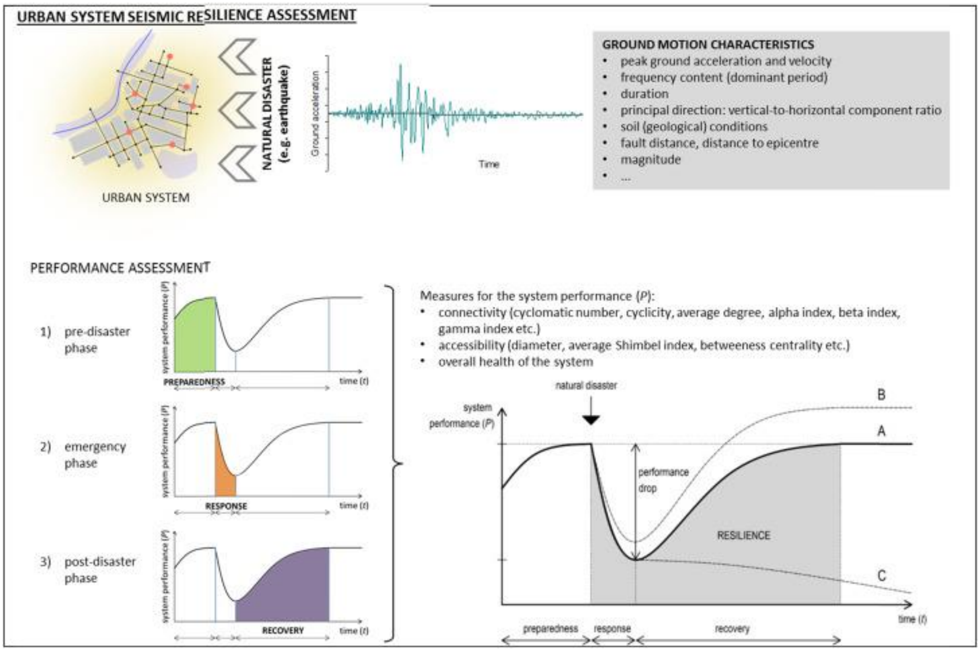

Fig. 2.5 A conceptual framework for quantitative seismic resilience assessment of an urban system: time-dependent system performance analysis [Rus et al., 2018]

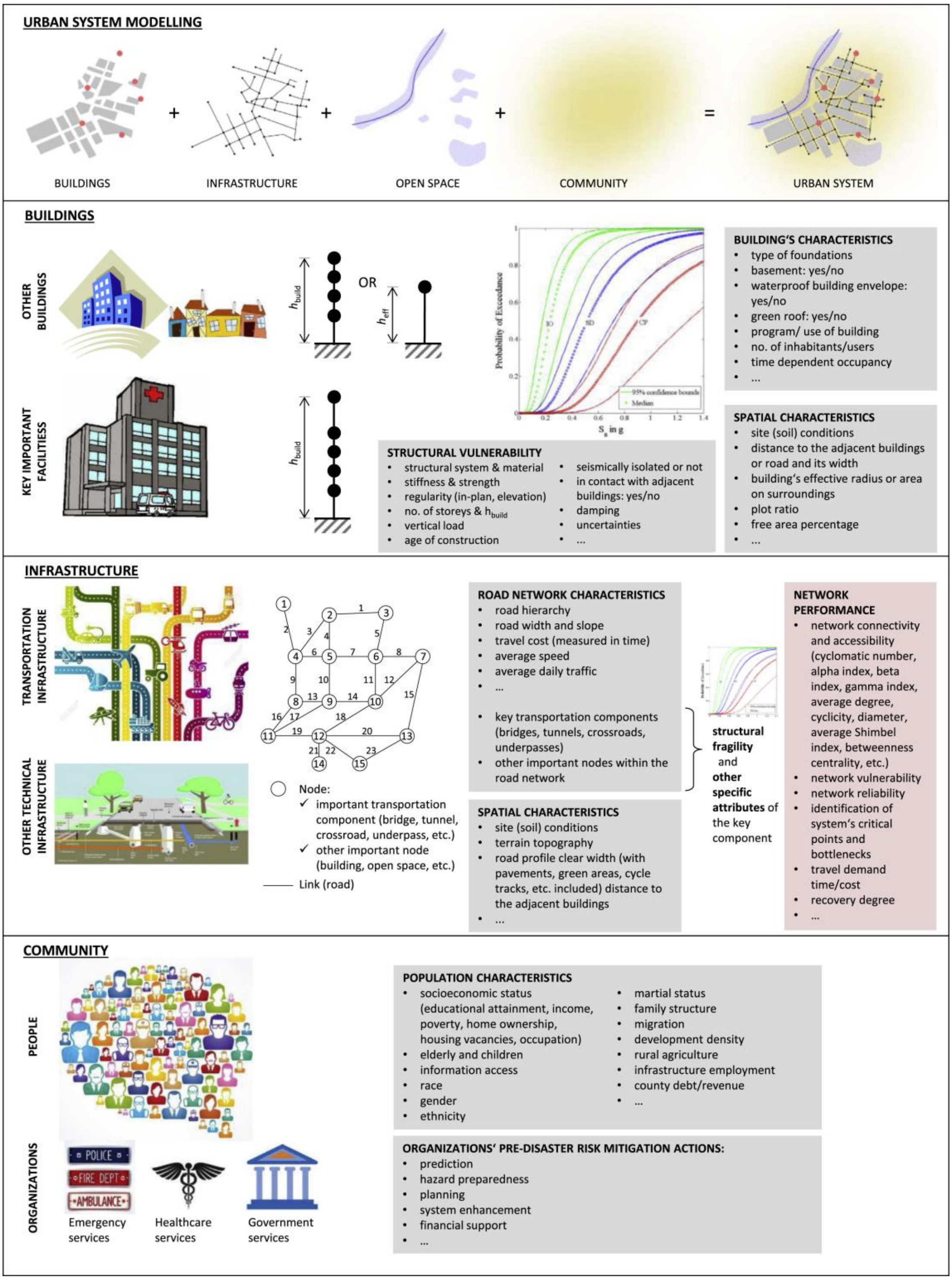

Fig. 2.6 A concept for the modelling of an urban system, its (sub)components and their attributes [Rus et al., 2018]

Chan et al. [2019] reported that, in rural areas of Asia, the number and severity of climate-related natural disasters were increased. In the process of the assessment and management of natural disasters in rural areas, it was necessary to jointly consider local culture, economic level and sustainable development. In addition, current studies on natural disasters in rural areas mostly focused on earthquakes. The number of studies on other natural disasters, such as droughts and floods, were somehow limited. It was proposed that the popularization of disaster prevention and response knowledge should be enhanced in rural areas, and disaster emergency exercises appropriately stepped up to improve the disaster prevention and risk avoidance ability of the local governments and ordinary people.

Kreibich et al. [2014] comprehensively reported the risk assessment and management for the most important natural disasters including floods, earthquakes, extreme temperatures and storms in Germany. It was pointed out that, in the process of risk management, multiple risk factors should be considered comprehensively. As a result, the interrelationship among various factors in natural disasters can be accurately identified, and the impacts and roles of natural disasters quantified.

Jahangiri et al. [2017] reported that the current policies related to natural disaster risk assessment and management were mainly developed based on previous experiences. Using forward-looking tools or methods was helpful for effective risk management.

Therefore, the applications of far-sighted methods, models and tools were important in natural disaster risk assessment and management.

2.3 Studies on the thermal environments inside disaster-relief temporary houses including PTHs

Following a natural disaster, disaster-relief temporary houses were widely deployed during post-disaster transition, post-disaster reconstruction and resettlement period. Disaster-relief temporary houses can meet victims' basic living needs, provide victims with safe shelters, sufficient water, food and clean sanitation facilities. In addition, the use of disaster-relief temporary houses also helped people recover from the trauma of natural disasters and provide strong support for future reconstruction.

When deploying disaster-relief temporary houses, four types of factors should be considered [Bashawri et al., 2014]:

- Technical factors: materials and insulations, classification of hazards and performance, easy to erect and dismantle, physical and psychological effects;
- Economic factors: cost, lifetime, type of shelters, livelihood;
- Environmental factors: recycling, upgrading and disposal, climate variations, hygiene, locations;

- Sociocultural factors: dignity and security, cultural difference, communication;

2.3.1 Types of disaster-relief temporary houses

Disaster-relief temporary houses mainly included disaster-relief PTHs and tents, which will be discussed in detail in this Section. Other types may include a paper tube disaster-relief temporary house, and an example is shown in Fig. 2.7.

Fig. 2.7 The inside of a paper tube disaster-relief temporary house

2.3.1.1 Disaster-relief PTHs

Disaster-relief PTHs have been massively used in disaster relief reconstructions due to the advantages of convenient transport, easy installation and short construction period [Tang et al., 2017; Aye et al., 2012; Wang et al., 2016b]. For example, after the mega-scale 2008 Wenchuan Earthquake in China, more than 21 million victims were resettled in PTHs during a post-disaster transitional period of up to 36 months. A photo illustrating PTHs erected in Whenchuan is shown in Fig. 2.8.

Fig. 2.8 Disaster-relief PTHs erected following the Whenchuan Earthquake in 2008

Felix et al. [2013] found that due to the continuous occurrence of natural disasters, the demands for disaster-relief PTHs became increasingly higher. Appropriate layout and scientific management of disaster-relief PTHs were necessary in effectively using disaster-relief PTHs during post-disaster rescue and transitional resettlement. By applying life cycle analysis evaluation method to the full cycle evaluation for two kinds of disaster-relief PTH in Turkey, Atmaca [2017] obtained the following two conclusions. Firstly, from the view of point of improving the energy efficiency in temporary disaster-relief PTHs and reducing carbon dioxide emissions, the selection of materials, the use of thermal insulation technology and recyclable facilities were the key factors to be considered. Secondly, during the operation of a PTH, its energy consumption and carbon dioxide emissions accounted for 86% and 95%, respectively, of those during building and installing the PTH. Similarly, Song et al. [2016] also discussed the issue of energy consumption from the viewpoint of full life cycle of PTHs. They pointed out that the use of recycled materials, lightweight structural materials and lightweight envelope materials were helpful to reduce the energy consumption in building and erecting PTHs.

Shinohara et al. [2013] measured the air exchange rate, VOCs release and radioactive energy levels in 19 PTHs after the earthquake in Minamisoma region, Japan. The time span was from August 2011 to January 2012. The measured results demonstrated that there was little difference in air exchange time duration in different post-disaster PTHs.

For the measured results of VOCs, it was shown that indoor air quality in post-disaster PTHs was good, and indoor radioactive energy level grade was low. Iwasa et al. [2012] found that two families who used to be neighbours would choose to live adjacent to each other in a post-disaster temporary building community. Setting up public areas such as "Bench Space", "Common Room" and "Farm Place" in a post-disaster temporary building community could better enhance the information and emotional communication of victims, and was an important way to promote their physical and mental recovery from the post-disaster trauma [Basile, 2020]. Arslan [2007] found that in the whole process of post-disaster reconstruction, the cost of post-disaster temporary housing took up to 10% of the total cost. But more attention should be paid to the effective recycling of post-disaster temporary housing, which was very important for environmental friendliness and sustainable development of a post-disaster residential ecosystem.

2.3.1.2 Tents

Tents that may be used as temporary houses for various purposes include nomadic tents, adventure tents, military tents and disaster-relief tents, etc.

For nomadic tents, in order to adapt to different environmental temperatures, three different structures of single, double and three-layer can be used. The advantages of single-layer tents include portability, low cost, small size and easy making. On the other hand, a double-layer tent adds an impermeable layer to a single-layer tent. Single-layer tents are mainly suitable for warmer areas or seasons, and double-layer tents for cooler seasons or areas. Furthermore, the design of a three-layer tent is based on a double-layer tent by adding a layer of cotton to further enhance the thermal insulation. In an outdoor environment of - 10 ^{o}C, the temperature inside a three-story tent can be kept at above 0 ^{o}C. Fig 2.9 shows three-layer nomadic tents.

Fig. 2.9 Three-layer nomadic tents

For adventure tents, as illustrated in Fig. 2.10, in the harsh climate of the high altitude mountains or polar regions, an adventure tent can provide shelter and warmth for explorers [Cena et al., 2003]. Adventure tents mainly include dome tents, geodesic tents and tunnel tents.

Dome tents are widely used in outdoor adventures, ranging from a single-person tent to a size that can accommodate a dozen people for dinner and meeting. The structure of dome tent is highly wind-resistant, so that dome tents are generally suitable for high altitude applications.

Fig. 2.10 Adventure tents

On the other hand, the poles in the structure of geodesic tents are repeatedly crossed, providing a very strong stability. They are hence highly suitable for use in harsh climate environments. For weight considerations, the number of poles in a geodesic tent may be reduced, provided that its stability would not be compromised.

Military tents, as illustrated in Fig. 2.11, are used for long-term or short-term stays for soldiers during a period of field investigation, camping, prospecting, construction and disaster relief. Steel frame structure adopted by military tents is convenient for exhibition and collection. Military tents can be erected or withdrawn within 30 minutes by 4 people. Jiang and Chen [2019] conducted comparative experiments on the thermal environments inside military tents having different structures. They also studied the contributions to the improvement in the thermal environment inside military tents from shading.

Fig. 2.11 A military tent [Jiang and Chen, 2019]

Following the occurrence of disasters, disaster-relief tents, with an example shown in Fig. 2.12, are also massively used for disaster-relief management and emergency medical treatment, and as temporary school buildings, transit storage of disaster-relief materials and personnel accommodation, etc. [Easton, 2008; Wang et al., 2015].

Fig. 2.12 Disaster-relief tents erected in Wenchuan in 2008

2.3.2 Studies on the thermal environments inside disaster-relief temporary buildings/tents

A number of studies on the methods of improving the thermal environment inside temporary houses have been reported [Jiang and Chen, 2019; Cena et al., 2003; Liu et al., 2016]. Jiang and Chen [2019] reported that having shading measures on top of a tent, such as a sunshade net, could effectively reduce the solar radiation received by the tent, so as to improve the thermal environment inside the tent in summer. It was demonstrated that the thermal environments inside the tested tent were improved by different degrees when using different densities of sunshade nets. The resulted shading rate when using a 6-pin shading net was 28% higher than that when using 3-pin shading net, and the air temperature inside the two nets was reduced by 8^{o}C and 5 ^{o}C, respectively. The inner surface temperature of the shaded tent was dropped by as much as 17 ^{o}C. Fig. 2.13 shows the experimental setup used in the study by Jiang and Chen [2019].

Fig. 2.13 The shaded tent studied by Jiang and Chen [2019]

Naylor et al. [2018] proposed a disaster-relief building made of wood and multi-layer cork panels, as shown in Fig. 2.14. Cork had the characteristics of good sound insulation, fire retardant, environmental protection, mould and microorganisms resistance. They measured the thermal environments inside this cork-based disaster-relief building. By comparing the measured indoor air temperatures in July, it was found that when the outdoor air temperature was lower than 30 ^{o}C, the maximum air temperature inside this cork-based disaster-relief building still exceeded the maximum outdoor air temperature. Therefore, the thermal environment inside the cork-based disaster-relief building should be improved. Shinohara et al. [2014] conducted a 7-month long study on 19 disaster-relief temporary buildings located in Fukushima, Japan. Combined with the results of questionnaire survey of residents and field measurements in disaster-relief buildings, it was found that the thermal environment inside disaster-relief buildings was worse than that of ordinary buildings in summer. It was proposed that an improvement in the thermal insulation for disaster-relief buildings should be considered during the construction of disaster-relief buildings in the future. Cornaro et al. [2015] studied the thermal environment inside disaster-relief temporary tents. The experimental results showed that at the highest outdoor air temperature of 23 ^{o}C, as shown in Fig. 2.15, the air temperature inside a disaster-relief tent can reach as high as 45 ^{o}C, as shown in Fig. 2.16, far above the upper limit of the air temperature for thermal comfort. These results suggested that the thermal environment inside disaster-relief temporary buildings/tents in summer should be significantly improved.

Fig. 2.14 A disaster-relief building made of cork panel [Naylor et al., 2018]

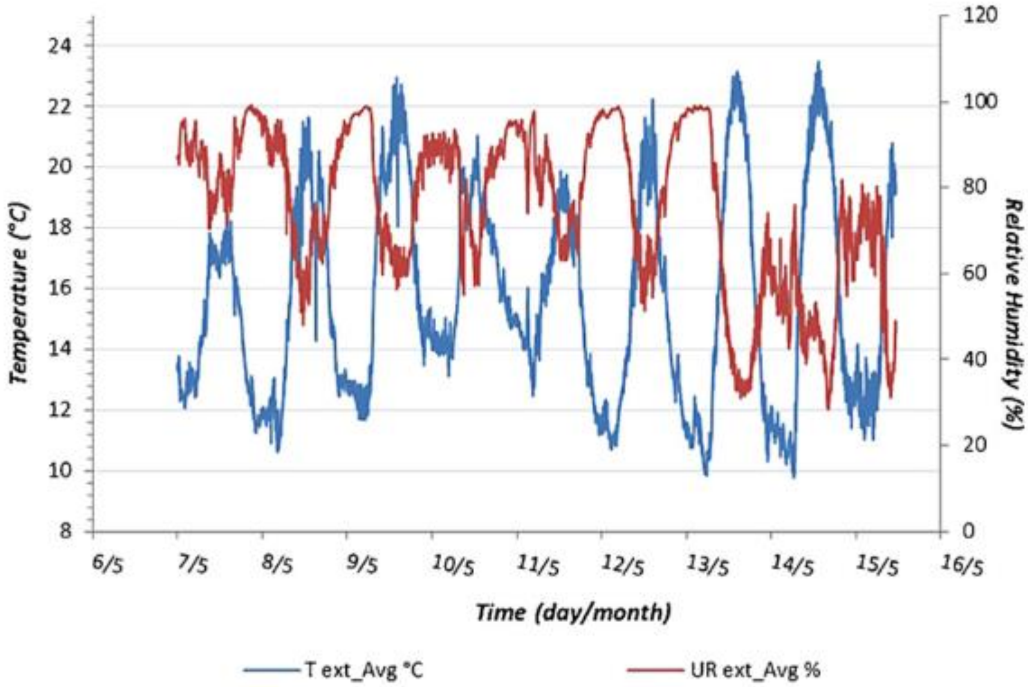

Fig. 2.15 Measured outdoor air temperature where a disaster-relief tent was erected [Cornaro et al., 2015]

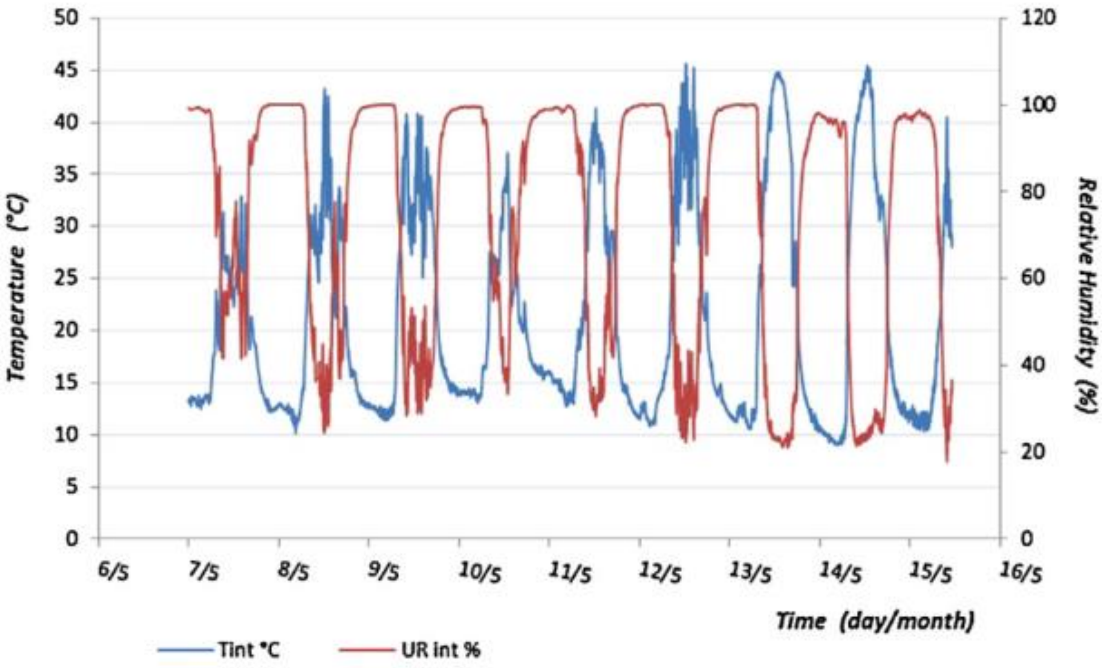

Fig. 2.16 Measured air temperature inside the disaster-relief tent [Cornaro et al., 2015]

2.3.3 Studies on the thermal environments inside disaster-relief PTHs

As an important form of disaster-relief temporary houses, disaster-relief PTHs have been widely used during post-disaster resettlements. Therefore, a number of studies have been carried out to evaluate the thermal environment, and to examine the measures for improving thermal comfort level, inside PTHs.

Combined with measurements and questionnaire surveys, Shinohara et al. [2014] studied the thermal environments inside both a PTH and a wooden temporary house. The study results demonstrated that in winter, the air temperatures inside the PTH and the wooden temporary house were both very low, hence their thermal environments were poor. In summer, the thermal comfort level inside the PTH was lower than that inside the wooden temporary house due to a higher air temperature inside the PTH.

Kim et al. [2015] investigated the thermal environment inside an experimental mobile energy PTH in Korea. The results showed that the PMV range inside the experimental mobile energy PTH was between - 0.08 and - 0.85. The thermal environments inside the PTH were found uncomfortable during certain periods in summer and winter. However, the comfort level of occupants can be improved by adjustment of clothing and using appropriate mechanical ventilation.

Wang et al. [2016a] studied the thermal environments inside a full-scale experimental disaster-relief PTH. The study results demonstrated that in both summer and winter, the thermal environments inside the full-scale experimental PTH were intolerable for disaster victims. The indoor air temperature peaked at 42 ^{o}C which was 8 ^{o}C higher than outdoor air temperature. Therefore, it was urgently needed to improve the thermal environment inside a disaster-relief PTH by effective and low cost passive measures. As a follow-up, Wang et al. [2017] further numerically investigated four different passive measures applied to the full-scale PTH for improving its indoor thermal environment. The effects of using single passive measures and multiple passive measures on improving the thermal environments inside the PTH were compared in detail. The comparison results showed that the use of external window blinds and movable sunshade curtains on the roof and walls could effectively reduce the air temperature, and improve the thermal comfort level, inside the PTH in summer.

Asfour [2019] studied disaster-relief PTHs erected in Gaza Strip. The study results demonstrated that if appropriate and effective measures were not employed, the thermal environments inside disaster-relief PTHs would become intolerable. It was difficult for occupants to live in such a harsh environment. In their study, three methods were proposed to improve the thermal environments inside PTHs. The first was to shade PTHs so as to reduce the solar radiation received by PTHs. The second was to make the appropriate layout for PTHs in order to reduce the total external envelope surface area of PTHs. The last was to add thermal insulation materials to PTHs' envelopes, such as walls and roofs. By taking these measures, the average PMV level inside PTHs was increased by 0.6 in winter and decreased by 0.9 in summer, respectively.

2.4 Studies on applying PCMs in buildings for improving indoor thermal environments

In order to improve the thermal environments inside buildings, various passive measures for regulating indoor air temperatures using new technologies and materials have been developed. As one of these measures, PCMs have been widely used for improving indoor thermal environments in various buildings [Hirmiz et al., 2019; Mourid et al., 2018; Sun et al., 2018].

2.4.1 Classifications of PCMs

PCMs release or absorb energy by phase transition reaction, which is a reversible process. The phase transition process of PCMs has three different forms, including solid-liquid, solid-solid and solid-gas phase transition. In these three forms, a solid-gas phase transition has a low heat transfer coefficient and a large change in volume and pressure, while the energy storage capacity in a solid-solid phase transition is relatively lower [Sun et al., 2020a; Yan et al., 2019a]. PCMs based on solid-liquid phase transition are widely used in the construction industry [Umair et al., 2019]. Generally, PCMs are classified into three main categories, eutectic mixtures [Cai et al., 2015; Zhang et al., 2014a; Zhang et al., 2014b], organic [Choi et al., 2019; Wang et al., 2019a; Xie et al., 2019] and inorganic [Mohseni et al., 2020; Peng et al., 2019; Sun et al., 2020b; Cunha and Aguiar, 2020].

Extensively used organic PCMs include paraffin [Qu et al., 2020; Vasu et al., 2019; Yao and Wu, 2020], polyethylene glycol [Kou et al., 2019; Wijesena et al., 2020] and fatty acids [Umair et al., 2019]. Organic PCMs have a wide applicability temperatures range, high latent heat of phase change, high nucleation, low phase segregation rate, low undercooling capability, good thermochemical stability, non-toxic and high recycling utilization rate [Kalnaes and Jelle, 2015; Lin et al., 2018; Oliver et al., 2012]. Their disadvantages however include leakage problem, flammability, low density and low thermal conductivity. Umair et al. [2019] reported that shape-stabilization was an effective method to solve the leakage problem of organic PCMs by microencapsulation, as illustrated in Fig. 2.17.

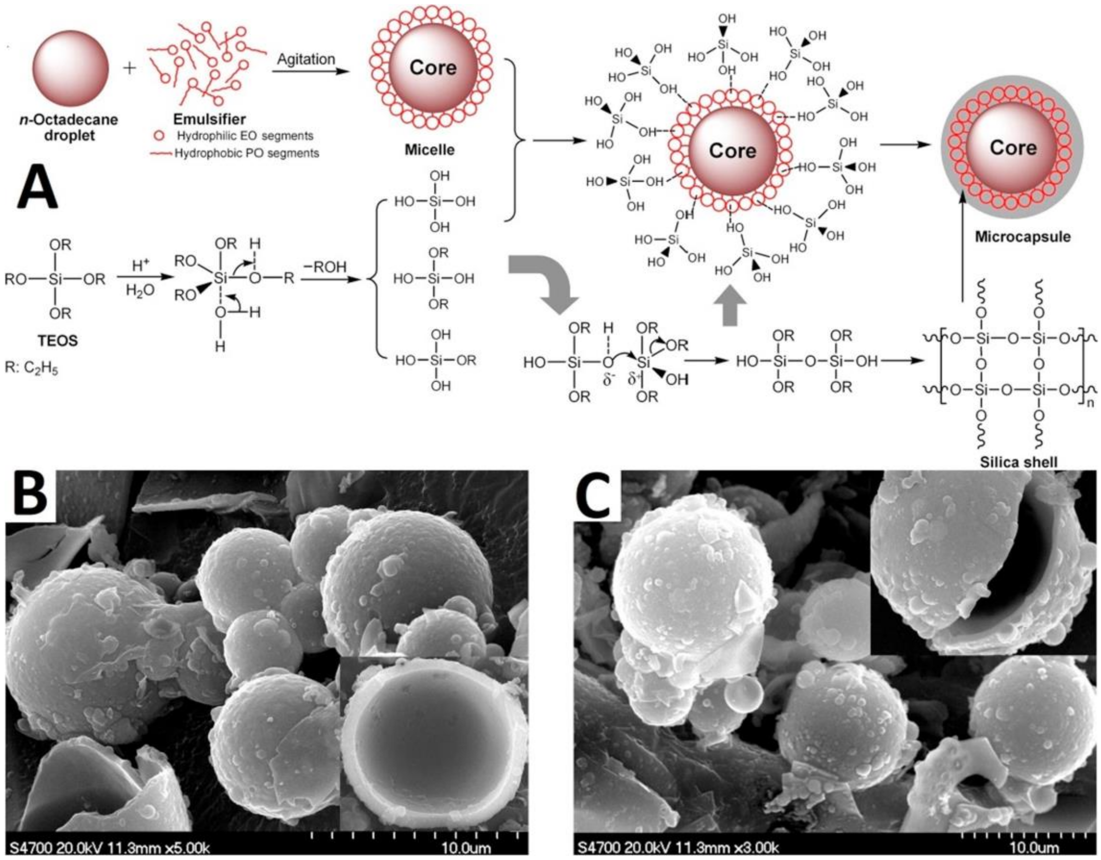

Fig. 2.17 (A) Schematic formation of the silica-microencapsulated n-octadecane via sol–gel method. (B) SEM images of MEPCMs containing n-octadecane/TEOS with 50/50 mass ratio at pH 2.45, and (C) 70/30 mass ratio at pH 2.89 [Umair et al., 2019]

As a representative of organic PCMs, paraffin wax is introduced in details as follows. Paraffin wax, a product of petroleum refining, is a mixture of pure alkanes. The general chemical formula of paraffin is C_nH_{2n+2}. Paraffin has the advantages of no undercooling, non-corrosiveness, high chemical stability, high latent heat of phase transformation, no phase separation and low cost. However, its main disadvantages include low density, flammability and low thermal conductivity [Hasnain, 1998a; Hasnain, 1998b; Lv et al., 2016].

Inorganic PCMs mainly include hydrated salts, molten salts, metal and alloy. Their advantages are large phase change temperature ranges, high thermal conductivity, non-flammability, low volume change and low cost. Their disadvantages however include low nucleation, high phase segregation rate, sub-cooling problems, toxic and low thermochemical stability [Cunha and Aguiar, 2020; Lin et al., 2018].

Hydrated salt is a kind of inorganic PCM containing crystal water, and its general chemical formula is $AB \cdot X\ H_2O$. Hydrated salt has relatively high latent heat and thermal conductivity of phase transition and is non-flammable and cheaper than paraffin wax. However, it has certain shortcomings, such as insufficient durability, easy for phase separation to occur, undercooling and corrosiveness. In practical application, hydrated salt is widely used in buildings [da Cunha and Eames, 2016; Tyagi and Buddhi, 2008].

For eutectic mixtures, due to their appropriate combining of inorganic and organic PCMs, they have the advantages of good thermochemical stability, low undercooling capability, high thermal conductivity and low liquid leakage. Eutectic mixtures are a mixture of organic and inorganic PCMs, such as microencapsulated PCMs, porous composite PCMs, polymer composite PCMs. However, the high cost of eutectic mixtures limits their application [Cunha and Aguiar, 2020]. The melting temperature of eutectic mixtures is lower than that of their components [Campos-Celador et al., 2014; Rezaei et al., 2013].

On the other hand, according to the phase change temperature, PCMs can also be divided into high temperature energy storage materials (above 250 ^{o}C), medium temperature energy storage materials (100 ^{o}C - 250 ^{o}C) and low temperature energy storage materials (below 100 ^{o}C) [Kalnaes and Jelle, 2015; Lin et al., 2018; Sharma et al., 2009].

For practical application, factors that should be considered in the selection of PCMs include phase change temperature, phase change latent heat, thermal conductivity, undercooling, volume change rate, flammability, stability and corrosion [Cunha and Aguiar, 2020]. An ideal PCM should have suitable thermos-physical, kinetic, safety, environmental and economic properties [Forbes et al., 2018], detailed as follows:

- Thermos-physical property: operating temperature, thermal conductivity, density, energy storage density, latent heat, heat capacity, thermal stability, volume variation, segregation;
- Kinetic property: nucleation rate, crystallization rate;
- Safety property: toxicity, flammability, degradation, corrosion properties;
- Environmental property: energy consumption, recycling life, environmental impact;
- Economic property: abundance of raw materials, cost;

2.4.2 Methods for incorporating PCMs into building materials

Incorporating methods of building materials and PCMs include: direct modification of building materials and PCMs, incorporating encapsulated PCMs into building materials, PCMs immersion in building materials [Cunha and Aguiar, 2020].

The definition of direct modification of building materials and PCMs is that, in the preparation stage of building materials, PCMs are directly incorporated into building materials. For example, in the process of preparing concrete, PCMs are directly added in the raw materials to modify concrete. However, direct modification has the risk of properties changing for building materials. For example, the strength of mortar and the durability of gypsum may be reduced due to the modification of PCMs.

Yun et al. [2019] experimentally added PCMs into mass concrete. The experimental results showed that adding PCMs to concrete would reduce the compressive strength of concrete, reduce the heat of hydration, and decrease the cracking caused by heat. Bahrar et al. [2018] used experimental and numerical methods to study the PCMs composited concrete. The study results demonstrated that the thermal conductivity of the composited concrete was decreased with an increase in the number of PCMs added. The phase transition temperature of the PCMs was verified by heating and cooling experiments. An established numerical model was also validated by experiments.

Incorporating building materials with encapsulated PCMs is another suitable method. Commonly encapsulating materials include microcapsules [Cabeza et al., 2020; Raj et al., 2019; Yan et al., 2020] and large-volume containers [Aziz et al., 2018; Yan et al., 2019b]. Large-volume PCMs containers mainly include plates, tubes and large-volume blocks.

Microencapsulation materials can be formed through physical, chemical and mechanical actions. The main advantage of microencapsulated PCMs is that the encapsulated PCMs can be directly added into building materials. For example, microencapsulated PCMs can be added into mortar or concrete in the form of aggregate. The heat transfer, the durability and mechanical shock resistance of PCM are enhanced due to microencapsulation. However, the incorporation of microencapsulated PCMs into building materials also has certain disadvantages, such as reducing the strength and increasing the production cost of building materials. In the production process of microcapsule PCMs, the cost of microencapsulation of PCM accounts for 70% of the total cost.

The cost of PCMs encapsulation in large-volume containers is considerably lower than microencapsulation materials. In addition, PCMs encapsulated in large-volume containers are more convenient to transport and install. For some buildings, PCMs in large-volume containers are prefabricated in buildings' envelopes. However, several factors should be taken into consideration during the selection and design process of large-volume containers, such as convenient installation, method of incorporation and coefficient of heat transfer.

The third incorporating method is to impregnate building materials with PCMs. PCMs are immersed into the building materials through the capillary action. This method is mainly used for porous building materials, such as lightweight concrete aggregates with porous structures impregnated with PCMs [Uthaichotirat et al., 2020]. Materials used for PCMs immersion should have sufficient porosity, suitable specific surface area and pore size. Commonly used lightweight aggregates for PCMs immersion are perlite, slate and shale [Umair et al., 2019; Cunha and Aguiar, 2020]. Fig, 2.18 shows a process of impregnating PCMs into building materials.

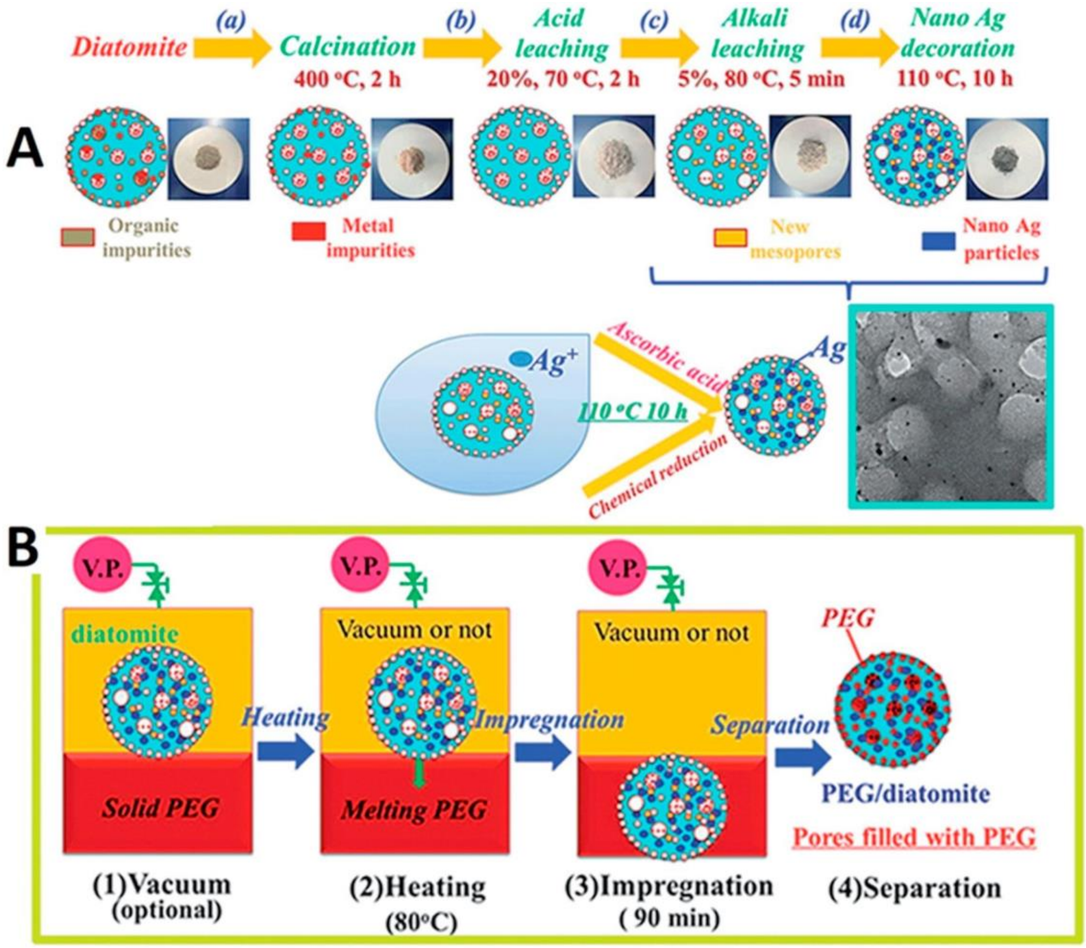

Fig. 2.18 (A) Schematic preparation of AgNP-decorated diatomite powder; (B) shape stable PCM fabrication via vacuum impregnation method [Umair et al., 2019]

In the study by Qian and Li [2018], PCM and carbon nano-diatomite were compounded and mixed into concrete as aggregates. The multi-layer porous structure of carbon nano-diatomite was beneficial to the recombination of PCMs. The energy storage capacity of PCM concrete was improved. PCM concrete had good chemical and mechanical stability and excellent durability which was helpful to modulate the fluctuation of indoor air temperature and improve indoor thermal comfort.

Uthaichotirat et al. [2020] completed a serious of studies about high porous aggregates impregnated with PCMs mixed with concrete. Workability, density, compressive strength and modulus of rupture and sound transmission loss of the aggregates were examined. The experimental results showed that with an increase in PCMs content in aggregate, the slump, density, compressive strength, flexural strength and sound transmission loss of aggregates were all increased. As the content of PCMs was increased from 0 to 100%, the slump, density, compressive strength and flexural strength of concrete were increased by 19.2%, 8.6%, 8.6% and 8.2%, respectively.

2.4.3 Application of PCMs to buildings for improving indoor thermal environments

PCMs chemically store energy by high latent heat. In the process of phase transformation, PCMs change from solid to liquid or from liquid to solid, during which a large amount of heat is absorbed or released. The melting temperature of PCMs used in passive buildings is usually at between 10 ^{o}C and 35 ^{o}C. Beside suitable temperature range of phase change, PCMs used in passive buildings should also meet other requirements, such as thermodynamic properties, kinetic properties, chemical properties, economy, realizability [Song et al., 2018; Zhu et al., 2018; Tao and He, 2018].

Studies of applying PCMs to buildings can be divided into three categories, based on the way of incorporating PCMs into buildings: direct modification of PCMs into building materials; independent operation of PCMs inside or outside a building; incorporating PCMs into building envelopes [Dardir et al., 2019; Rao et al., 2018; Rathore and Shukla, 2019].

Cabeza et al. [2007] developed an innovative concrete, by incorporating PCMs into the concrete. Good structural properties together with thermal comfort improvement performances were demonstrated. It was shown that in buildings using the innovative concrete, a more comfortable indoor thermal environment can be provided, as compared with the buildings using conventional concrete.

Zhao et al. [2019] analysed the specific geo-climatic characteristics of Tibet, including high altitude, abundant solar radiation, long sunshine duration, low ambient temperature at nighttime and low water boiling point. It was proposed that in the design process of a PCMs based solar heating system, both active and passive heating methods should be considered. The use of flat plate solar collectors can prevent explosion hazard caused by water vaporization at low boiling point, while considering the risk of sandstorm and glass breakage. The efficiency of using solar energy through the implementation of a PESS may be enhanced.

PCMs can also be composited into building envelopes [Lu et al., 2020; Park and Kim, 2019; Lu et al., 2017]. When a PCM is composited into the inner surface, outer surface or middle layer of a building envelope, the PCM can help increase the thermal resistance of building envelopes. Experimental and numerical studies suggested that the application of PCMs to building envelopes can improve the thermal environment inside buildings.

Tyagi et al. [2012] observed that a PESS was very important when energy supply and demand mismatched. Such a PESS can regulate indoor air temperature efficiently in low energy demand buildings. In their experimental work, they firstly charged the PESS with cooling energy, and then increased the heat gain for an experimental room by 1 kW, 2 kW and 3 kW, respectively. From the experimental results, it was found the duration when comfortable indoor air temperature was maintained was at 9 h, 3.5 h and 2.5 h, respectively. Lin et al. [2016] provided a solution of thermal performance improvement by compositing a residential building with PCMs and using solar photovoltaic thermal (PVT) collectors. They undertook a series on-site tests, considering the arrangement of different PCMs and thickness of insulation materials.

A common method of using PCMs in building envelopes was to combine PCMs with the inner surface, outer surface or middle layer of building walls. PCMs can enhance the heat capacity of building envelopes. A number of experimental and numerical studies [Kuznik et al., 2016; Imani, 2019; Kolaitis and Founti, 2017] have proved that PCMs can improve the indoor thermal environment and have a positive impact on reducing energy consumption.

2.5 Conclusions

Following global natural disasters, disaster-relief temporary houses have been massively used during post-disaster transition, post-disaster reconstruction and resettlement period to provide disaster victims with temporary shelters. Among various disaster-relief temporary houses, disaster-relief prefabricated temporary houses (PTHs) were the mostly commonly employed due to their advantages of convenient transport, easy installation and short construction period. In many cases, such fast-installed PTHs were the only choice for disaster victims during a post-disaster transitional period, which may unfortunately last for up to several years. Furthermore, given their temporary nature, few indoor thermal environmental control systems were usually installed and therefore, the thermal environments inside PTHs can become intolerable, as shown in Section 2.3.3. In particular, in summer, the air temperature inside a disaster-relief PTH can be much higher than the outdoor air temperature. For example, the indoor air temperature peaked at 42 ^{o}C which was 8 ^{o}C higher than outdoor air temperature. The long-term severity in indoor thermal environment may result in physical and mental problems for PTHs' occupants, which can be particularly true for those disaster victims. Therefore, improving the indoor thermal comfort for the occupants in disaster-relief PTHs using simple and low-cost measures, such as passive designs, has been urgently needed. As illustrated in Section 2.3.3, although certain passive measures, such as shading and ventilation, for improving the thermal environments inside PTHs had certain effects, they were still inadequate in maintaining acceptable thermal environments inside disaster-relief PTHs. Alternative but yet effective passive measures on improving the indoor thermal comfort for occupants in disaster-relief PTHs in summer were still urgently needed.

On the other hand, as presented in Section 2.4, previous experimental and numerical studies showed that the use of PCMs could help improve the thermal comfort in buildings. A considerable number of studies were carried out to study the applications of PCMs to various permanent buildings for enhancing their indoor thermal environmental control. However, full-scale applications of PCMs to disaster-relief PTHs were rarely seen. This may also be due to the temporary nature of disaster-relief PTHs since they were not expected for long-term use. Nonetheless, as the actual use of PTHs may no longer be temporary, it became highly necessary also to study the use of PCMs, as an alternative to other passive measures, in PTHs for improving their indoor thermal environments in summer, for the well-beings of disaster victims.

The extensive literature review presented in this Chapter has identified a number of important areas where further in-depth research work is urgently required, to provide the disaster victims in PTHs with an acceptable indoor thermal environment in summer using passive measures of applying PCMs to PTHs. These are the expected study targets of the programed research work presented in this Thesis.

Chapter 3

Proposition

3.1 Background

It is clear from the literature review presented in Chapter 2 that the thermal environment inside disaster-relief PTHs in summer was severe and therefore harmful to the physical and mental health of their occupants. It became highly necessary to take measures to effectively improve the thermal environment inside disaster-relief PTHs in summer. Although certain passive measures, such as shading and ventilation, were applied to disaster-relief PTHs to improve their indoor thermal environments, their effectiveness was limited and alternative measures should be developed.

On the other hand, although PCMs have been widely applied to conventional buildings for reducing energy consumption and demand, and for improving indoor thermal comfort, they were rarely applied to disaster-relief PTHs. This may be due to the temporary nature of disaster-relief PTHs since they were not expected for long term use. Given the success of applying PCMs to conventional buildings in regulating the energy demand and improving indoor thermal comfort, it became highly necessary to study the application of PCMs in disaster-relief PTHs, as an alternative measure to other passive measures, for improving their indoor thermal environment in summer.

3.2 Project title

A programmed research work on applying PCMs to improve the thermal environments inside disaster-relief PTHs has been therefore carried out and is presented in this Thesis. There are three parts in the programmed research work: 1) experimentally studying the application of PCMs to disaster-relief PTHs for improving their internal thermal environment in summer; 2) establishing and experimentally validating a numerical model for an experimental PTH, and using the validated model to numerically optimize the designs of applying PCMs to the PTH in order to improve its indoor thermal environment in summer; 3) numerically studying the application of a movable PESS to disaster-relief PTHs used in different climate regions around the world to improve their indoor thermal environments in the summer month of July. The programmed research work is therefore entitled "Applying phase change materials (PCMs) to disaster-relief prefabricated temporary houses (PTHs) for improving their indoor thermal environments in summer time".

3.3 Aims and objectives

The aims and objectives of the programmed research work are as follows:

1) To establish two experimental MHs, a full-scale experimental PTH and a PCM-based energy storage system, to enable the required experimental work and model experimental validation;
2) To experimentally study the application of PCMs to disaster-relief PTHs for improving their indoor thermal environments in summer, using the experimental MHs and the full-scale experimental PTH;
3) To establish and validate a numerical model for the experimental full-scale PTH incorporating with PCMs and to use the validated model to numerically study the optimization of the designs of applying PCMs to a full-scale disaster-relief PTH to improve its indoor thermal environment in summer;
4) To use the validated model to numerically study the application of a movable PESS to disaster-relief PTHs used in different climate regions around the world to improve their indoor thermal environments in the summer month of July.

3.4 Research methodologies

Experimental and numerical approaches will be used throughout the programmed research work.

Firstly, two experimental MHs, an experimental full-scale PTH and a PESS, to be placed on the flat roof of a four-story building in the campus of Sichuan University, will be purposely established. The operating thermal and environmental parameters for the experimental MHs, full-scale PTH and PESS, including outdoor air temperature, air temperatures inside the MHs and the full-scale PTH, internal surface temperatures of the MHs and the full-scale PTH, will be measured, to experimentally study the application of PCMs to the MHs and the full-scale PTH and to validate a numerical model to be established for the experimental full-scale PTH.

Secondly, a numerical model for the experimental full-scale PTH will be established using EnergyPlus platform and experimentally validated with the measured data from the experimental full-scale PTH. With the validated model, a detailed numerical study on optimizing the designs of applying PCMs to the full-scale PTH will be carried out. The numerical study will include two parts. In the first part, a total of 16 different designs will be defined and numerically evaluated. In the second part, an appropriate thickness for a PCM layer will be recommended as a reference design value for practical applications.

Thirdly, a further numerical study on applying a movable PESS to PTHs in 12 selected cities of different climates around the world will be undertaken. The experimentally validated EnergyPlus based simulation model for the full-scale experimental PTH incorporating the movable PESS will be deployed. To evaluate the effectiveness of applying PCMs to disaster-relief PTHs, an evaluating criteria will be proposed. Based on the thermal and environmental parameters for the PTH incorporating the movable PESS, such as outdoor air temperature, air temperatures inside PTHs (the maximum temperature, the monthly averaged air temperature, the daily peak and daily average indoor air temperature on the hottest day) obtained in the numerical study and the proposed evaluating criteria, cities which are suitable for applying PCMs to PTHs will be identified.

Chapter 4

Experimental setups for the two designs and their associated measuring instrumentations

4.1 Introduction

In the experimental part of the programmed research work, two different designs, named as Design 1 and Design 2, respectively, were examined. In Design 1, two MHs were used and in Design 2, a full-scale experimental PTH was used. Design 2 was implemented following the experimental outcomes for Design 1. The experimental setups for the two designs are detailed in this Section.

4.2 Design 1

In Design 1, two model PTHs, a reference MH and a PCM based MH, were purposely built. Both were the scaled down models of a full-scale PTH, and of identical dimensions of 1.0 m × 0.8 m × 1.3 m. Both MHs used light-weight prefabricated insulation panels for their envelopes. However, for the PCM based MH, a PCM layer of 20 mm-thick was added to the internal surfaces of its envelope, as shown in Fig. 4.1

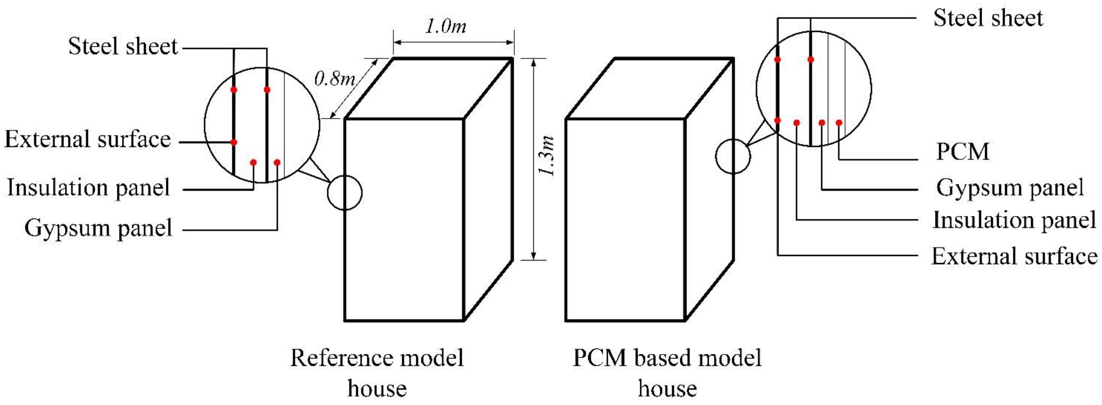

Fig. 4.1 Details of the two experimental MHs for Design 1

The details of envelope materials, and the physical and thermal properties of these materials are given in Table 4.1 and Table 4.2, respectively. In addition, there were no windows or doors in the two MHs.

The two MHs were placed on the flat roof of a four-story building in the campus of Sichuan University, Chengdu, China. To ensure an accurate comparison between the thermal environments inside the two MHs, they were placed side by side, with a distance of only 1.2 m in between.

Table 4.1 Materials of building envelope used in the two MHs

Building envelope	Reference MH	PCM based MH
Floor	Steel panel EPS insulation panel	Steel panel EPS insulation panel
Roof and Walls	Steel panel EPS insulation panel Gypsum panel	Steel panel EPS insulation panel Gypsum panel Phase change material

Table 4.2 Physical and thermal properties of the materials used in the two MHs

Materials	Thickness (mm)	Thermal conductivity (W/m·K)	Density (kg/m^3)	Specific heat (J/kg·K)
Steel	0.5	45.28	8000	460
EPS	75	0.035	20	1100
Gypsum	8	0.18	580	870
PCM	20	0.25 - 0.5	1300	1780

To measure and compare the thermal performances inside the two MHs, T-type thermocouples with an accuracy of ± 0.5 ^{o}C were used. All T-type thermocouples were calibrated before they were used in the experiments, and were connected to a data logger where all the measured temperatures were recorded at an interval of 5 minutes.

The arrangement of locating thermocouples for the two MHs is shown in Fig. 4.2, and their details are given in Table 4.3. All the thermocouples for measuring envelope surface temperatures were located at the center of each of the surfaces, and those for measuring air temperatures inside the two MHs at the center point of the two MHs.

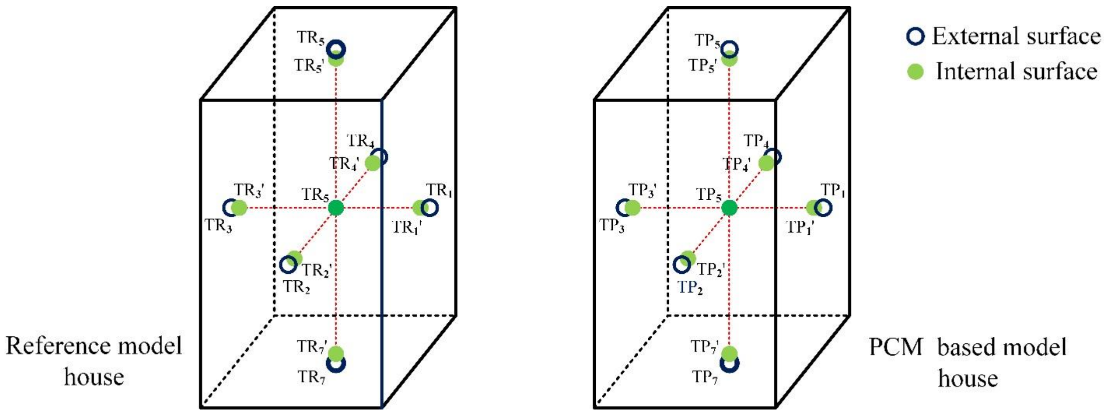

Fig. 4.2 The locations of T-type thermocouples in the two MHs

Table 4.3 Temperature measuring locations for the two MHs

Locations	Reference MH	PCM based MH
External surface of east wall	TR_1	TP_1
External surface of south wall	TR_2	TP_2
External surface of west wall	TR_3	TP_3
External surface of north wall	TR_4	TP_4
Internal surface of east wall	TR_1’	TP_1’
Internal surface of south wall	TR_2’	TP_2’
Internal surface of west wall	TR_3’	TP_3’
Internal surface of north wall	TR_4’	TP_4’
External surface of roof	TR_5	TP_5
Internal surface of roof	TR_5’	TP_5’
Indoor air	TR_6	TP_6
Internal surface of floor	TR_7’	TP_7’
External surface of floor	TR_7	TP_7

4.3 Design 2

The experimental results with Design 1, to be reported in Chapter 5, suggested that in summer time, the use of PCM in a PTH on a permanent basis was only good for improving the indoor thermal comfort at daytime, but counter-productive at nighttime. It was therefore considered necessary to apply PCM to PTHs on a movable basis. However, the two MHs were too small to install a movable PESS, and therefore Design

2 was implemented.

In Design 2, a full-scale experimental PTH, having a dimension of 5.6 m × 3.8 m × 2.7 m, with two 1.7 m × 0.9 m windows and one 2.0 m × 0.8 m door, was used, as shown in Fig. 4.3. The full-scale PTH was made of light-weight prefabricated insulation panels and wood. The details of envelope materials, and the physical and thermal properties of these materials are given in Table 4.4 and Table 4.5, respectively. This full-scale experimental PTH represented those typical conventional PTHs in the current Chinese market, in terms of both dimensions and envelope materials.

The full-scale experimental PTH was also placed on the flat roof of the same four-story building in the campus of Sichuan University, where the two MHs were previously placed. The flat roof was surrounded by a 1.5 m-high parapet, and there was a 7.5 m-high elevator shaft 2 m away from the south wall of the full-scale PTH.

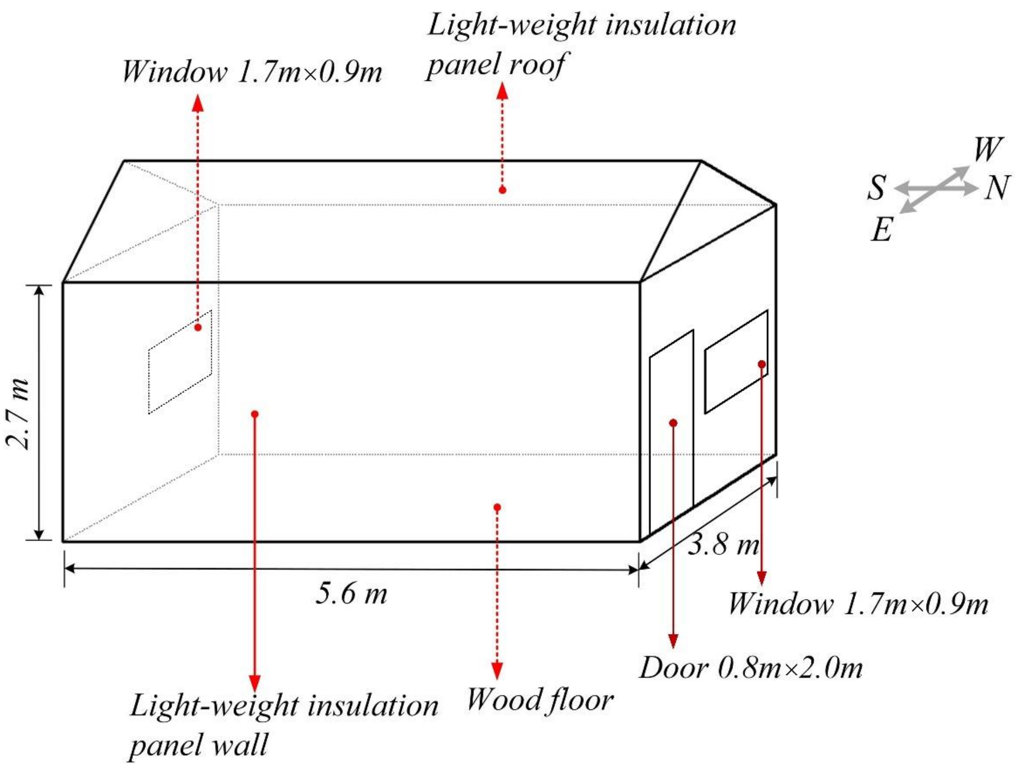

Fig. 4.3 3D-Illustration of the full-scale experimental PTH

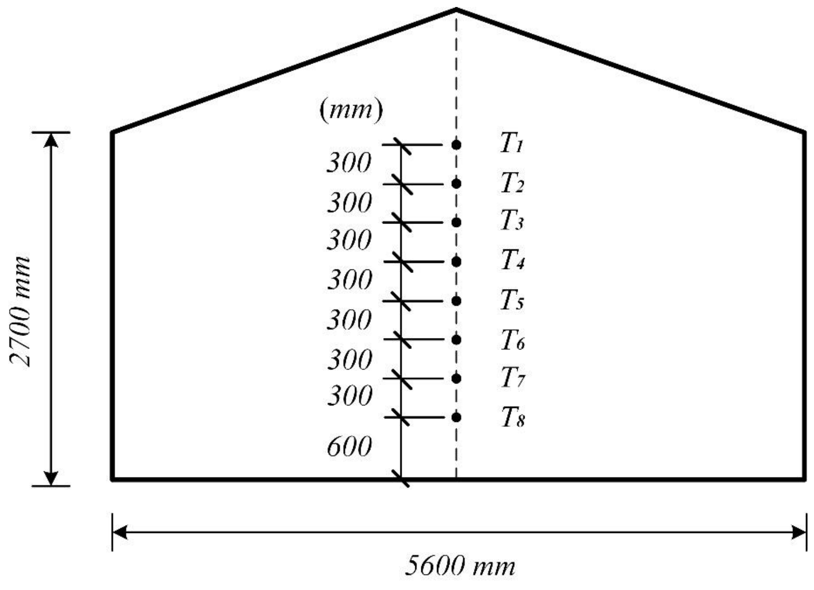

Fig. 4.4 The locations of T-type thermocouples inside the full-scale experimental PTH

Inside the full-scale PTH, eight thermocouples were placed and their locations are shown in Fig. 4.4. These eight thermocouples were located at the center of the full-scale PTH, with a distance of 300 mm between any two of them. The indoor air temperature (T_i) inside the full-scale experimental PTH was obtained by averaging the readings from the eight thermocouples. In addition, a thermocouple was also used to measure the outdoor air temperature (T_o).

Table 4.4 Materials of building envelope used in the full-scale experimental PTH

Building envelope	Materials
Roof and external wall	Steel
	EPS
Floor	Wood

Table 4.5 Physical and thermal properties of the materials used in the full-scale experimental PTH

Materials	Thickness (mm)	Thermal conductivity (W/m·K)	Density (kg/m^3)	Specific heat (J/kg·K)
Steel	0.5	45.28	8000	460
EPS	75	0.035	20	1100
Wood	13	0.15	521	1630

A movable PESS was specially made to be placed inside the full-scale experimental PTH. It consisted of (i) a supporting steel shelf, (ii) a plastic net-shape container for holding PCM-tubes and (iii) PCMs inside tubes. The physical and thermal properties of PCMs and the details of PESS are given in Table 4.6 and Table 4.7, respectively. Totally there were 1240 tubes which were horizontally tiled onto the plastic net-shape container. Inside each tube, 120 g PCM was filled. The container was suspended on the steel shelf, with variable distances from the west wall, as shown in Fig. 4.5. Such a configuration for the PESS would enable the largest possible heat transfer surface area between the PCMs and indoor air. Furthermore, since the solar heat gain by the west wall would be the highest in the afternoon, the PESS was therefore placed close to the west wall, as shown in Fig. 4.6. In addition, since the PESS was movable, experiments can be carried out with and without the PESS placed inside the full-scale PTH for comparison purposes.

Fig. 4.5 The movable PESS placed inside the full-scale experimental PTH

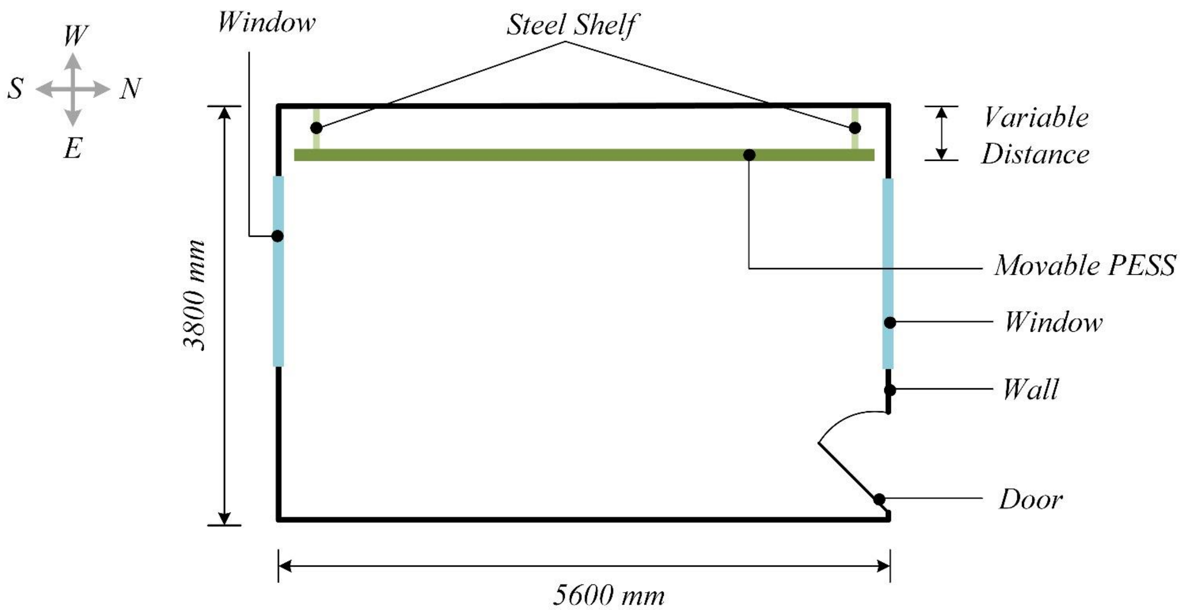

Fig. 4.6 Top view of the PESS placed inside the full-scale experimental PTH

Table 4.6 Physical and thermal properties of PCMs in the movable PESS

Physical and thermal properties	Values
Base material	Inorganic salts
Phase change temperature	18 - 26 °C
Operating temperature	0 - 60 °C
Latent heat	216 kJ/kg
Specific heat capacity	1785 J/(kg·K)
Thermal conductivity (solid)	0.5 W/(m·K)
Thermal conductivity (liquid)	0.25 W/(m·K)
Density at (16-28 °C)	1300 kg/m^3
Total enthalpy at 16-28 °C (heating)	50 kWh/m^3
Total enthalpy at 16-28 °C (cooling)	58 kWh/m^3
Encapsulation material	Aluminum composite membrane
Flammable	Nonflammable
Toxicity	Non-toxic

Table 4.7 Details of the movable PESS

Parameters	Values
Parameters of phase change material tube	
Weight of one PCM tube	120 g
Length of one PCM tube	175 mm
Width of one PCM tube	35 mm
Thickness of PCM tube	20 mm
Total PCM tubes in PESS	1240
Dimensions of PCMs energy storage system (PESS)	
Length of PESS	5500 mm
Height of PESS	2700 mm
Thickness of PESS	20 mm

4.4 Conclusions

Experimental setups for the two designs of applying PCMs to disaster-relief PTHs were established to facilitate carrying out all the experimental part of the programmed research work. The two MHs and full-scale experimental PTH were fully instrumented for measuring all the operating parameters. The availability of the experimental setups was expected to be essential in experimentally evaluating the thermal environment inside PTHs, and in establishing and validating a numerical model for the full-scale PTH.

Chapter 5

An experimental study on applying PCMs to disaster-relief PTHs for improving their internal thermal environments in summer

5.1 Introduction

With the availability of the experimental setups of the two designs of applying PCM to disaster-relief PTHs, as described in Chapter 4, an experimental study on applying PCMs to disaster-relief PTHs for improving their indoor thermal environments in summer has been carried out and the study results are presented in this Chapter. The experimental MHs shown in Fig. 4.1, the experimental full-scale PTH shown in Fig. 4.3, and the movable PESS shown in Fig. 4.5 were used in the experimental study. In this Chapter, firstly, the experimental results for the two designs are reported. Secondly, discussions on the research approach, the energy sources for charging PCMs, a comparison between the two Designs, the amount of PCM used and a proposed practical design of a PESS for future PTHs are presented. Finally, a conclusion is given.

5.2 Experimental results

5.2.1 Experimental results of Design 1

Experiments using the two MHs in Design 1 were carried out in the summer for three days starting from 12 June and ending 14 June, 2014. During the three-day periods, the measured outdoor air temperature (T_o) varied from 17 ^oC to 30.5 ^oC, and the air temperatures inside the two MHs were continuously monitored. Also during the experiments, the PCM based MH was not provided with any measure to charge its PCM, so that the only source for charging the PCM was the outdoor air at a lower temperature at nighttime.

In Fig. 5.1, the measured outdoor air temperature, the measured air temperatures inside the reference MH and the PCM based MH during the three days are profiled. As seen from Fig. 5.1, during the three days, the air temperature inside the reference MH (TR_6) varied from 17.5 ^oC to 37.5 ^oC. Clearly, there was a synchronization in the variation patterns of the outdoor air temperature and the air temperature inside the reference MH. Actually, due to the greenhouse effect and no ventilation, the air temperature inside the reference MH could be much higher than outdoor air temperature. For example, when the highest outdoor air temperature was 30.5 ^oC on the sunny day of 12 June, the indoor air temperature was at 37.5 ^oC due to greenhouse effect, much higher than outdoor air temperature. Hence, indoor air temperature in the reference MH was intolerably high [Wang et al., 2016c] throughout most of the daytime on that day. However, on the cloudy day of 14 June, as solar radiation was weaker and outdoor air temperature lower, the highest indoor air temperature was also lower than that on Day 1, 12 June, but still higher than comfort air temperature, at 30.5 ^{o}C. Furthermore, the air temperature inside the reference MH at nighttime on the three days was only slightly higher than outdoor air temperature.

However, as also seen in Fig. 5.1, the air temperature inside the PCM based MH (TP_6) exhibited a variation profile which was significantly different from that inside the reference MH. Firstly, TP_6 was always lower than TR_6 at daytime, and even lower than T_o in the afternoon, during the three days. This was considered due to the effect of the discharged cooling energy from the PCM which was charged with cooling energy during nighttime. Secondly, TP_6 was actually higher than both TR_6 and T_o during nighttime over the three days. This suggested that while the PCM absorbed heat at daytime to achieve a lower indoor air temperature, the absorbed heat was discharged at nighttime, leading to a higher TP_6.

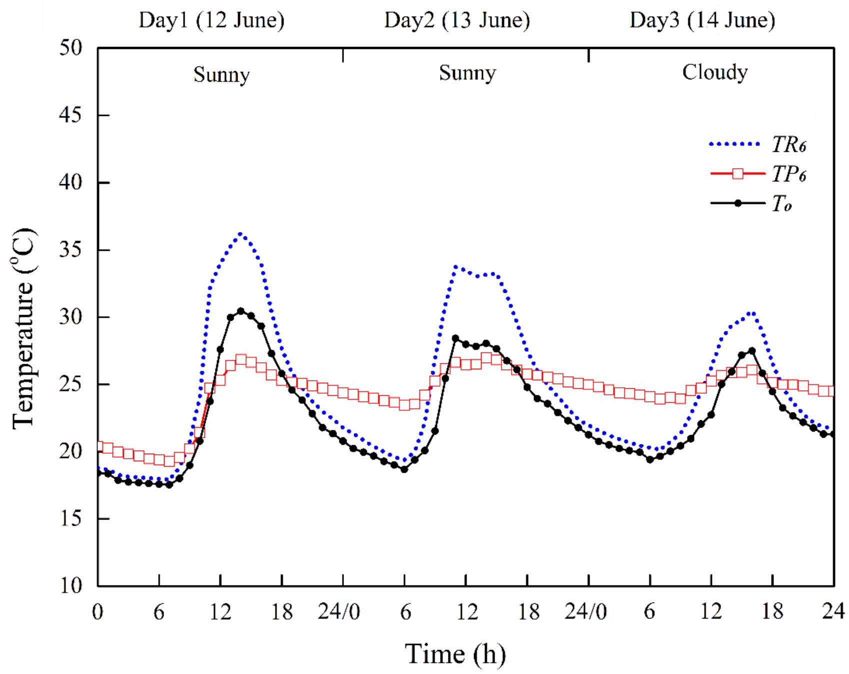

Fig. 5.1 Measured outdoor air temperature, air temperatures inside the reference MH and the PCM based MH

For evaluating the thermal conditions inside the two MHs, an index of TD_{ia} was used, which was defined as the temperature difference between the upper limit of tolerable air temperature inside a MH of 29 °C [Wang et al., 2016c] and the air temperature inside a MH. Hence TD_{ia_r} was for the temperature difference in the reference MH, and TD_{ia_p} that in the PCM based MH. A positive TD_{ia} suggested an acceptable indoor thermal environment, and vice versa. From Fig. 5.2, it can be seen that while TD_{ia_p} values remained positive throughout the three days, negative TD_{ia_r} values were present at 37% of the three days duration, mostly in the afternoons. This suggested that the use of PCM inside PTHs can help significantly improve the indoor thermal environment.

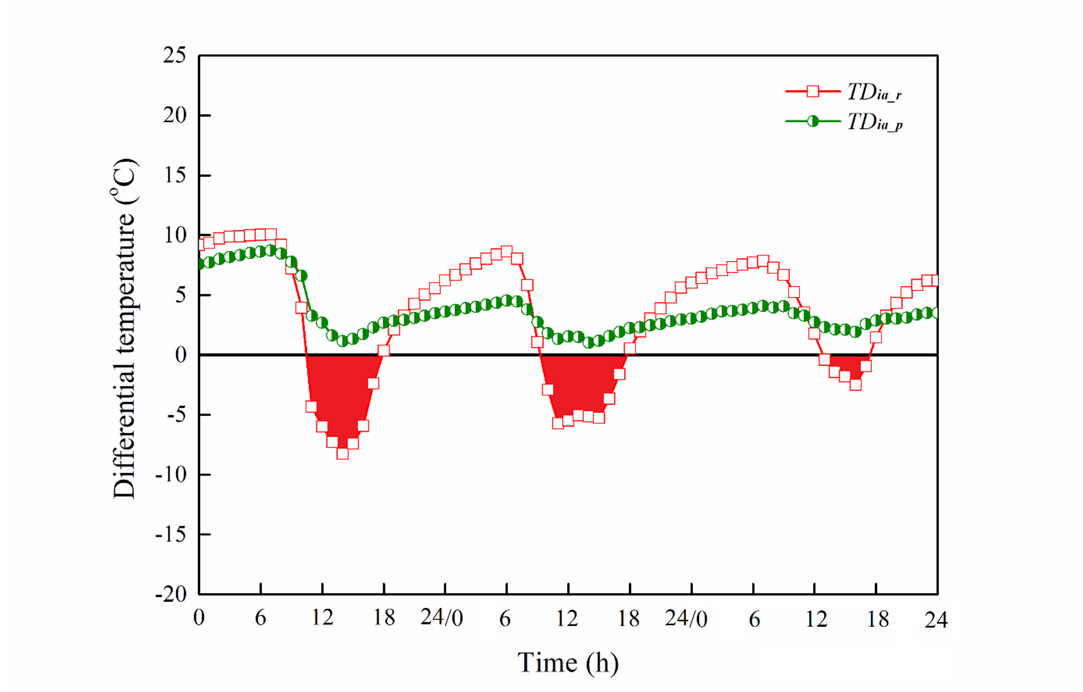

Fig. 5.2 The comparison between the TD_{ia} for the reference MH and that for the PCM based MH

Furthermore, the temperatures of the internal surfaces of both MHs were also measured during the three days period and the selected measured results for the roof and west wall are shown in Fig. 5.3 and Fig. 5.4, respectively. Fig. 5.3 shows the measured internal surface temperatures of roofs for both the reference MH (TR_5') and the PCM based MH (TP_5'). As seen, at the daytime of the three days, TP_5' was always lower than TR_5', and the largest difference between the two was in the afternoon during the three days. The highest TR_5' was at 41 °C, but the highest TP_5' was only at 31.5 °C on 12, June. Nonetheless, similar to the air temperature inside both MHs, TP_5' was always higher than TR_5' at nighttime, as PCM discharged the heat absorbed at daytime. Furthermore, Fig. 5.4 shows the measured internal surface temperatures of west walls for both the reference MH (*TR_3*') and the PCM based MH (*TP_3*'). Similar to those shown in Fig. 5.3, as seen in Fig. 5.4, *TP_3*' was lower than *TR_3*' at daytime, and the difference between the two was increased in the afternoons of the three days. The highest of *TR_3*' was at 39.5 ^{o}C, but the highest of *TP_3*' was only at 29 ^{o}C on 12, June. However, at nighttime *TP_3*' was also always higher than *TR_3*'.

Therefore, from the results shown in Fig. 5.3 and Fig. 5.4, it can be seen that the use of PCMs in the PCM based MH can also help remarkably reduce its internal surface temperatures at daytime, which would consequently lead to a lower internal radiant temperature. A lower internal radiant temperature was certainly beneficial to achieving a more thermally comfortable environment [Wang et al., 2018]. Nonetheless, a higher internal surface temperature at nighttime was counter-productive to a better internal thermal environment.

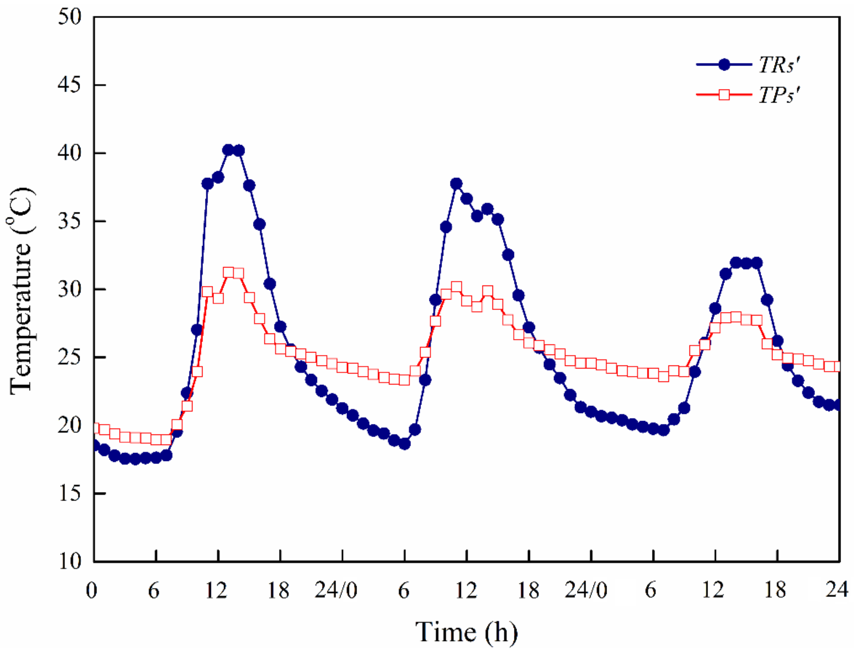

Fig. 5.3 Measured internal surface temperatures of the roofs of the reference MH and the PCM based MH

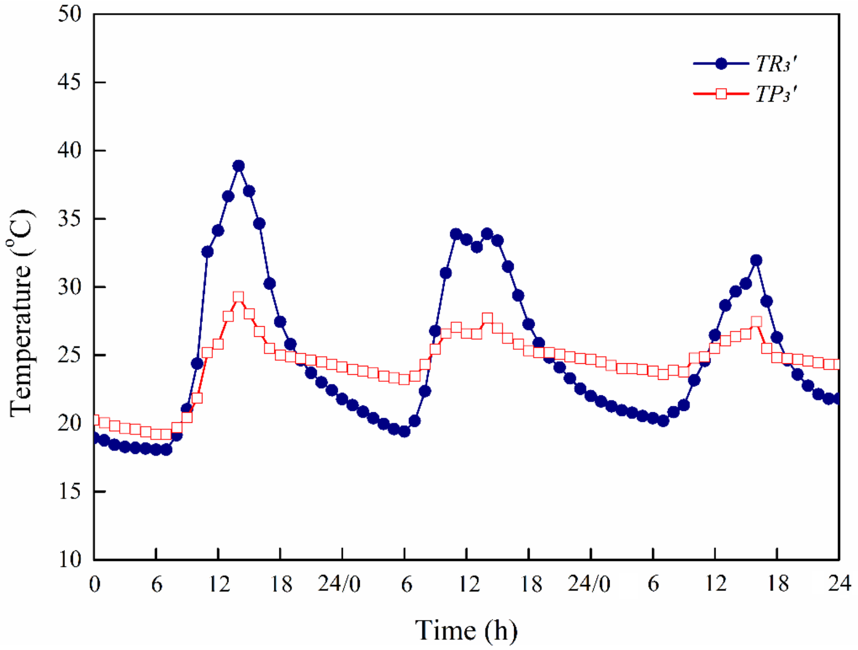

Fig. 5.4 Measured internal surface temperatures of the west walls of the reference MH and the PCM based MH

5.2.2 Experimental results of Design 2

Experiments using the full-scale PTH in Design 2 were carried out in the summer time of August and September, 2016, with two stages. In Stage One, the movable PESS was not placed inside the full-scale PTH, and in Stage Two, the movable PESS was placed inside for experimental purpose. Also in Stage Two, a room air conditioner was added to the full-scale experimental PTH and turned on at nighttime from 20:00 on the day prior to experiments to 8:00 on the day of experiments, so as to charge the movable PESS for releasing the charged cooling energy at daytime for experimental purpose. During all experiments, doors and windows were closed with the windows further covered by sunshades, and there was no mechanical ventilation provided.

The measured indoor and outdoor air temperatures on the selected days in the two stages are shown in Fig. 5.5 and Fig. 5.6, respectively. In Fig. 5.5, the measured outdoor air temperature and average indoor air temperature in Stage One, T_o and T_i, on a sunny day, and those in Stage Two, T_o' and T_i', on another sunny day, are shown. As seen, although on two different days, T_o and T_o' had similar hourly variation trends, with the starting and ending temperatures at around 26 ^oC and 32 ^oC, and the lowest and the highest temperatures at around 25 ^oC and 38 ^oC, respectively. For both days, the daily average outdoor air temperatures were at around 31 ^oC. On the other hand, the air temperature inside the full-scale experimental PTH in Stage One, T_i, was always higher than T_o, with the highest value of 42.5 °C at 13:00. However, in Stage Two, the air temperature inside the PTH from 0:00 to 8:00 was less than 20 °C due the operation of the air conditioner. As the air conditioner was turned off at 8:00, indoor air temperature, T_i, started to increase, and reached the highest at 38.1 °C, also at around 13:00. However, T_i' was consistently lower than T_i, at daytime, mainly due to the discharged cooling energy from the movable PESS. In addition, the average air temperature inside the full-scale experimental PTH from 10:00 to 20:00 in Stage One was 3.2 °C higher than that in Stage Two. Furthermore, at 20:30, T_i' started to over pass T_i, but the difference between T_i' and T_i was not as large as that in Design 1, due possibly to the difference in the amount of the cooling energy stored.

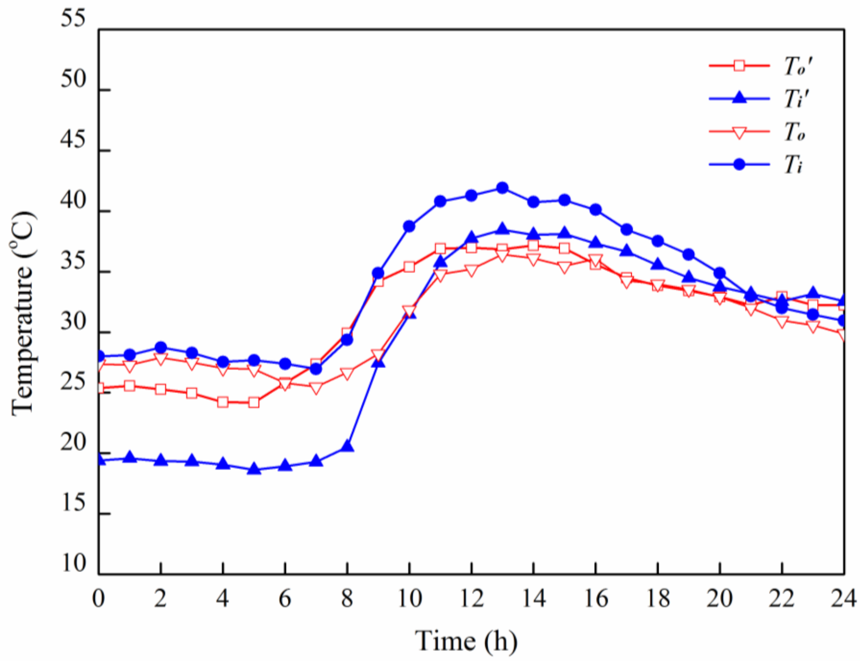

Fig. 5.5 Comparisons of indoor and outdoor air temperatures in selected sunny days

In Fig. 5.6, the measured T_o and T_i in Stage One on a cloudy day, and the measured T_o' and T_i' in Stage Two, also on another cloudy day, are shown. As seen, although on two different days, T_o and T_o' had similar hourly variation trends, with the starting and ending temperatures at around 26 ^{o}C and 29 ^{o}C, and the lowest and the highest temperatures at around 25 ^{o}C and 32 ^{o}C, respectively. The daily average outdoor air temperatures were at around 27.6 ^{o}C on both days. On the other hand, in Stage One, since there was no direct solar heat gain, the air temperature inside the full-scale experimental PTH, T_i, was not as high as that on a sunny day, but stayed higher than T_o from 24:00 onwards. In Stage Two, after the air conditioner was turned off at 8:00, indoor air temperature, T_i', started to increase, but unlike that in Stage One, stayed consistently lower than T_i after 24:00 to the end of the day. This was because the experiment was carried out on a cloudy day and the cooling loads were smaller than those in Stage One. However, the cooling energy provided by the air conditioner to charge the PESS was the same on both days, so that there was an adequate amount of cooling energy to maintain a lower T_i' to the end of the experimental day. In addition, the average air temperature inside the full-scale experimental PTH from 10:00 to 20:00 in Stage One was 3.6 ^{o}C higher than that in Stage Two.

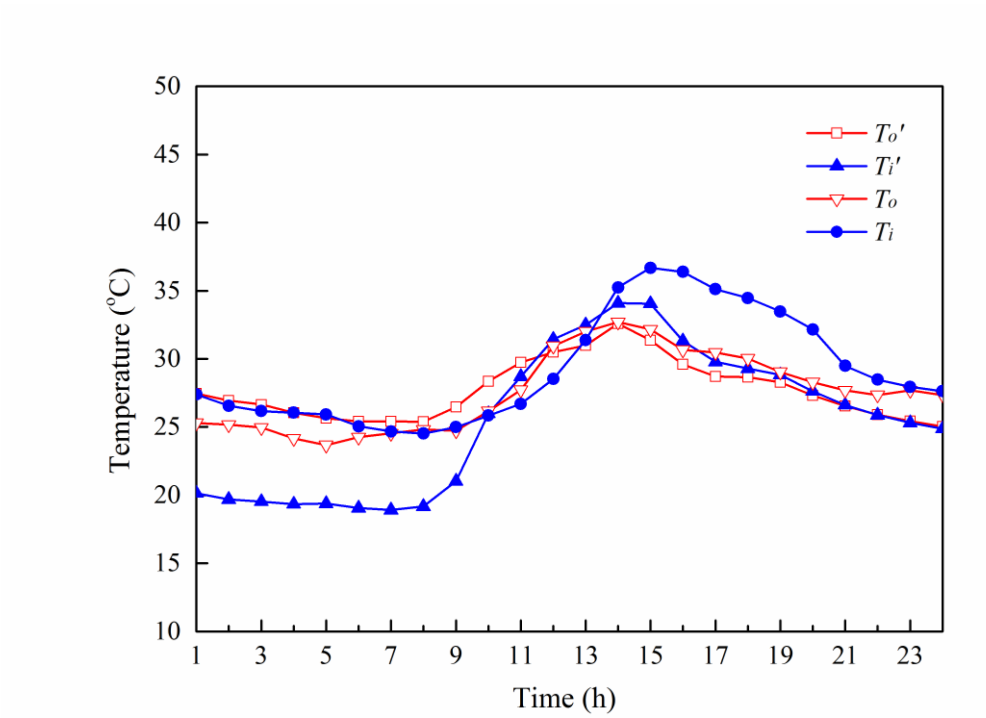

Fig. 5.6 Comparisons of indoor and outdoor air temperatures in selected cloudy days

Therefore, as seen from Fig. 5.5 and Fig. 5.6, the use of the movable PESS helped lower the air temperatures inside the full-scale experimental PTH at daytime on both a sunny day and a cloudy day, thus providing an improved thermal environment inside the full-scale experimental PTH in summer.

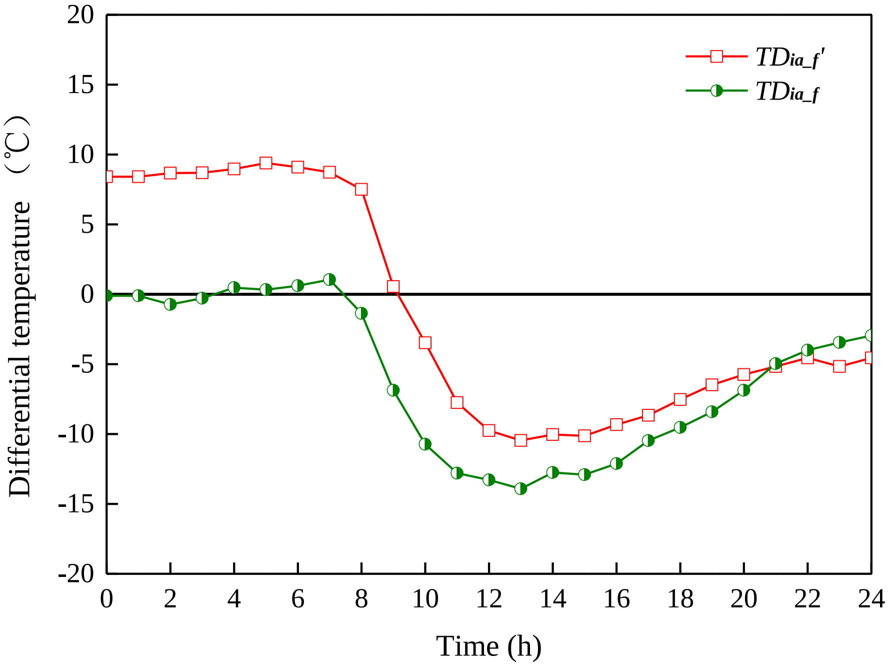

Fig. 5.7 The comparison between the *TDia* for the full-scale experimental PTH with and without PESS in the selected sunny days

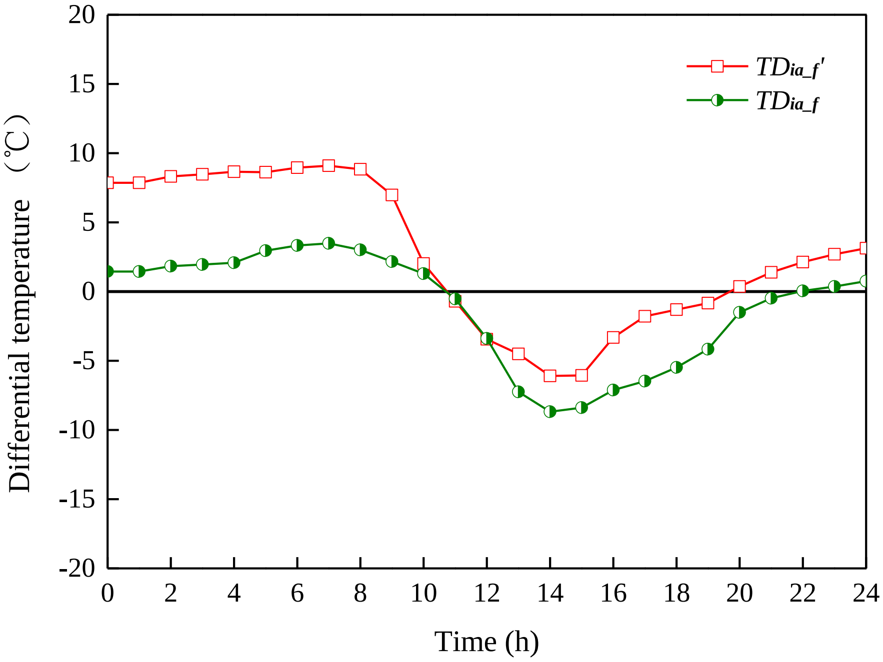

Fig. 5.8 The comparison between the *TDia* for the full-scale experimental PTH with and without PESS in the selected cloudy days

For evaluating the thermal conditions inside the full-scale PTH, similar to those for the MH based experiments reported in Section 5.2.1, the index of TD_{ia} was also used. Hence TD_{ia_f} ' was for the temperature difference in the full-scale PTH with the movable PESS, and TD_{ia_f} in the full-scale PTH without the movable PESS. Fig. 5.7 and Fig. 5.8 show the TD_{ia} values for the full-scale PTH on the selected sunny days and cloudy days, respectively. From Fig. 5.7, it can be seen that the total area for the negative TD_{ia_f} values was larger than that for TD_{ia_f}' from 10:00 to 20:00 in sunny days. In Fig. 5.8, it also can be seen that the total area for the negative of TD_{ia_f} values was also larger than that for TD_{ia_f} ' from 10:00 to 20:00 in cloudy days. These also suggested that the use of PCM helped improve the thermal environment inside the full-scale PTH.

5.3 Discussions

In Section 5.2, the experimental results for the two Designs of applying PCMs to disaster-relief PTHs for improving their internal thermal environments in summer are reported. Although the results demonstrated that the use of PCM based thermal energy storage in PTHs can, to a certain extent, help improve the thermal environments inside both the PCM based MH and the full-scale PTH, a number of related issues should be carefully considered, as follows.

5.3.1 The research approach

In this study, two different Designs for applying PCMs to PTHs were considered. In Design 1, two MHs were used, with 2.5 kg PCMs applying to one of the MHs. In Design 2, a full-scale PTH was used, using 148.8 kg PCMs. Although the sizes of the PTHs and the amounts of the PCMs used in the two Designs were different, the ratio of the amount of the PCMs used in Design 1 to that in Design 2 was the same as the ratio of the space volume in Design 1 to that in Design 2. Furthermore, the experiments with the two designs were not carried out at the same time, with that for Design 1 undertaken first. The study results for Design 1 suggested that the use of PCMs could help improve the thermal comfort level in disaster-relief PTHs effectively at daytime. At nighttime, the experimental results, however, demonstrated that the air temperature inside the PCM based MH was 3 ^{o}C higher than that in the reference MH. Hence, the design of a movable PESS, or Design 2, was proposed and implemented. The experimental results for Design 2 demonstrated that the movable PESS may be effectively used to help eliminate the negative effect of the PCMs inside PTHs at nighttime and could also be practically applied to PTHs used for future disaster-relief reconstructions.

5.3.2 Energy sources for charging PCMs

In the current experiments with the full-scale PTH in Design 2, an air conditioner was used to provide cooling energy to charge the PCM at nighttime. The air conditioner was turned on from 20:00 on the day prior to experiments for 12 hours. Such an arrangement was purely for the purpose of the current experimental work. However, in Design 1, there were no additional measures of providing cooling source for charging the PCM. Hence, it became essential that a suitable source of cooling energy for charging the PCM should be made available. One of potential energy sources was due to the diurnal change in outdoor air temperature. For instance, in Qinghai Province, Tibet Autonomous Region and Xinjiang Uygur Autonomous Region of western China, in summer, the outdoor air temperature difference between day and night is on average at 12 ^{o}C. For certain locations such as Yinchuan and Kashi, the days whose nighttime temperature of lower than 16 ^{o}C and daytime temperature of greater than 29 ^{o}C account for 87% of the total number of days in summer [22]. In the current study, when carrying out experiments with the MHs in Design 1, there were no additional measures for providing cooling sources for charging the PCM. However, the diurnal changes in outdoor air temperature in June in Chengdu city were large, with the lowest outdoor air temperature at 17 ^{o}C, so that certain cooling energy from outdoor air at nighttime was available for charging the PCM.

It may be however argued that in certain places with a large outdoor air temperature difference between daytime and nighttime, the use of nighttime ventilation may help improve the thermal comfort inside PTHs during nighttime and provide cooling energy to charge those permanently installed PCMs. However, the use of nighttime ventilation may actually have the following disadvantages: a) additional fan energy consumption is required; b) with PCM placed indoor, the amount of cooling energy charged can be less than placed outdoor since indoor air temperature and the temperatures of internal surfaces of a PTH may be higher; c) it is not possible to use the additional cooling energy due to sky radiation at nighttime to charge PCMs if placed indoor with nighttime ventilation. Furthermore, if outdoor air temperature is very low, while directly using nighttime ventilation may effectively charge the PCMs placed indoor, it may also cause thermal discomfort for PTHs' occupants at nighttime.

5.3.3 Comparison between the two Designs

In this experimental study, two different designs of applying PCMs were experimentally evaluated. In Design 1, a PCM layer of 20 mm thick was fixed to the internal surfaces of the PCM based MH. Since the PCM layer was at a fixed place, while it can be charged with cooling energy at nighttime, it can also be charged with heat energy at daytime, in particular in the afternoons, so that the resulted air temperatures and internal surface temperature inside the PCM based MH at nighttime during the experimental period (except the indoor air temperature on the first night) were both higher than those in the reference MH. Since PCM was fixed indoor, at a higher indoor air temperature at nighttime, it can only absorb less cooling energy to be discharged at daytime for lowering down indoor air temperature. This may hence be seen as an inadequacy in Design 1. However, in Design 2, the PESS was designed as being movable. Therefore, it can be moved from indoor to outdoor, so that the PCM after absorbing the heat in the afternoons can release heat to colder outdoor air at nighttime. Consequently, both a lower indoor air temperature may be resulted in and more cooling energy can be charged to the PCM at a lower outdoor air temperature. Hence, a movable PESS should be preferred when applying PCMs to disaster-relief PTHs for improving their indoor thermal environments in summer.

5.3.4 The amount of PCM used

It is obvious that the more PCM is used, the greater improvement in indoor thermal environment can be expected. In the current experiments using the full-scale PTH in Design 2, a total of 148.8 kg PCM was used and helped reduce averaged daytime indoor air temperature from 10:00 to 20:00 from 39.3 ^{o}C in Stage One to 36.1 ^{o}C in Stage Two on sunny days, and from 33.7 ^{o}C to 30.1 ^{o}C on cloudy days. In order to achieve an improvement in the thermal environments inside PTHs, proper sizing of the movable PESS should be carefully carried out, taking into account a number of factors such as locations and climates, thermal loads in PTHs, thermal properties of PCM, etc.

On the other hand, the amount of PCM used would affect the cost of applying PESS to PTHs. In the current experiments using the full-scale PTH, the total cost of the movable PESS with 148.8 kg PCMs was at RMB 1200, which was 11.6 % of the cost for a full-scale PTH. However, the cost of the actual application can be remarkably lower if PESSs were massively produced. Furthermore, the cost of a PESS appeared comparable to that of an electrical driven basic room air conditioner. However, using room air conditioners was not possible for disaster-relief PTHs, as usually there would only be limited essential power supply for disaster relief over a long period of time.

5.3.5 A proposed practical design of a PESS for future PTHs

From the experimental results presented in this Chapter, it was clear that the use of the movable PESS could improve the thermal environment inside the PTHs. However, the practical design of a movable PESS in a future disaster-relief temporary house will be certainly a key issue for its future wide application. One of the practical designs can be that PCMs may be attached to the envelopes of a PTH during its prefabrication. The envelopes with PCMs attached may be divided into several pieces and each piece can be rotated along its axis, thus providing a convenient way to move PCMs from indoor to outdoor, as shown schematically in Fig. 5.9. Such a movable PESS can be massively produced and conveniently used.

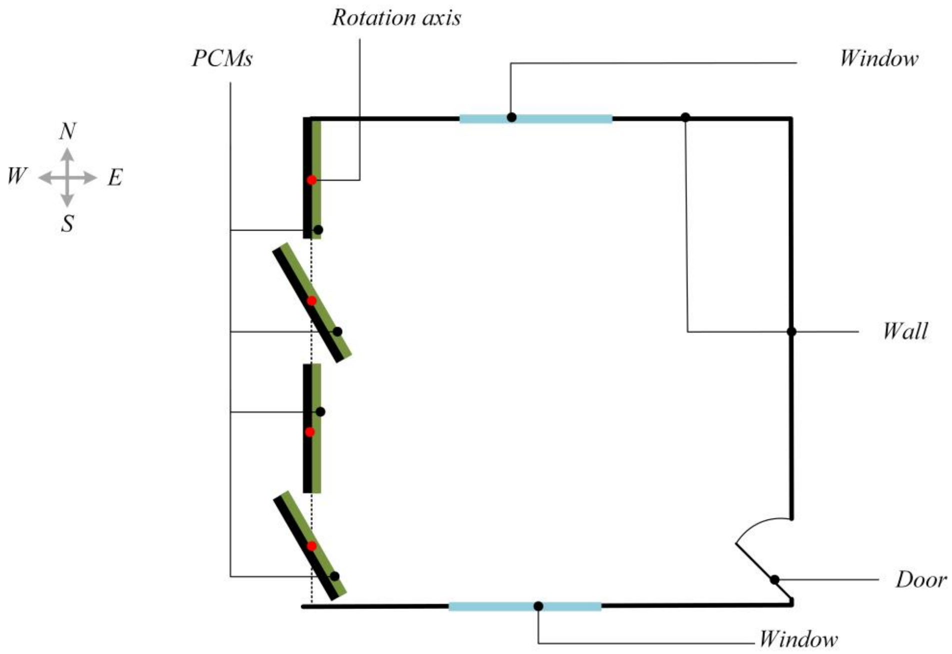

Fig. 5.9 A proposed practical design of a movable PESS for future PTHs

5.4 Conclusions

This Chapter reports an experimental study on applying PCMs to disaster-relief PTHs for improving their internal thermal environments in summer. Two different designs of applying PCMs to PTHs were examined. In Design 1, PCM was fixed to the internal surfaces of the PCM based MH, but a movable PESS was used in Design 2. The experimental results for Design 1 demonstrated that in summer, the use of PCM helped reduce not only indoor air temperature, but also internal surface temperature at daytime when solar radiation was present. In Design 2, the use of the movable PESS with a total charge of 148.8 kg PCM helped reduce average daytime indoor air temperature from 10:00 to 20:00 by 3.2 ^{o}C on sunny experimental days and by 3.6 ^{o}C on cloudy experimental days. The experimental results from both Designs demonstrated that the use of PCM can help improve the thermal environment inside PTHs at daytime in summer. However, the comparison between the two Designs suggested that, since outdoor air at a lower temperature at nighttime may be the only cooling energy source available for charging the PCM, using the movable PESS was preferred. This was because a movable system can be moved to outdoor at nighttime to absorb more cooling energy from outdoor air at a lower temperature, but at the same time not to lead to a relatively higher indoor air temperature.

Furthermore, the use of PCM in PTH was subject to the availability of cooling energy source for charging the PCM. Given the nature of disaster relief, it was not practical to use electrical-based means to charge the PCM. However, as demonstrated by the results of the comparison between the two Designs, due to the diurnal change in outdoor air temperature, outdoor air at a lower temperature at nighttime may potentially be used for charging the PCM. Furthermore, to achieve a suitable balance between the cost of a PESS and the level of thermal environment improvement inside a disaster-relief PTH, the PESS must be properly sized. Finally, a practical design of applying the movable PCMs to future disaster-relief PTHs was also proposed for the future wider application of the PCMs to disaster-relief PTHs.

The results of the experimental study presented in this Chapter demonstrated that applying PCMs to disaster-relief PTHs can help effectively improve their internal thermal environments in summer. However, the experimental study was based on a fixed design of applying PCMs to PTHs and fixed outdoor climates. Therefore, it was considered necessary to follow up the experimental study by carrying out numerical studies on optimizing designs and on applications to PTHs installed in locations with different climates. These numerical studies will be reported in Chapter 6 and 7, respectively.

Chapter 6

A numerical study on optimizing the designs of applying PCMs to a disaster-relief PTH to improve its summer daytime indoor thermal environment

6.1 Introduction

The experimental results reported in Chapter 5 demonstrated that the use of PCMs could help improve the thermal comfort in disaster-relief PTHs effectively at daytime in summer. Two different designs of applying PCMs to disaster relief PTHs for improving their internal thermal environments at daytime in summer were experimentally compared and a movable PESS was preferred due to its flexibility of utilizing cooling energy of both cold outdoor air and sky radiation at nighttime for discharging the stored heat absorbed from indoor air at daytime, when the PESS was moved to outdoors. However, as limited by the nature of an experimental study, only one fixed design for applying a PESS to PTHs with a fixed amount of PCM was experimentally examined. Hence, aiming at improving the thermal environment inside PTHs at daytime in summer using PCMs, it becomes highly necessary to optimize the designs of applying PCMs to disaster-relief PTHs.

To this end, as a follow-up to the previously reported experimental study reported in Chapter 5, a numerical study on optimizing the designs of applying PCMs to a full-scale PTH has been carried out and the study results are reported in this Chapter. In this Chapter, firstly, the development and experimental validation for a numerical model for a full-scale PTH using the well-known building energy simulation platform, EnergyPlus, are reported. Secondly, two parts of the numerical study, i.e., evaluating different designs of applying PCMs to the PTH and examining the effects of different amounts of PCM to be used, were carried out by using the validated model and the numerical study results from the two parts are presented. Finally, a conclusion is given.

6.2 Model development and validation

6.2.1 Model establishment

A simulation model for a full-scale PTH was established using the famous building thermal load and energy analysis simulation platform, EnergyPlus [Zhang et al., 2017b; Costanzo et al., 2016; Morakinyo et al., 2017; Karachaliou et al., 2016; Foustalieraki et al., 2017; Silva et al., 2016b; Zeng et al., 2017], which has been extensively used in indoor thermal environmental analysis and building energy efficiency evaluation. EnergyPlus could be used to evaluate the thermal loads and energy consumption of a building based on its physical configurations and details of HVAC installations, and can be applied to both conditioned and unconditioned buildings. In the current numerical study, the algorithm of CondFD in EnergyPlus was selected to simulate the heat transfer of PCM in the full-scale PTH. The temperature of PCM at each time interval could be calculated iteratively according to the first-order full implicit differential heat transfer method.

The model developed in this Chapter was based on the full-scale experimental PTH used in the experimental study reported in Chapter 5, as shown in Fig. 4.3. A movable PESS was placed near the west wall inside the full-scale experimental PTH, as shown in Fig. 4.6. In addition, since the PESS was movable, experiments can be carried out with and without the PESS placed inside the full-scale PTH for comparison purposes. The details of envelope materials, the physical and thermal properties of these envelope materials and the physical and thermo-physical parameters of the PCM used in the experimental study are given in Tables 4.4 - 4.6, respectively.

6.2.2 Model validation

The indoor air temperature and internal surface temperatures of four walls, roof and floor of the experimental PTH were measured for the purpose of model validation. As previously shown in Fig. 4.4, eight thermocouples were placed inside the experimental PTH. These eight thermocouples were located at the center of the full-scale PTH, with a distance of 300mm between any two of them. The indoor air temperature of the experimental PTH (T_i) was obtained by averaging the readings from the eight thermocouples. On the other hand, T-type thermocouples with an accuracy of ± 0.5 °C used to measure the internal surface temperatures of envelopes were located at the center of the internal surface of each envelope component.

In addition, the following weather parameters were recorded by a meteorological and weather station nearby: dry bulb air temperature, air dew point temperature, air relative humidity, atmospheric pressure, extra-terrestrial horizontal radiation, extra-terrestrial direct normal radiation, horizontal infrared radiation intensity from sky, global horizontal radiation, direct normal radiation, diffuse horizontal radiation, global horizontal illuminance, direct normal illuminance, diffuse horizontal illuminance, zenith luminance, wind direction, wind speed, total sky cover and opaque sky cover.

All the measuring instruments were calibrated before they were used in the experiments, and were connected to data loggers where all the measured parameters were recorded at an interval of 5 minutes. The measurements were taken in the summer months from June to September, 2016, to collect data for model validation.

The simulation model used in this numerical study was validated by the collected experimental data. As shown in Fig. 6.1 and Fig. 6.2, the simulated parameters of indoor air temperature, internal surface temperatures of the west wall, roof and floor of the experimental PTH, with and without the movable PESS placed inside the PTH, were compared with the measured ones.

Fig. 6.1 shows the comparisons between the measured and simulated indoor air temperatures, internal surface temperatures of west wall, roof and floor of the experimental PTH without the PESS placed inside during three selected days of the entire measurement period. As seen, both the measured and simulated indoor air temperatures, internal surface temperatures were increased at daytime, and decreased at nighttime. Good agreements between the measured and simulated temperatures were achieved.

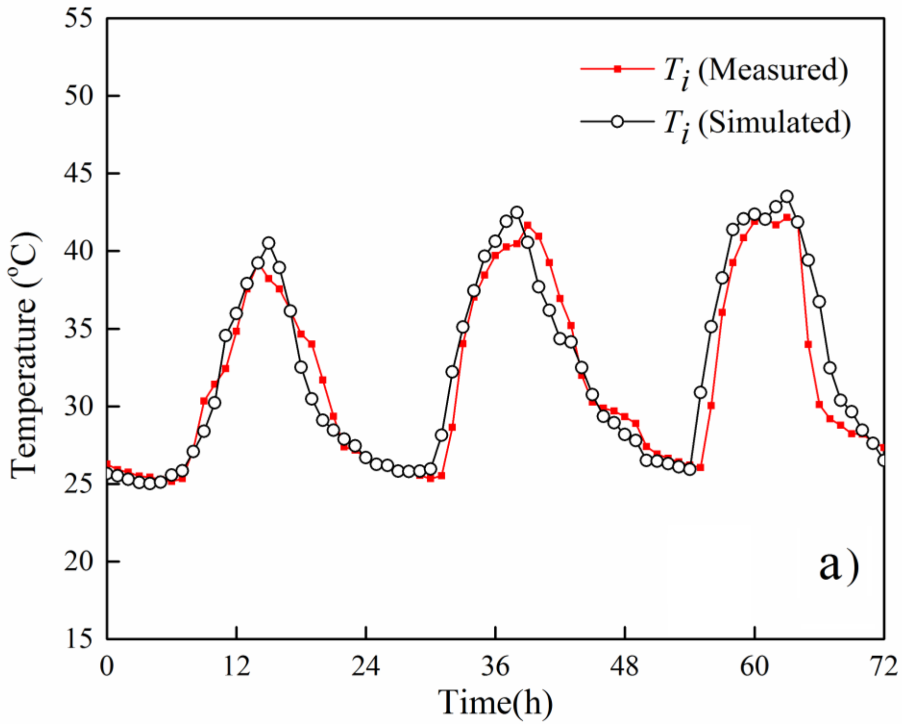

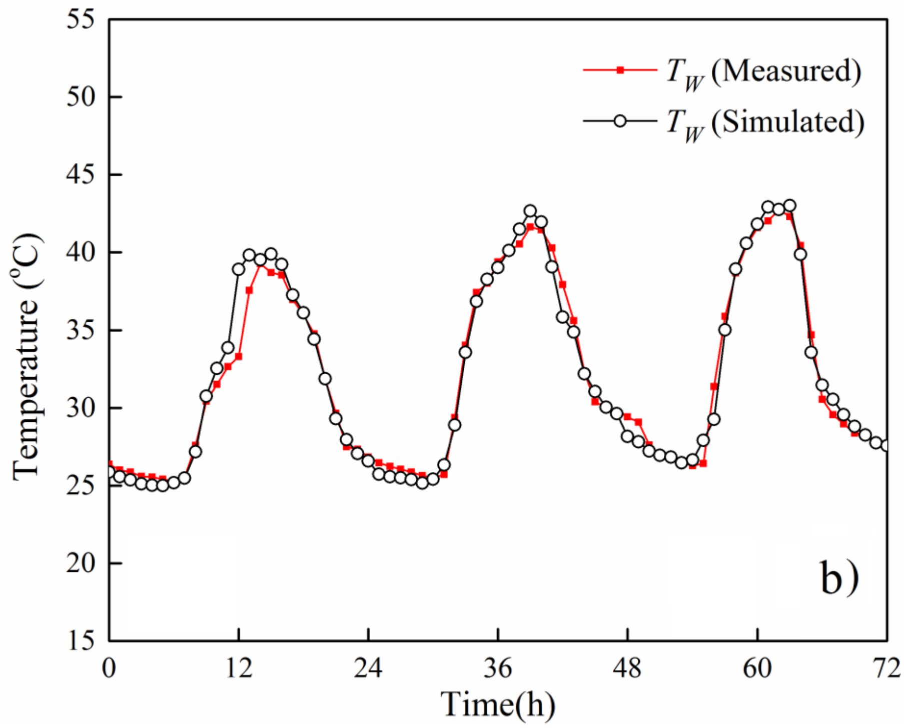
T_W (Measured)
T_W (Simulated)
Temperature (°C)
Time(h)
b)

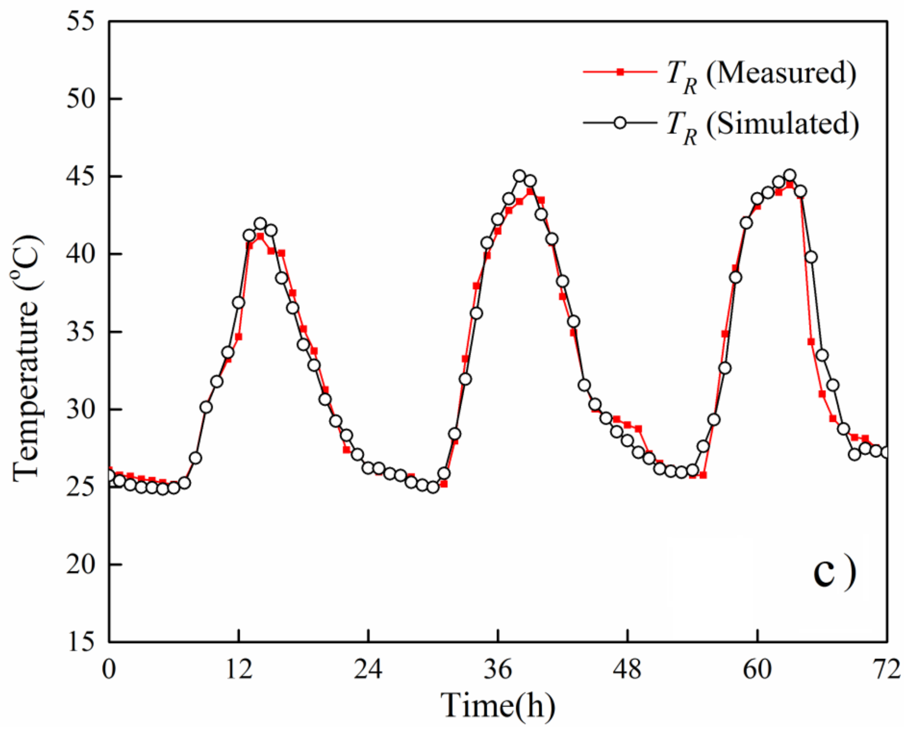
T_R (Measured)
T_R (Simulated)
Temperature (°C)
Time(h)
c)

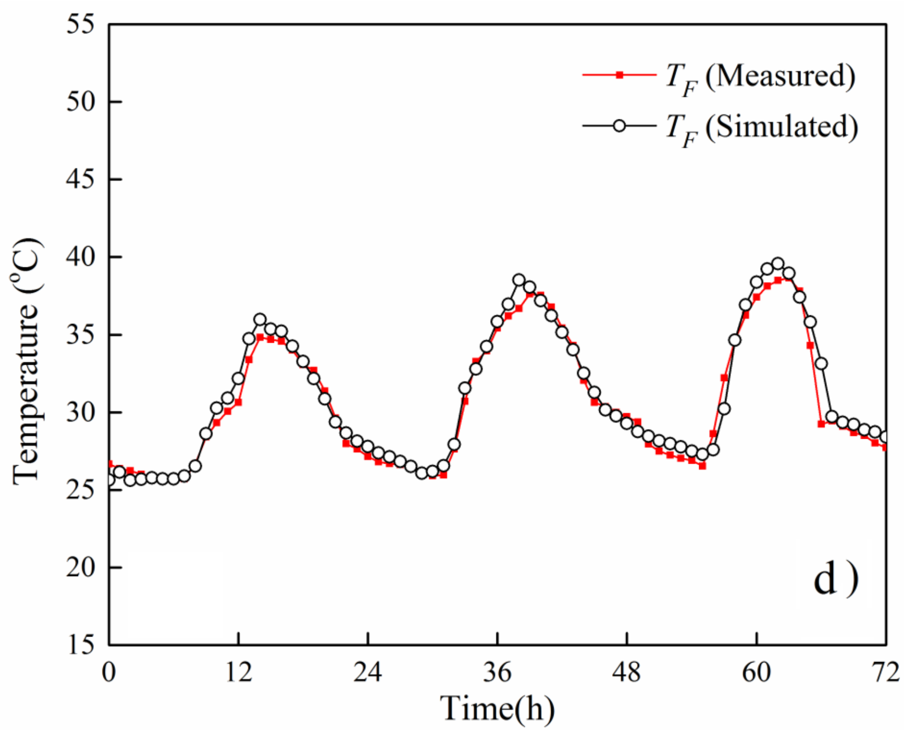

Fig. 6.1 Comparisons between the measured and simulated a) indoor air temperatures; b) internal surface temperatures of west wall; c) internal surface temperatures of roof; d) internal surface temperatures of floor inside the PTH, without the PESS placed inside

Fig. 6.2 shows the comparisons between the measured and simulated indoor air temperatures, internal surface temperatures for west wall, roof and floor of the experimental PTH with the movable PESS placed inside during another three days. The movable PESS were placed near the west wall inside the experimental PTH throughout the three days. As seen, both the measured and simulated indoor air temperatures, internal surface temperatures for west wall, roof and floor were also increased at daytime, and decreased at nighttime. Again, good agreements between the measured and simulated temperatures were also achieved.

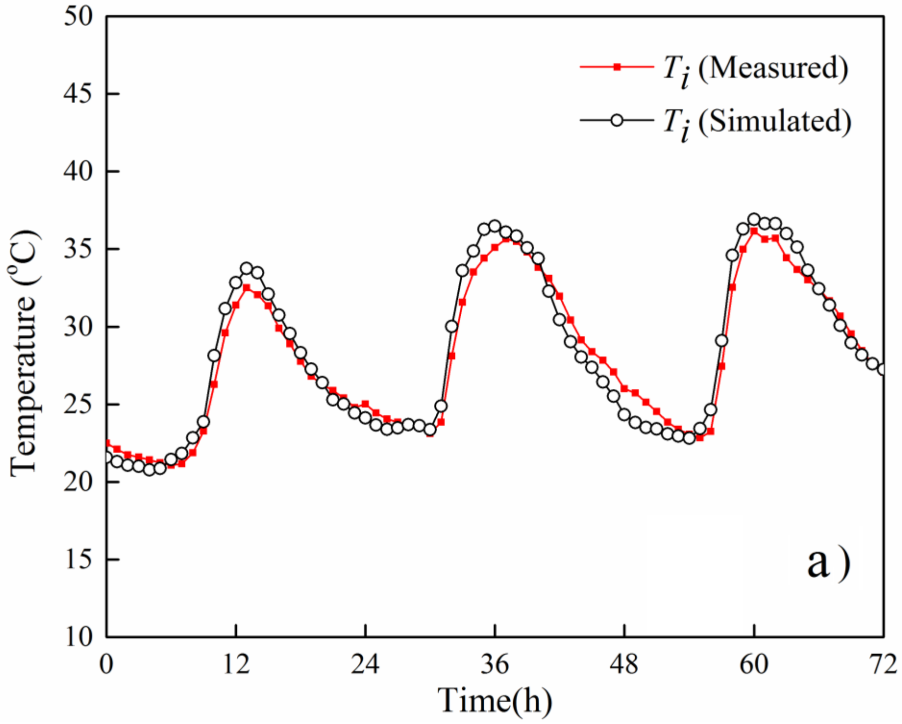

T_i (Measured)
T_i (Simulated)
a)
Temperature (°C)
Time(h)

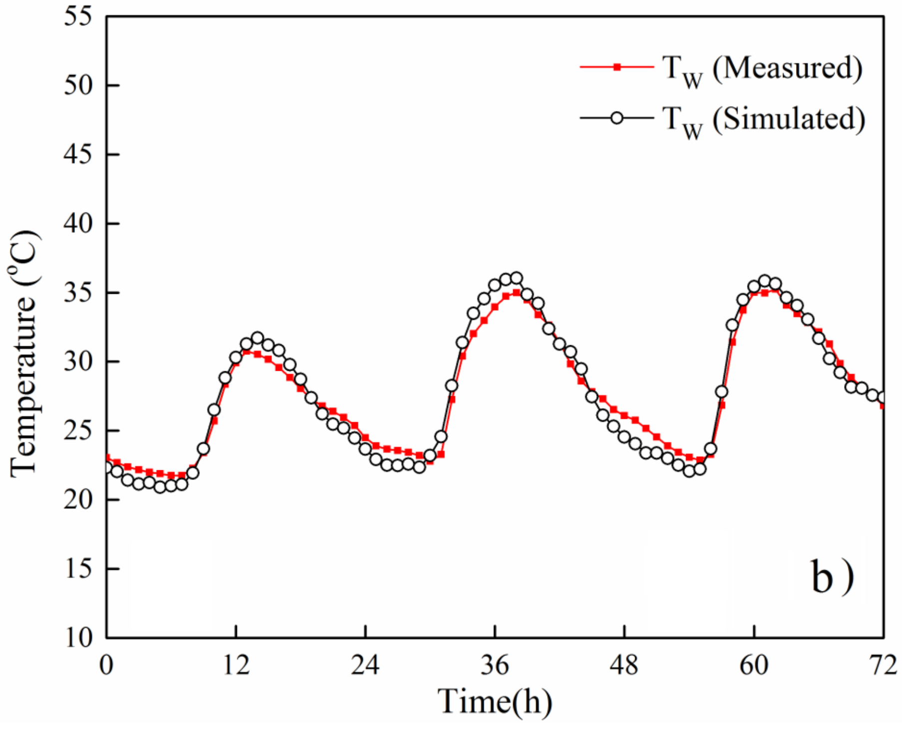

T_W (Measured)
T_W (Simulated)
b)
Temperature (°C)
Time(h)

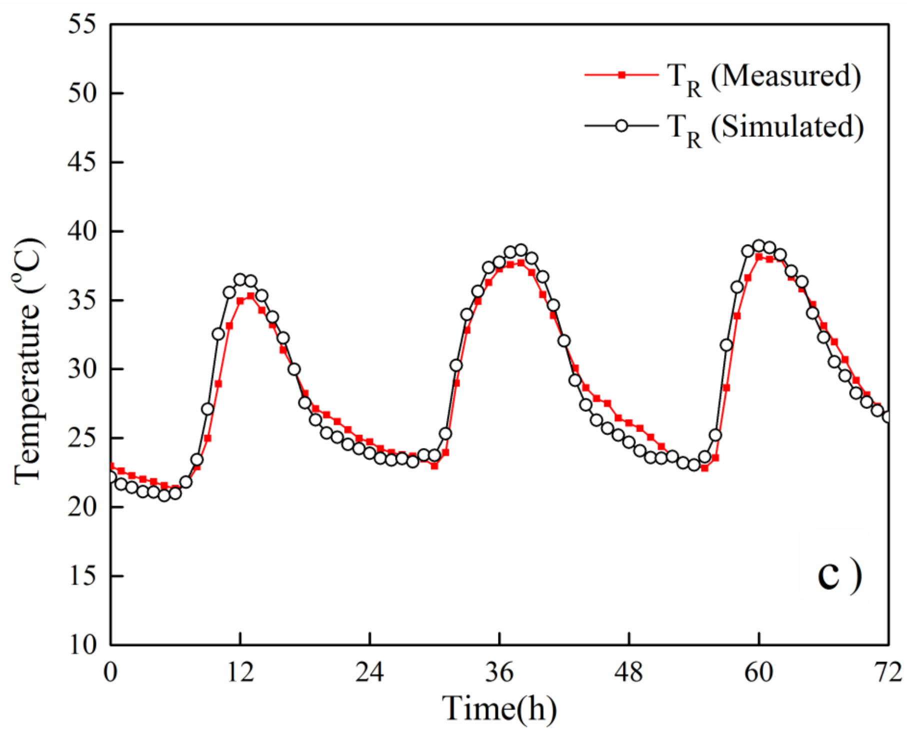

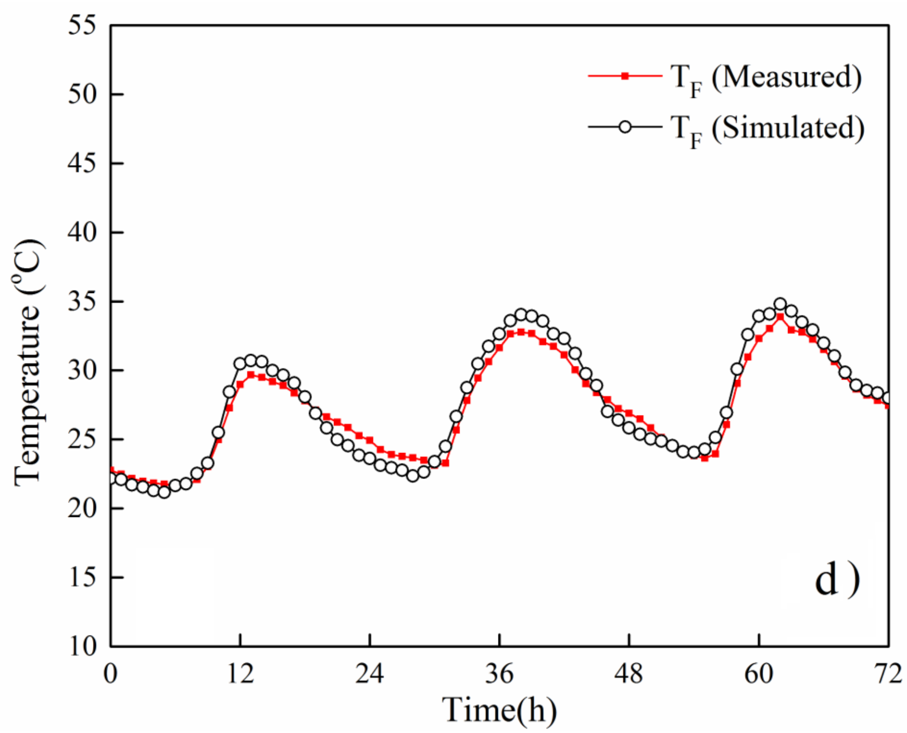

Fig. 6.2 Comparisons between the measured and simulated a) indoor air temperatures; b) internal surface temperatures of west wall; c) internal surface temperatures of roof; d) internal surface temperatures of floor inside the PTH, with the PESS placed inside

In addition, all the simulated and measured maximum and minimum indoor air and internal surface temperatures of the PTH's envelopes and their variation ranges are listed in Table 6.1 without, and Table 6.2 with the PESS placed inside the PTH, respectively.

Table 6.1 Simulated and measured maximum and minimum indoor air and internal surface temperatures and their variation ranges without the PESS placed inside the PTH

Measured	T_i	T_E	T_W	T_S	T_N	T_R	T_F
Maximum	42.17	42.73	42.75	43.52	43.23	44.45	38.65
Minimum	25.16	25.42	25.28	25.64	25.02	25.09	25.61
Variation range	17.01	17.31	17.47	17.88	18.21	19.35	13.04
Simulated	T_i	T_E	T_W	T_S	T_N	T_R	T_F
Maximum	43.51	43.12	43.01	43.16	43.92	45.08	39.57
Minimum	25.02	25.04	25.00	25.19	24.87	24.85	25.62
Variation range	18.49	18.08	18.01	17.97	19.05	20.23	13.95

Table 6.2 Simulated and measured maximum and minimum indoor air and internal surface temperatures and their variation ranges with the PESS placed inside the PTH

Measured	T_i	T_E	T_W	T_S	T_N	T_R	T_F
Maximum	36.17	36.12	36.05	36.63	36.28	38.13	33.88
Minimum	21.08	20.83	20.90	21.16	21.02	21.35	21.64
Variation	15.08	15.29	15.15	15.47	15.26	16.78	12.23
Simulated	T_i	T_E	T_W	T_S	T_N	T_R	T_F
Maximum	36.90	36.49	36.23	36.49	36.43	38.93	34.81
Minimum	20.77	20.85	20.75	20.44	20.51	20.83	21.17
Variation	16.13	15.64	15.48	16.05	15.92	18.10	13.64

As seen from Table 6.1 and Table 6.2, except for south wall, the simulated maximum internal surfaces temperatures for other envelops were all slightly higher than the measured values, and the simulated variation ranges were also all slightly higher than the measured ones. However, the differences between the simulated and measured were small.

In order to ensure the validation accuracy, two metrics: Root Mean Square Deviation (RMSD) and Coefficient of Variation ($CV_{(RMSD)}$), were employed. While RMSD measured the average spread of errors which provided a measure for model's dispersion [Inman et al., 2013], $CV_{(RMSD)}$ was the coefficient of variation in RMSD, as expressed by Eq. (6.1) and (6.2), respectively, as follows:

$$RMSD = \sqrt{\frac{1}{N}\sum_{t=1}^{N}(T_{Mt} - T_{St})^2} \tag{6.1}$$

$$CV_{(RMSD)} = \frac{RMSD}{\bar{y}} \tag{6.2}$$

Where T_{Mt} and T_{St} are the respective measured and simulated temperatures at each hour 't', ^{o}C, N the total number of hours, and $\bar{y}$ the average measured temperature during the entire measurement period, ^{o}C.

The RMSD and $CV_{(RMSD)}$ for indoor air temperature, and internal surface temperatures for all envelopes of the PTH, with and without the PESS placed inside were calculated and the calculated results are shown in Table 6.3. As seen, the highest RMSD value of 1.89 ^{o}C and $CV_{(RMSD)}$ value of 5.9% were for the air temperature inside the experimental PTH. The $CV_{(RMSD)}$ values were all less than 6%, suggesting that the model developed can be used to predict the thermal environment in terms of indoor air temperature and internal surface temperatures inside the PTH well, with an acceptable accuracy. Therefore, the model can be considered validated and may be used in the numerical study for both optimizing the designs of applying PCMs to a PTH and examining the amount of PCM to be used to improve its indoor daytime thermal environment in summer.

Table 6.3 Summary of RMSD and $CV_{(RMSD)}$, both with and without the movable PESS placed inside the PTH

Without the PESS placed inside the PTH							
Parameters	T_i	T_E	T_W	T_S	T_N	T_R	T_F
RMSD	1.89	0.99	1.07	1.12	1.25	1.10	0.90
$CV_{(RMSD)}$	5.9%	3.1%	3.4%	3.6%	4.0%	3.4%	2.9%
With the PESS placed inside the PTH							
Parameters	T_i	T_E	T_W	T_S	T_N	T_R	T_F
RMSD	1.04	0.91	0.91	0.97	1.03	1.17	0.92
$CV_{(RMSD)}$	3.7%	3.3%	3.2%	3.4%	3.5%	4.0%	3.3%

6.3 The numerical study

Using the validated model reported in Section 6.2, a numerical study on optimizing the designs of applying PCMs to, and examining the amount of PCM to be used in, a PTH located in Chengdu city, Sichuan Province, China, for improving its internal thermal environment at daytime in summer, has been carried out and the study results are presented in this Section.

6.3.1 Assumptions used in the numerical study

The period of simulation was from June to September, which is the representative period of summer in Chengdu, China, using the weather data of Chengdu City from the files for International Weather for Energy Calculation (IWEC) [ASHRAE, 2001]. Furthermore, the numerical study was carried out under the following assumptions:

- The PTH was occupied by 3 average adults (of 1.73 m tall, 70 kg, DuBois area = 1.8 m^2) [ASHRAE, 2013a];
- The activity level of the occupants was at 60 W/m^2 (1.0 met) [ASHRAE, 2013b];
- The thermos-physical properties of the PCM used were the same as those shown in Table 4.6;
- The PCM of 20 mm thickness was sandwiched by two 0.5 mm steel sheets as a PCM panel;
- The hourly internal heat gains from lighting and electric appliance remained constant at 100 W;
- The windows and door of the PTH remained closed throughout the simulation period.

The numerical study included two parts: 1) optimizing the designs of applying PCM to the PTH, and 2) examining the amount of PCM to be used. The study results for the two parts are presented in Sections 6.3.2 and 6.3.3, respectively.

6.3.2 Optimizing the designs of applying PCM to the PTH

In the experimental study reported in Chapter 5, only one fixed design for the PCM located near the indoor side of the PTH's west wall was examined. However, whether this design was the best remained to be examined when locating the PCM at different positions inside or outside the PTH. Hence, optimizing the designs of applying PCM at different positions inside and outside the PTH was numerically studied.

Therefore, various designs of locating the PCM in different positions relative to the PTH's envelopes were firstly defined. As shown, PCM was located on the outdoor side and the indoor side of the roof, as Position ①, ② and ③ in Fig. 6.3a, 6.3b and 6.3c, respectively. Furthermore, PCM was located on the outdoor side and the indoor side of a wall, as Position ④, ⑤ and ⑥, as shown in Fig. 6.4a, 6.4b and 6.4c, respectively. Consequently, a total of sixteen different designs for locating the PCM at different positions, i.e., D1 to D16, were hence defined, as detailed in Table 6.4.

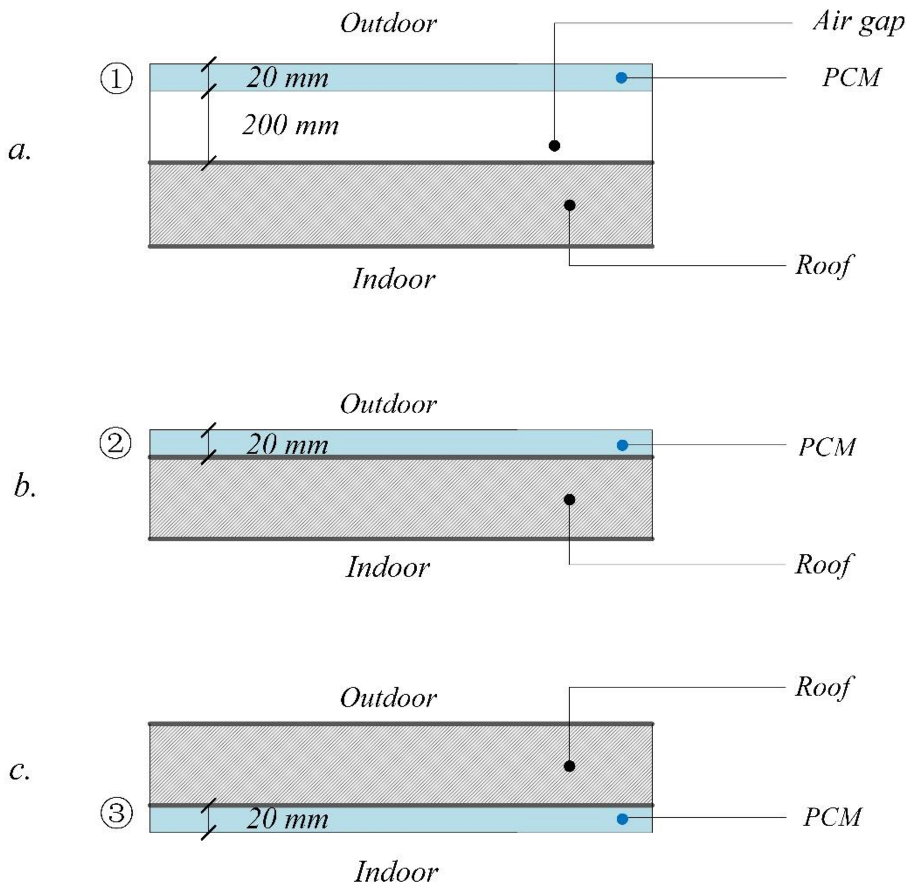

Fig. 6.3 Different positions of the PCM relative to the roof of the PTH

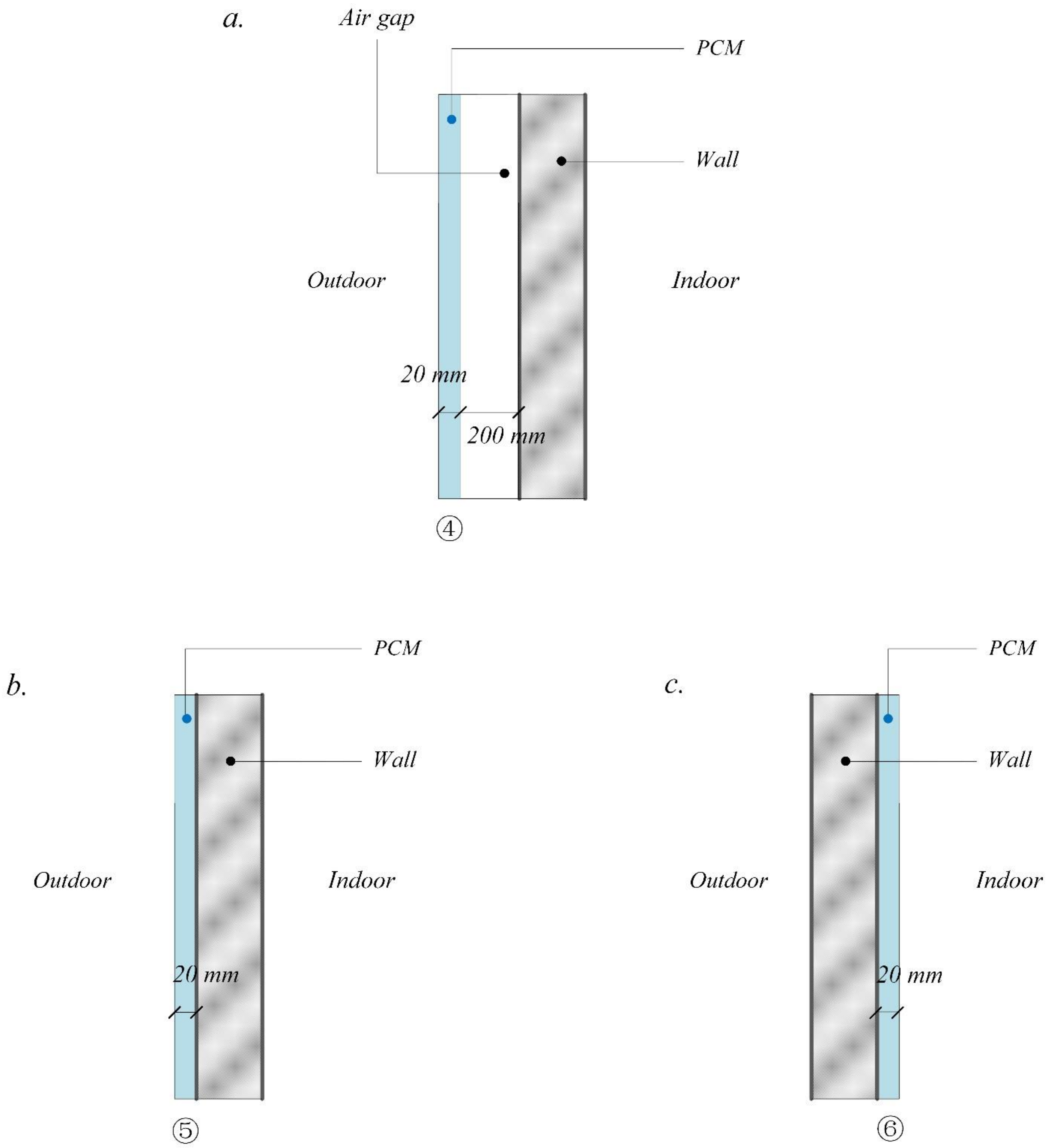

Fig. 6.4 Different positions of the PCM relative to a wall of the PTH

Table 6.4 Details of the sixteen different designs

Design	Details
1	Without PCM- Baseline design
2	PCM always at ① for Roof
3	PCM always at ② for Roof
4	PCM at ③ for Roof at daytime, but moved to outside the PTH at nighttime
5	PCM always at ④ for East Wall
6	PCM always at ⑤ for East Wall
7	PCM at ⑥ for East Wall at daytime, but moved to outside the PTH at nighttime
8	PCM always at ④ for West Wall
9	PCM always at ⑤ for West Wall
10	PCM at ⑥ for West Wall at daytime, but moved to outside the PTH at nighttime
11	PCM always at ④ for South Wall
12	PCM always at ⑤ for South Wall
13	PCM at ⑥ for South Wall at daytime, but moved to outside the PTH at nighttime
14	PCM always at ④ for North Wall
15	PCM always at ⑤ for North Wall
16	PCM at ⑥ for North Wall at daytime, but moved to outside the PTH at nighttime

As examples, the simulated air temperatures inside the PTH in D1, D11-13, together with outdoor air temperature over a total of four selected days within the period of simulation, are shown in Fig. 6.5 and Fig. 6.6, respectively. In Fig. 6.5, the outdoor air temperature and the simulated indoor air temperature in D1, T_o and $T_{i\ (D1)}$, are shown. As seen, during the four days, the indoor air temperature inside the PTH in D1, $T_{i\ (D1)}$, varied from 18.87 ^{o}C to 41.77 ^{o}C, and $T_{i\ (D1)}$ was always higher than T_o at daytime. Clearly, there was a similar trend in the variation patterns for both outdoor air temperature and the simulated indoor air temperature. However, due to the greenhouse effect and without ventilation at daytime, indoor air temperature in D1 could be much higher than outdoor air temperature. For example, when the highest outdoor air temperature was 31.1 ^{o}C on the second day, indoor air temperature was at 41.77 ^{o}C due to the greenhouse effect, and without ventilation. Hence, the air temperature inside the PTH was intolerably high [Wang et al., 2016c] throughout most of the daytime on that day. Furthermore, indoor air temperature at nighttime on the four simulation days was only just slightly higher than outdoor air temperature.

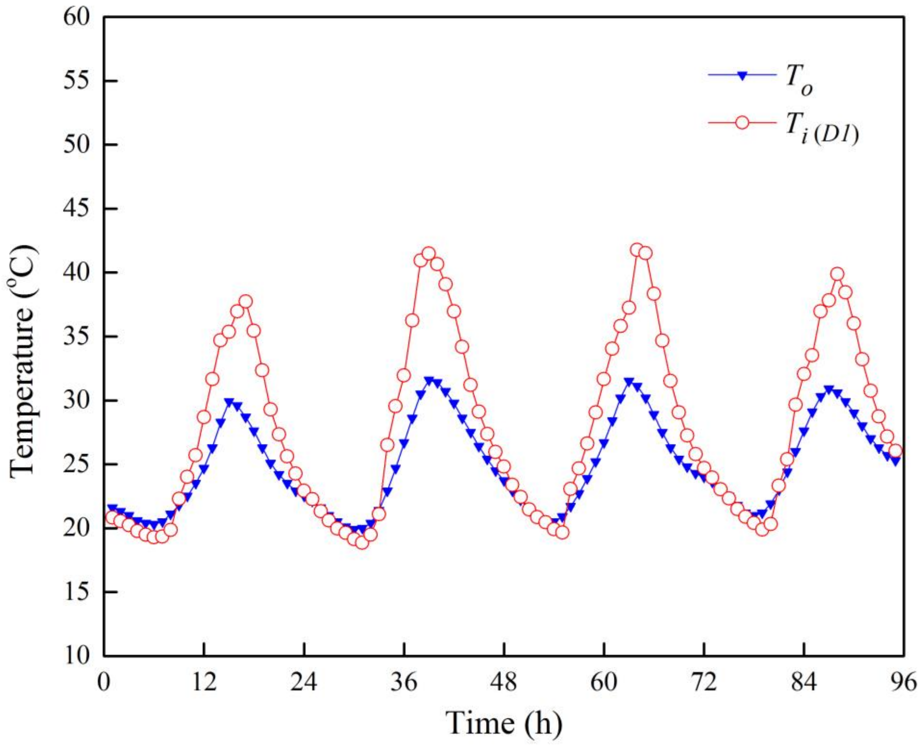

Fig. 6.5 The outdoor air temperature and simulated indoor air temperature over the four selected days in D1

In Fig. 6.6, the simulated indoor air temperatures in D11-13, $T_{i\,(D11)}$, $T_{i\,(D12)}$ and $T_{i\,(D13)}$, are shown. In D11, PCM was located outside the south wall of the PTH, 200 mm away from its external surface. In D12, PCM was placed outside the PTH close to the outside surface of south wall. In D13, PCM was located close to the indoor side of south wall and was moved to outside of the PTH from 20:00 to 8:00 on the following day, for releasing the absorbed heat to low temperature outdoor air at nighttime. As seen, over the four days, the simulated indoor air temperature in D13, $T_{i\,(D13)}$, varied from 18.91 °C to 37.76 °C, the lowest at both daytime and nighttime among the three designs. This suggested that the use of PCM on a movable base, which was placed on the indoor side of the south wall at daytime, could help improve the thermal environment inside the PTH most effectively when compared with the use of PCM in both D11 and D12 at daytime. At nighttime, the simulated results demonstrated that $T_{i\ (D13)}$ exhibited similar variation profile with $T_{i\ (D11)}$ because PCM was moved to outside of the PTH at nighttime, and $T_{i\ (D12)}$ was higher than $T_{i\ (D11)}$ and $T_{i\ (D13)}$ at nighttime because heat was released from the PCM on the external surface of the south wall and transferred into indoor via conduction through the wall.

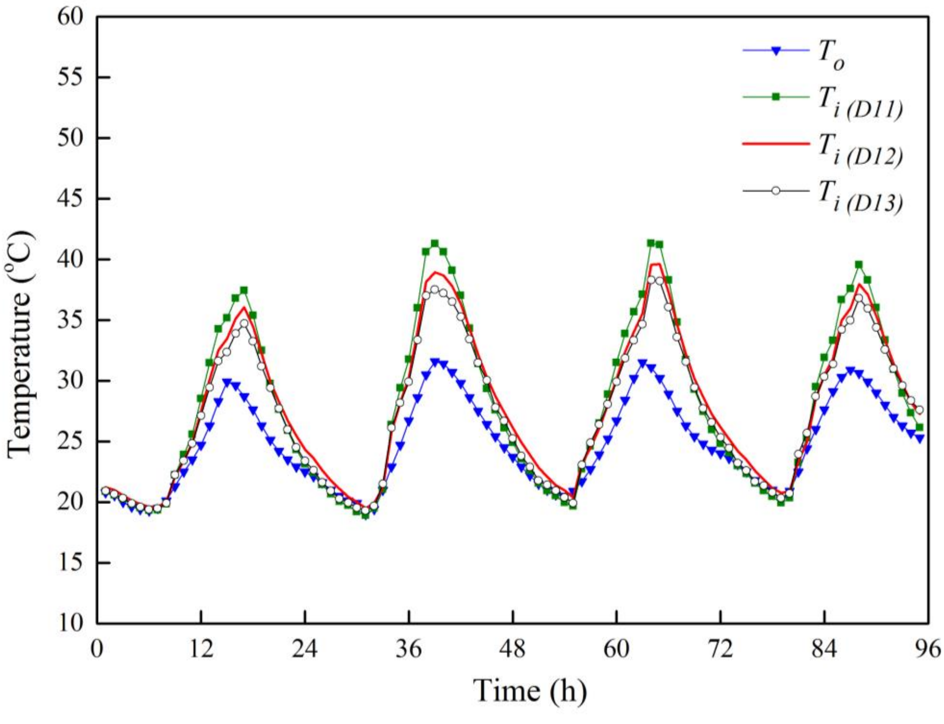

Fig. 6.6 The simulated indoor air temperatures in D11-13

Similar to the results shown in Fig. 6.6 for the south wall, locating the PCM on the indoor side of the other walls and moving it to outside the PTH could also improve the thermal environment in the PTH more than the use of PCM on the outdoor side of the walls at daytime.

The simulated results for D2-16 suggested that locating the PCM on the indoor side of roof and the four walls, i.e., in D4, D7, D10, D13 and D16, could help improve the thermal environment in the PTH more than the use of PCMs on the outdoor side of roof and the four walls at daytime. In addition, in these designs, as the PCM may be moved to outside the PTH at nighttime, the use of PCM at daytime would not, therefore, impair the thermal environment inside PTH at nighttime. Hence, the design of a movable PESS like that used in the experimental study reported in Chapter 5 should be preferred. The simulated results clearly demonstrated that a movable PESS may be used to help eliminate the negative effect of placing PCM inside the PTH at nighttime, while it can effectively improve the thermal environment in the PTH at daytime.

The simulated maximum and minimum T_o and T_i in D1-16 are shown in Table 6.5. As seen, as compared to those for D1, all the maximum values of T_i in D2-16 were lower, suggesting the effect of using PCM for improving indoor thermal environment at daytime in summer. However, there was a large variation in the 16 maximum T_i values, from 36.61 ^oC in D10 to 41.77 ^oC in D1, i.e., the baseline design. On the other hand, in D2-16, their minimum values of T_i stayed relative stable with a small variation range from 18.87 ^{o}C in D10 to 19.88 ^{o}C in D3. Furthermore, the average T_i in D10 was the lowest at 26.9 ^{o}C. These further suggested that, again, the use of PCM on the indoor side of roof and four walls was more effective for improving the thermal environment at daytime inside the PTH than on the outdoor side of roof and four walls. In addition, the designs with PCM to be moved to outdoor were more effective for improving the thermal environment inside the PTH than placing PCM near outdoor side of four walls at both daytime and nighttime. This was because while the use of a design with movable PCM could help not only reduce the air temperature inside the PTH at daytime, but also eliminate the negative effect of placing the PCM inside the PTH at nighttime. Hence a movable PESS such as that used in the experimental study reported in Chapter 5 provided a convenient way to move PCM from indoor to outdoor at nighttime, so as to eliminate the heat release from the PCM to indoor and re-charge the PCM with cooling energy from both the sky radiation and a low temperature outdoor air at nighttime.

Table 6.5 Simulated maximum and minimum T_o and T_i for D1-16

	T_o	$T_{i\ (D1)}$	$T_{i\ (D2)}$	$T_{i\ (D3)}$	$T_{i\ (D4)}$	$T_{i\ (D5)}$
Maximum	31.60	41.77	40.80	37.92	37.84	41.50
Minimum	19.90	18.87	18.96	19.88	19.01	18.91
Average	24.84	27.76	27.69	27.57	27.13	27.76
	$T_{i\ (D6)}$	$T_{i\ (D7)}$	$T_{i\ (D8)}$	$T_{i\ (D9)}$	$T_{i\ (D10)}$	$T_{i\ (D11)}$
Maximum	39.03	37.45	41.64	39.05	36.61	41.33
Minimum	19.74	18.92	18.92	19.73	18.93	18.90
Average	27.70	26.93	27.77	27.69	26.90	27.76
	$T_{i\ (D12)}$	$T_{i\ (D13)}$	$T_{i\ (D14)}$	$T_{i\ (D15)}$	$T_{i\ (D16)}$	
Maximum	39.62	37.76	41.71	39.85	37.73	
Minimum	19.51	18.91	18.90	19.52	18.92	
Average	27.70	27.08	27.76	27.71	27.04	

The simulated resultant thermally acceptable hours inside the PTH for all the designs are shown in Fig. 6.7. A thermally acceptable hour was defined as an hour during which indoor air temperature inside a PTH was below the occupants' thermal ultimate temperature in temporary shelters after natural disasters at 34 ^oC [Wang et al., 2016c]. As seen, compared with the baseline design, the number of acceptable hours for D10 was at 90 h during the four days, the highest among all designs. This was consistent with the earlier simulation results that D10 would lead to the lowest averaged indoor air temperature at 26.9 ^oC, among all designs.

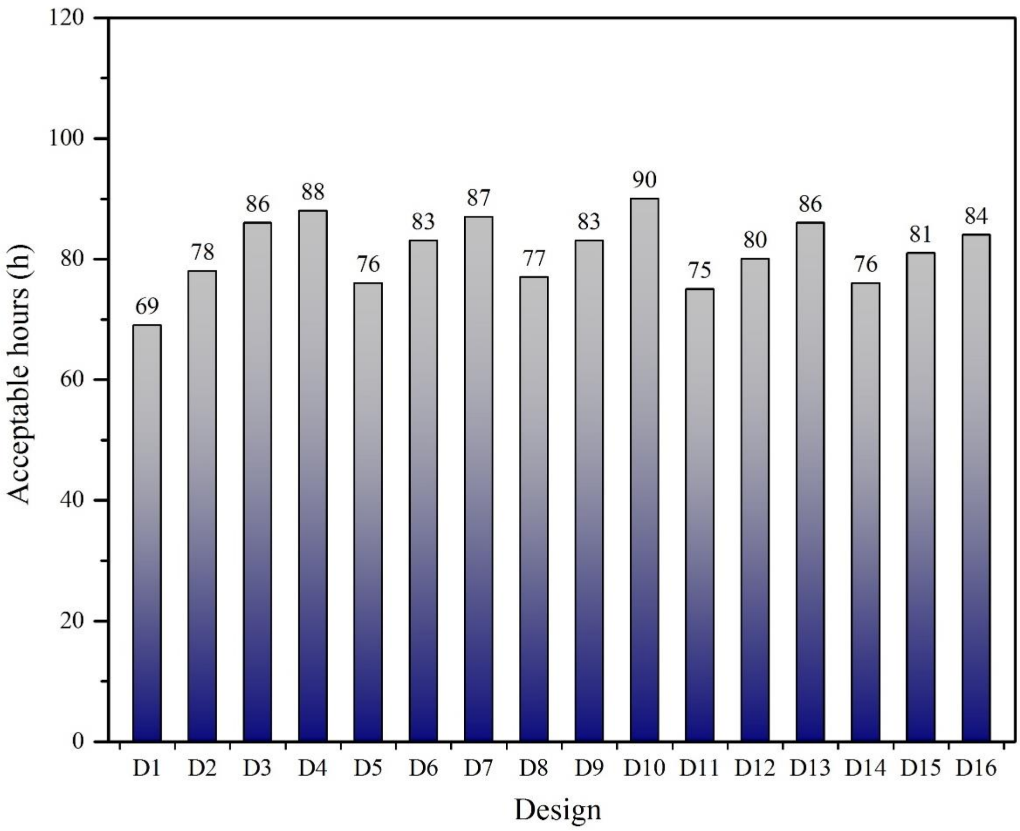

Fig. 6.7 Simulated thermally acceptable hours inside the PTH for D1-16

6.3.3 The amount of PCM to be used

It was obvious that the more PCM was used, the greater improvement in indoor thermal environment can be expected. However, the amount of PCM used would have a financial impact on applying PCMs to PTHs. Hence, the numerical study reported in this Chapter also covered an analysis on the impacts of the amount of PCM used on the thermal environment inside a PTH in summer, which is reported in this Section. To simplify the analysis, the amount of PCM to be used was indirectly represented by its thickness.

From the simulated results shown in Section 6.3.2, it can be seen that D10 was the most effective design on improving the PTH's indoor thermal environment at daytime in summer among the 16 designs, and hence selected to exam the relationship between the amount of the PCM used and the improvements in the thermal environment inside a PTH. Seven different levels of PCM thickness at 0 mm, 5 mm, 10 mm, 20 mm, 30 mm, 40 mm and 50 mm, were used in the analysis, with 0 mm thickness representing baseline design.

Table 6.6 shows the analysis results. As seen, the maximum indoor air temperatures, average indoor air temperatures and daytime average indoor air temperatures (from 8:00 to 20:00) inside the PTH were decreased with an increase in PCM's thickness. On the other hand, the rates of the decreases in these temperatures at different levels of thickness are shown in Fig. 6.8. As illustrated, the changes in these temperatures at 0 - 20 mm PCM thickness were greater than those at 20 - 50 mm PCM thickness. More remarkably, the rates of decrease in these temperatures at 20 - 50 mm PCM thickness were fairly small and almost stayed unchanged at 30 - 50 mm PCM thickness. Therefore, increasing PCM's thickness 1) from 0 mm to 20 mm, would have an obvious impact on regulating PTH's indoor thermal environment, and 2) to beyond 20 mm thickness, would have negligible impacts on further improving PTH's indoor thermal environment. Hence, the PCM thickness of 20 mm may be taken as a reference design value for future practical applications.

Table 6.6 Simulated maximum and average *Ti* in D10 at different thickness PCM

PCM's thickness	0	5 mm	10 mm	20 mm	30 mm	40 mm	50 mm
Maximum	41.77	39.80	38.39	36.61	36.21	36.13	36.05
Average	27.76	27.43	27.12	26.90	26.24	26.18	26.14
AVE_{day}	33.63	31.64	30.29	28.93	28.28	27.86	27.53

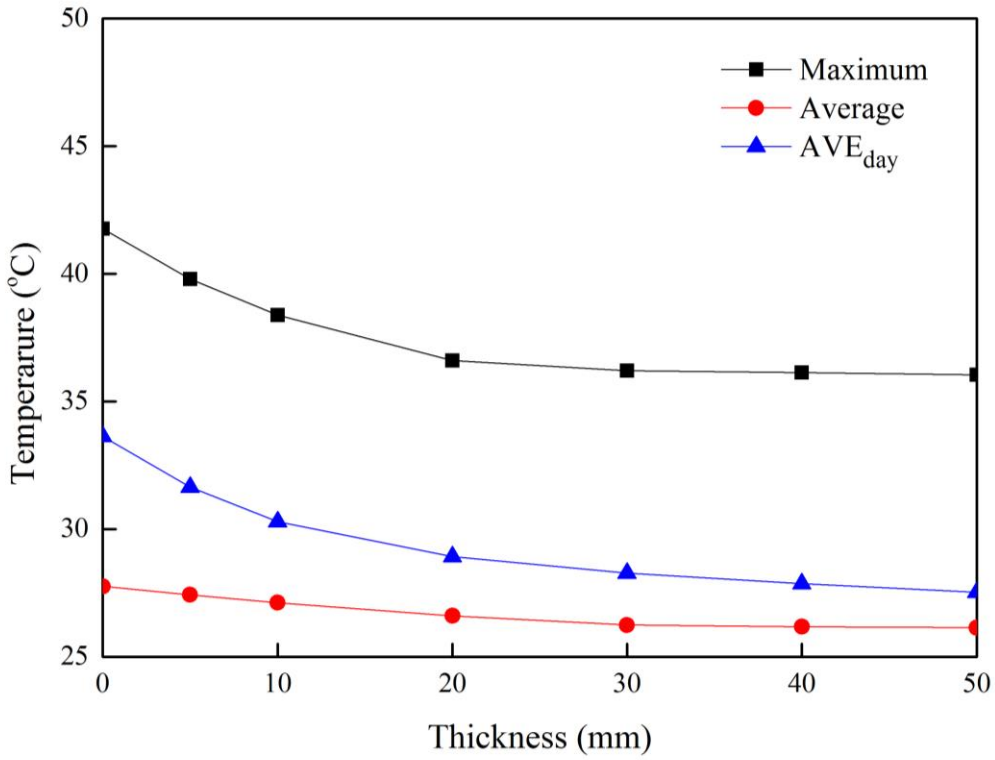

Fig. 6.8 Simulated rates of decrease in indoor air temperatures at different levels of PCM thickness

With the identified reference design PCM thickness of 20 mm, D10 was further revised to D17 by placing PCM of 20 mm thickness on the indoor sides of roof and all four walls of the PTH at daytime, with the PCM to be moved to outside the PTH at nighttime. As shown in Table 6.7, the simulated maximum T_i was reduced from 36.61 ^oC in D10 to 32.30 ^oC in D17, and the daytime average temperature from 28.93 ^oC in D10 to 26.82 ^oC in D17. Hence, these results suggested that it would be more effective to distribute a fixed amount of PCM to all envelope surfaces, rather than simply increasing the amount of PCM for just one particular envelope element.

Table 6.7 Simulated maximum and average T_i in D10 and D17

Indoor air temperature (^oC)	D10 (Shown also in Table 6.6)	D17
Maximum	36.61	31.30
Average	26.90	25.39
AVE_{day}	28.93	26.82

6.4 Conclusions

This Chapter reports a numerical study on optimizing the designs of applying PCM to a full-scale disaster-relief PTH in order to improve its indoor thermal environment in summer. The numerical study included two parts: 1) optimizing designs of applying PCMs at different positions relative to PTH's envelopes for improved indoor thermal environment at daytime in summer and 2) an analysis on the impacts of the amount of PCM used on the thermal environment inside the PTH.

In the first part, in order to find the best design of applying PCM to a PTH, a total of 16 designs to place PCM at different positions relative to the PTH's envelopes were defined and simulation studies with the 16 designs carried out. The study results demonstrated that in summer, D4, D7, D10, D13 and D16, among the 16 designs, can lead to a better thermal environment inside the PTH, than all the other designs, because in D4, D7, D10, D13 and D16, PCM was placed on the indoor side of all envelope components and may be moved to outside the PTH for charging the PCM with cooling energy from both the sky radiation and low temperature outdoor air at nighttime. Based on the simulation results, D10 was identified as the most effective design among all the 16 designs, and could result in the highest number of acceptable hours at 90 hours.

In the second part, the simulation results based on D10 demonstrated that increasing PCM's thickness from 0 mm to 20 mm would have noticeable improvements in the thermal environment inside the PTH, but to beyond 20 mm, would be negligible on further improving indoor thermal environment. Hence, the thickness of 20 mm for PCM was recommended as a reference design value for future practical applications.

Chapter 7

A further numerical study on applying the movable PESS to disaster-relief PTHs used in different climate regions to improve their indoor thermal environments in summer

7.1 Introduction

The experimental and numerical studies presented in Chapter 5 and Chapter 6, respectively, were carried out to investigate applying PCMs to disaster-relief PTHs installed in Chengdu, China. The study results of the previous experimental [Wang et al., 2018] and numerical [Wang et al., 2019b] studies demonstrated that in Chengdu in summer, applying PCMs to disaster-relief PTHs can help improve their internal thermal environments and the application of the movable PESS to PTHs was effective in transferring heat between indoor at daytime and outdoor at nighttime. However, natural disasters may also occur in other places globally. Given that the success of applying the movable PESS to PTHs for improving indoor thermal environments also depended on outdoor climates, but Chengdu only represented the “warm temperate-fully humid-hot summer” climate, it was therefore necessary to study the effectiveness of applying the movable PESS to PTHs installed in other climate regions globally.

To this end, as a follow-up to the previously reported experimental and numerical studies, respectively, a further numerical study on applying the movable PESS to disaster-relief PTHs installed in different climate regions around the world to improve their indoor thermal environments in the summer month of July has been carried out and the study results are reported in this Chapter. Firstly, the selection of the representative cities in different climate regions is reported. The mathematical model for a full-scale PTH with the movable PESS used in the numerical study reported in Chapter 6 was used in this further numerical study reported in this Chapter. Secondly, results of this further numerical study and the related analysis are presented. Finally, a conclusion is given.

7.2 Selection of the representative cities in different climate regions

The global climate classification by Köppen distribution method [Kottek et al., 2006] divided the world climatic regions into 31 types, as shown in Fig. 7.1 The division was based on three factors: temperature, main climates and precipitation.

Given the majority of both the lands and populations on the Earth is in the northern hemisphere, in this study, all the cities selected were therefore in the northern hemisphere. For locations in the southern hemisphere, reference may however be made to the locations of similar climate types in the northern hemisphere.

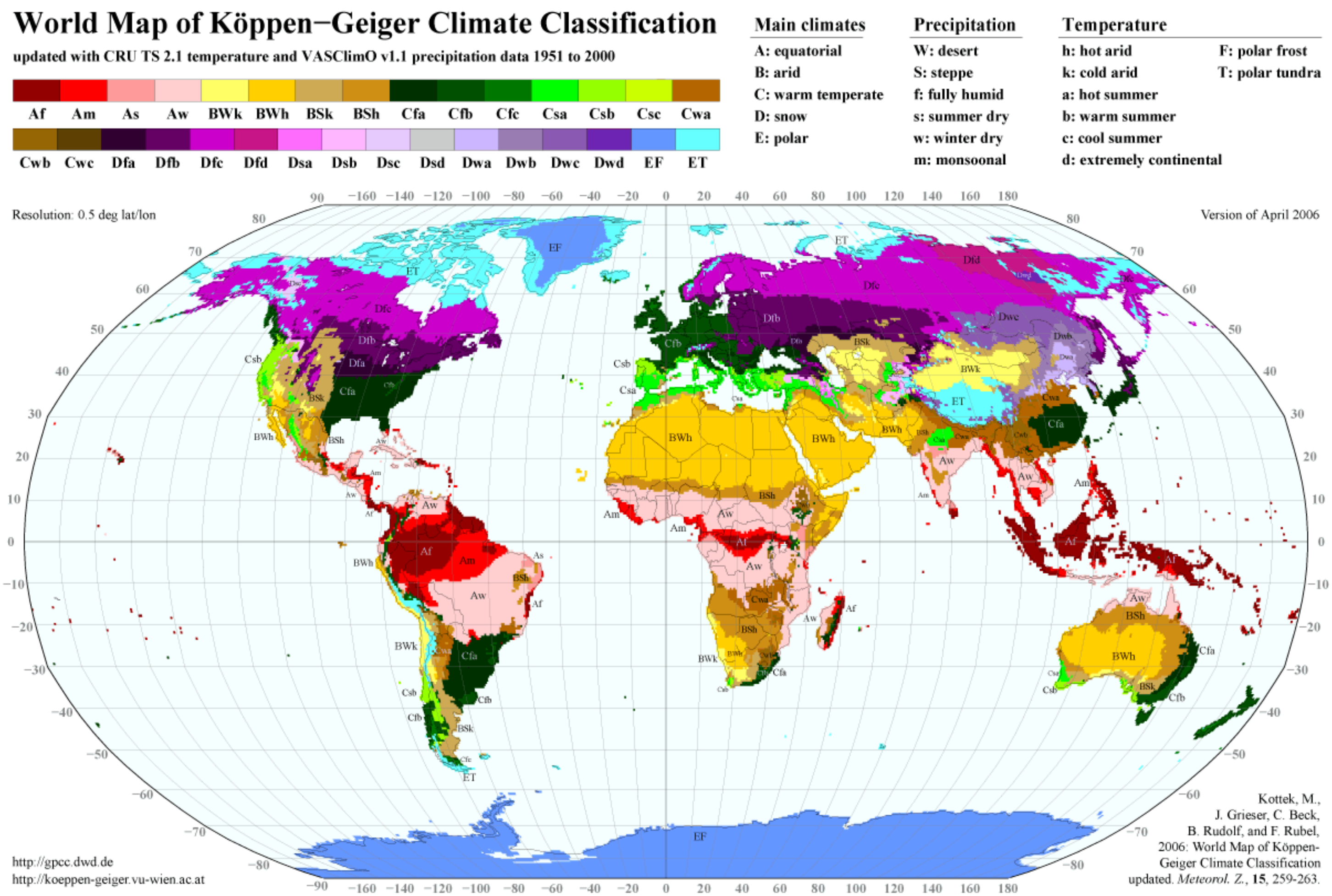

Fig. 7.1 The global climatic region distribution (Köppen distribution method) [Kottek et al., 2006]

The selection of the representative cities in the northern hemisphere in this further numerical study was based on a comprehensive consideration of a number of factors. Given the purpose of this further numerical study, the first consideration was the types of natural disasters. Secondly, the climatic characteristics of the selected cities should have regional representativeness. Thirdly, the population of the selected cities should be relatively large. Finally, the climate data of the selected cities can be accurately available from official sources and freely used. As a result, a total of twelve cities, with four in the tropical region, four in the temperate region and the last four in the cold temperate region, were selected, and their summer climate conditions are summarized in Table 7.1.

Table 7.1 Summary of the summer climatic data in the 12 selected cities

	Unit	Tropical region				Temperate region				Cold temperate region			
		01 Singapore	02 Miami	03 Bangkok	04 Abu Dhabi	05 Tokyo	06 Chengdu	07 Damasc us	08 Hanoi	09 Incheon	10 Toronto	11 Hohhot	12 Urumqi
Climate type		Af	Aw	Am	BWh	Cfa	Cfa	Csa	Cwa	Dwa	Dfb	BSk	BWk
Time zone		UTC*+8	UTC+4	UTC+7	UTC+4	UTC+9	UTC+1	UTC+2	UTC+7	UTC+9	UTC-5	UTC+8	UTC+10
Elevation	m	58.00	30.00	2.00	150.00	37.00	33.00	690.00	16.00	45.00	76.00	1040.00	1748.00
Maximum daytime temperature	ºC	33.00	33.38	37.98	46.53	34.00	30.00	40.00	43.00	32.65	32.34	34.39	36.09
Average temperature	ºC	27.88	27.17	29.05	33.09	20.64	17.20	27.50	28.85	21.15	17.07	19.03	20.37
Daily maximum temperature difference	ºC	9.48	11.68	11.14	20.05	16.05	16.42	21.44	18.91	13.03	21.42	20.19	17.36
Average moisture content	g/kg	19.60	16.90	18.80	16.70	13.40	8.70	7.10	19.40	12.70	8.80	8.80	6.70
Solar radiation	W/m^2	406.58	414.64	417.86	416.87	344.50	339.92	415.50	406.18	335.66	304.91	331.13	330.24
Types of natural disasters#		ST, TH	FL, HU,	CO, EA, FL, TS	DR, SA	EA, SE,TY,	DE, EA, FL, LA	EA, HU, TS,	DR, FL, LA, TY,	FL, TY	BL, EA, HU,	DR, FL, FR, HA,WI,	DE, DR, EA, RO, WI

* Universal Time Coordinated.

BL=blizzard; CO=collapse; DE=debris flow; DR=drought; EA=earthquake; FL=flood; FR=frost disaster; HA=hail; HU=hurricane; LA=landslide; RO=road frost heave; SA=sandstorm; SE=severe convective weather; ST=storm surge; TH=thunderstorm weather; TS=tsunami; TY=typhoon; WI=wind disaster.

7.3 Numerical studies results

The validated mathematical model for a disaster-relief PTH incorporating the movable PESS, as detailed in Section 6.2 of Chapter 6, was used to study, numerically, the effectiveness of applying PCMs to disaster-relief PTHs located in the 12 selected cities in the different climate regions in the northern hemisphere to improve their indoor thermal environments in the summer month of July and the study results are reported in this Section.

7.3.1 The evaluating criteria for the thermal environment inside a PTH

As emergency shelters during a post-disaster transition period, the thermal environment inside disaster-relief PTHs was expected to be poorer than that in ordinary buildings. Hence, the criteria for evaluating thermal environment in ordinary buildings was not applicable to PTHs. In fact, the evaluation of the thermal environments inside disaster-relief PTHs should take into account the post-disaster nature. In order to quantitatively describe the degree of improvement in the thermal environment inside PTHs after implementing certain passive thermal regulation measures such as applying PCMs, an evaluating index of Unacceptable Degree Hour (UDH), defined by Eq. (7.1) was proposed,

$$UDH = 1 \text{ hour} \times \sum_{j=1}^{n} \left(T_{in,j} - T_{top} \right)_{+} \tag{7.1}$$

Where UDH is unacceptable degree hours inside a PTH, ^{o}C·h; T_{top} the upper limit of tolerable air temperature inside the PTH, ^{o}C; $T_{in,j}$ the hourly average air temperature at j^{th} hour inside the PTH,

^{o}C, and *n* the total number of hours in the summer month of July. The subscript on the bracket, plus sign, indicates that only positive values are to be counted.

Based on the results from a previous related study [Wang, 2020] of surveying indoor thermal environment in disaster-relief PTHs using questionnaire survey approach, T_{top} can be set at 29 ^{o}C. As a matter of fact, the questionnaire survey results showed that the upper limit of tolerable air temperature inside a PTH during a post-disaster transition period was higher than the upper limit of normal human comfort temperature range. This further confirmed that the thermal environment inside disaster-relief PTHs deviated far from the comfortable range for ordinary buildings. Hence, *UDH* was more suitable for the evaluation of the thermal environment inside disaster-relief PTHs.

From Eq. (7.1), it can be seen that given a fixed T_{top} at 29 ^{o}C, when T_{in} was higher or the number of hours when $T_{in,j} - T_{top}$ > 0 was larger, *UDH* was greater. Hence, a greater *UDH* value directly reflected a poorer thermal environment inside a PTH.

After the movable PESS was incorporated into the PTH, it can be expected that because of the cooling effect from the movable PESS, T_{in} can be lower at daytime from 8:00 to 20:00 and the number of hours when $T_{in,j} - T_{top}$ >0 reduced, resulting in a reduced *UDH* value. In this connection, *UDH* ', unacceptable degree hours inside a PTH after incorporating the movable PESS, defined by Eq. (7.2), was further proposed,

$$UDH' = 1 \text{ hour} \times \sum_{j=1}^{n} \left(T'_{in,j} - T_{top} \right)_{+} \tag{7.2}$$

Where $T'_{in,j}$ is the hourly average air temperature at j^{th} hour inside a PTH after incorporating the movable PESS, ^{o}C.

With the above definitions of *UDH* and *UDH* ', the impacts of applying the movable PESS to disaster-relief PTHs used in the 12 selected cities in different climate regions in the northern hemisphere to improve their indoor thermal environments in the summer month of July may be evaluated by the absolute difference between *UDH* and *UDH* ', as follows:

$$\Delta = UDH - UDH' \tag{7.3}$$

Where the unit of Δ is $^{o}C{\cdot}h$.

In addition, a relative difference between *UDH* and *UDH* ' was also defined as Δ':

$$\Delta' = \frac{UDH - UDH'}{UDH} \tag{7.4}$$

Where the unit of Δ' is %.

Eq. (7.3) reflects the absolute degree of improvements, and Eq. (7.4) the relative degree of improvements, in the thermal environment inside PTHs before and after incorporating the movable PESS.

7.3.2 Results of the further numerical study for PTHs located in the 12 selected cities

Using the validated mathematical model for the disaster-relief PTH incorporating the movable PESS detailed in Section 6.2 and the official meteorological data in the typical weather year of

1989 for the 12 selected cities, a further numerical study on applying the movable PESS to the PTHs located in the 12 selected cities to improve their indoor thermal environments in July was carried out. *UDH*, *UDH* ', Δ and Δ' defined in Section 7.3.1 were used to evaluate the degree of improvements in the thermal environment inside the PTH after incorporating the movable PESS. For each of the 12 cities, the outputs from the further numerical study would include the daytime hourly average air temperature inside the disaster-relief PTH without incorporating the movable PESS, T_{in}, and the daytime hourly average air temperature inside the disaster-relief PTH after incorporating the movable PESS, T_{in}'. Using these output parameters, and the daytime hourly average ambient temperature, T_o, *UDH*, *UDH* ', Δ and Δ' were, respectively, obtained for the PTHs located in the 12 selected cities.

In this Section, firstly as an example, the further numerical study results for the PTH located in one of the 12 selected cities, Bangkok, are explained in detail. The study results for the PTHs located in the remaining 11 cities are then summarized in Table 7.2 and Table 7.3, respectively.

Fig. 7.2 shows the variations in the three temperatures, T_o, T_{in} and T_{in}', for the PTH installed in Bangkok in July. As seen, in July, the variation range in T_o was from 24.00 °C to 35.22 °C with a monthly average of 30.08 °C, but that in T_{in} was from 25.31 °C to 35.38 °C with a monthly average of 31.65 °C. At daytime, T_{in} was always higher than T_o. However, for T_{in}', its variation range was from 25.03 °C to 31.89 °C with a monthly average of 29.39 °C. These results suggested that, after incorporating the movable PESS, the monthly average daytime air temperature inside the PTH was reduced by 1.76 °C. In addition, the maximum temperature inside the PTH after incorporating the movable PESS could also be lowered by 3.49 °C from 35.38 °C to 31.89 °C.

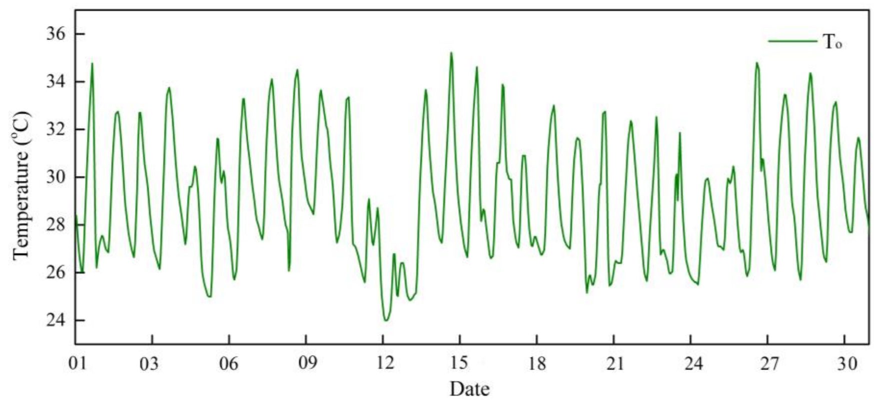

(a) Variations in hourly ambient air temperature in July in Bangkok

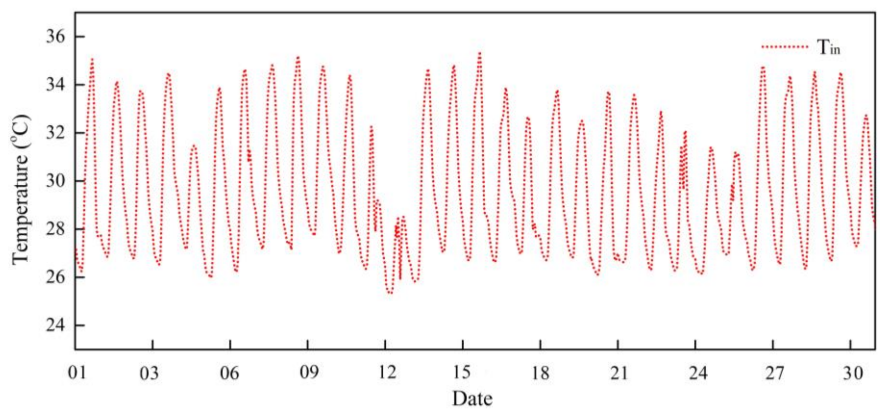

(b) Variations in the simulated hourly indoor air temperature without incorporating the movable PESS

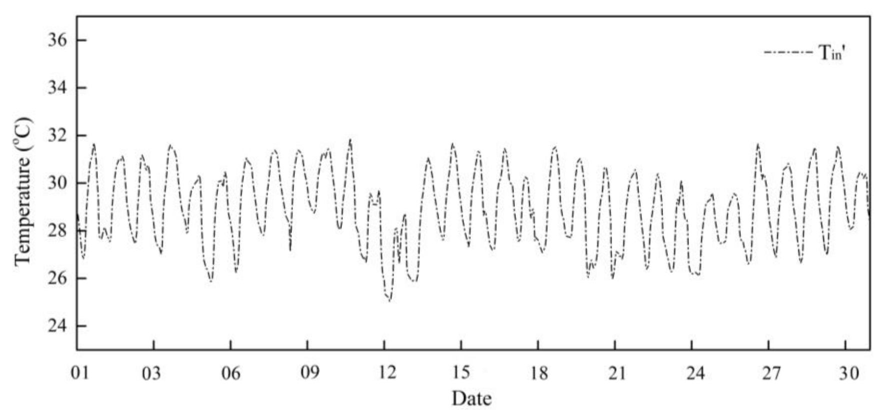

(c) Variations in the simulated hourly indoor air temperature after incorporating the movable PESS

Fig. 7.2 Hourly ambient air temperature and the simulated hourly air temperatures inside a disaster-relief PTH installed in Bangkok in July

Fig. 7.3 shows the variations in the three temperatures, T_o, T_{in} and T_{in}' for the PTH installed in Bangkok on the hottest day in July. As seen, on that day, the variation range in T_o was from 27.25 ^{o}C to 35.22 ^{o}C, but that in T_{in} from 27.31 ^{o}C to 35.36 ^{o}C. At daytime, T_{in} was always higher than T_o. However, for T_{in}', its variation range was from 27.50 ^{o}C to 31.66 ^{o}C. These results suggested that, on the hottest day in July, after incorporating the movable PESS, the daytime average hourly air temperature inside the PTH was reduced by 1.66 ^{o}C, and the maximum hourly air temperature inside the PTH reduced by 3.90 ^{o}C, respectively.

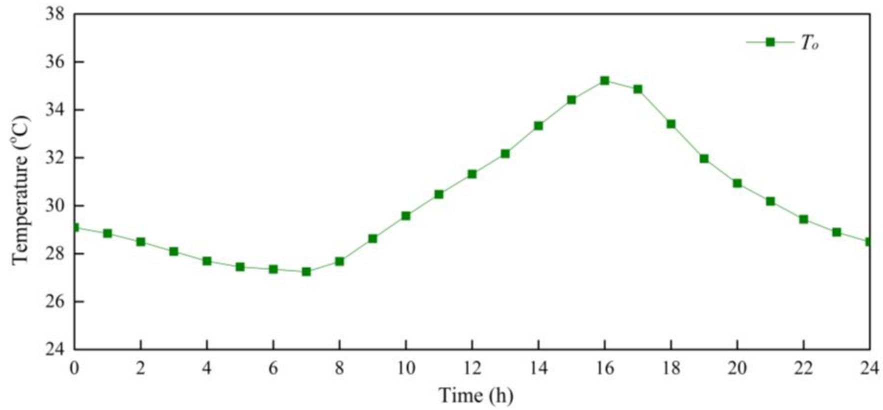

(a) Variations in hourly ambient temperature on the hottest day in July in Bangkok

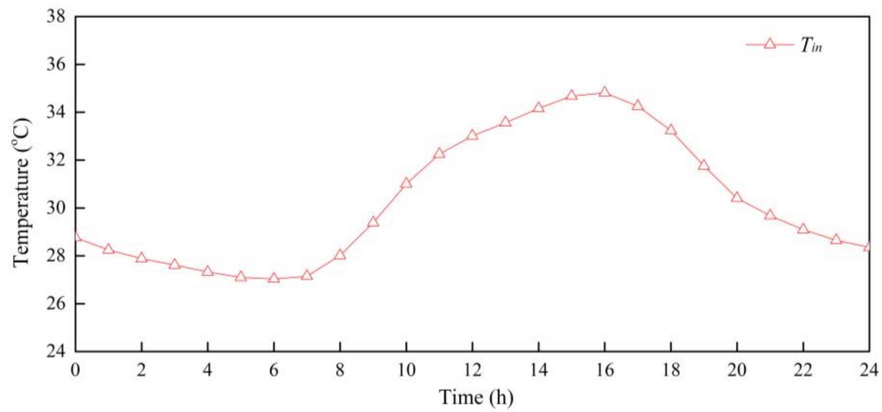

(b) Variations in the simulated hourly indoor air temperature without incorporating the movable PESS on the hottest day in July in Bangkok

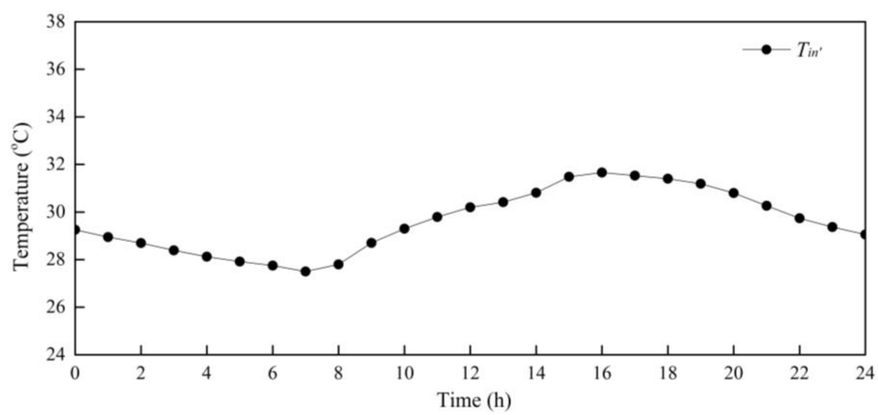

(c) Variations in the simulated hourly indoor air temperature after incorporating the movable PESS on the hottest day in July in Bangkok

Fig. 7.3 Hourly ambient air temperature and the simulated hourly air temperatures inside a disaster-relief PTH on the hottest day in July in Bangkok

Table 7.2 summarizes the variation ranges and the monthly averaged values in T_o, T_{in} and T_{in}' for PTHs located in the 12 selected cities in July. As seen, except for Abu Dhabi, in all other locations, the monthly averaged T_{in} values were all greater than the monthly averaged T_o values. This reflected the deteriorated thermal environments inside PTHs, which was consistent with the study results for the PTH located in Chengdu [Wang et al., 2019c]. Furthermore, in all the 12 selected cities in July, the highest values in the monthly variation ranges for T_{in} were always greater than those for T_{in}', and all the monthly averaged T_{in}' values were smaller than all the monthly averaged T_{in} values. These results suggested that the introduction of movable PESS to PTHs located in all the 12 selected cities was functional.

Table 7.2 The variation ranges and the monthly average values in T_o, T_{in} and T_{in}' for the PTHs located in the 12 selected cities in July (°C)

Region	City	Variation range in T_o	Monthly average T_o	Variation range in T_{in}	Monthly average T_{in}	Variation range in T_{in}'	Monthly average T_{in}'
Tropic region	Singapore	22.00 - 32.14	27.77	24.44 - 34.47	28.75	24.54 - 31.10	28.20
	Miami	23.20 - 32.20	27.96	24.66 - 33.81	28.99	24.47 - 31.01	28.24
	Bangkok	24.00 - 35.22	30.08	25.31 - 35.38	31.65	25.03 - 31.89	29.39
	Abu Dhabi	26.14 - 46.53	34.45	26.27 - 41.90	32.91	27.11 - 38.92	32.79
Temperate region	Tokyo	15.00 - 34.00	22.59	18.72 - 34.89	25.30	18.72 - 29.65	24.19
	Chengdu	20.30 - 34.64	25.81	22.53 - 35.43	27.52	21.89 - 31.34	26.76
	Damascus	13.69 - 39.00	26.34	19.32 - 37.29	28.08	19.41 - 32.57	26.83
	Hanoi	24.15 - 36.19	29.44	25.71 - 35.62	30.02	25.47 - 32.63	29.51
Cold temperate region	Incheon	17.81 - 32.65	23.58	21.58 - 32.87	25.97	20.04 - 29.43	24.87
	Toronto	8.78 - 31.81	20.81	15.87 - 33.48	24.81	17.20 - 29.54	23.58
	Hohhot	13.44 - 32.74	22.24	19.13 - 33.34	25.57	19.13 - 29.77	24.61
	Urumqi	13.11 - 36.09	23.97	18.63 - 36.07	26.81	19.96 - 33.74	25.73

Table 7.3 summarizes the variation ranges in, and the daily average values of T_o, T_{in} and T_{in}' for the PTHs located in the 12 selected cities on the hottest day in July. As seen, except for Abu Dhabi, Damascus and Urumqi, in the other nine cities, on the hottest day in July, the daily averaged T_{in} values were greater than the daily averaged T_o values, reflecting the deteriorated thermal environments inside PTHs without the use of PCMs. However, with the introduction of the movable PESS to PTHs, in all the 12 selected cities, both the daily peak and the daily averaged T_{in}' values were smaller than both the daily peak and the daily averaged T_{in} values, reflecting the effectiveness of applying movable PESS to PTHs to bring down their indoor air temperatures.

Table 7.3 The variation ranges and the daily average values of T_o, T_{in} and T_{in}' for the PTHs located in the12 selected cities on the hottest day in July (°C)

Region	City	Variation range in T_o	Daily average T_o	Variation range in T_{in}	Daily average T_{in}	Variation range in T_{in}'	Daily average T_{in}'
Tropic region	Singapore	26.75 - 32.14	30.26	26.46 - 34.26	31.64	27.56 - 31.02	30.11
	Miami	26.10 - 32.20	30.83	26.34 - 33.13	31.82	26.73 - 31.01	30.13
	Bangkok	27.25 - 35.22	31.85	27.31 - 35.36	32.35	27.50 - 31.66	30.39
	Abu Dhabi	26.48 - 46.53	39.88	26.57 - 41.33	37.31	27.55 - 37.38	35.33
Temperate region	Tokyo	23.00 - 34.00	30.15	24.81 - 34.89	31.63	23.96 - 29.55	28.21
	Chengdu	24.05 - 34.64	30.43	25.34 - 34.95	31.48	25.42 - 31.34	29.31
	Damascus	13.69 - 39.00	33.56	19.32 - 37.29	33.38	20.23 - 32.57	29.95
	Hanoi	27.45 - 36.19	32.84	26.95 - 34.77	33.60	28.02 - 32.63	30.85
Cold temperate region	Incheon	23.70 - 32.65	30.49	25.09 - 32.87	31.16	24.56 - 29.31	28.32
	Toronto	21.34 - 31.81	29.42	23.46 - 33.48	31.56	23.07 - 29.54	28.47
	Hohhot	15.79 - 32.74	29.60	20.41 - 33.34	30.65	20.78 - 28.80	27.09
	Urumqi	29.45 - 36.09	33.86	29.78 - 36.07	33.70	29.58 - 33.74	31.99

7.3.3 *UDH*, *UDH* ', Δ and Δ' values for PTHs located in the 12 selected cities

It is shown in Section 7.3.2 that applying the movable PESS to disaster-relief PTHs in all the 12 selected cities was functional. However, the levels of effectiveness in improving the indoor thermal environment for PTHs located in different cities may be different and are therefore evaluated in this Section.

Based on the output hourly average values of T_{in} and T_{in}' from this further numerical study, together with the hourly ambient air temperature values of T_o, *UDH*, *UDH* ', Δ and Δ' values for the PTHs located in the 12 selected cities in July were evaluated and are summarized in Table 7.4.

It can be seen from Table 7.4 that the differences in *UDH* values for the 12 selected cities were relatively large, with the maximum *UDH* value of 3085 $^oC{\cdot}h$ for Abu Dhabi and the minimum *UDH* value of 151 $^oC{\cdot}h$ in Incheon. The *UDH* values in Bangkok, Abu Dhabi, Damascus and Hanoi were higher than 1000 $^oC{\cdot}h$, those in Singapore, Miami and Urumqi between 500 $^oC{\cdot}h$ and 1000 $^oC{\cdot}h$ and those in Tokyo, Chengdu, Incheon, Toronto and Hohhot less than 500 $^oC{\cdot}h$. Without the introduction of the movable PESS to PTHs, there were 7 cities where the *UDH* values were higher than 500 $^oC{\cdot}h$. However, after introducing the movable PESS to PTHs, there were only 2 cities where the *UDH* ' values were higher than 500 $^oC{\cdot}h$. Furthermore, it can also be seen from Table 7.4 that for the 12 selected cities, *UDH* ' values were all smaller than *UDH* values, although there were large variations in the differences between the two values. These further suggested that incorporating the movable PCM to PTHs was an effective way to improve thermal environments inside PTHs in all the 12 selected cities.

Table 7.4 also shows the Δ values and Δ' values for the 12 selected cities. As seen, the differences in Δ values for the 12 selected cities were also relatively large, with the maximum of 869 °C·h for Damascus and the minimum of 147 °C·h for Incheon. The Δ values in Damascus (869 ℃·h), Bangkok (568 ℃·h), Hanoi (563 ℃·h), Miami (561 ℃·h) and Singapore (513 ℃·h) were higher than 500 °C·h, those in Urumqi (415 ℃·h) and Chengdu (382 ℃·h) between 300 °C·h and 500 °C·h and those in Hohhot (229 ℃·h), Toronto (229 ℃·h), Tokyo (224 ℃·h), Abu Dhabi (221 ℃·h) and Incheon (147 ℃·h) less than 300 °C·h. For Damascus, its Δ value of 869 ℃·h was the highest among the 12 selected cities. There can be three reasons for this. Firstly, its *UDH* value of 1260 ℃·h was relatively on the high side among all cities; Secondly, the variation range in hourly ambient air temperature in Damascus in July of 13.69 °C ~ 39.00 °C was the largest among the 12 selected cities; Thirdly, after incorporating the movable PESS in the PTHs, the difference in the peak values of T_{in} and T_{in}' at 4.72 °C was also on the high side among all cities. On the other hand, for Incheon, its Δ value of 147 ℃·h was the lowest among the 12 selected cities, because the *UDH* value in Incheon at 151 ℃·h was the lowest. Furthermore, with respect to different climate regions, there were 3 cities in the tropic region, 2 cities in the temperate region but 0 city, respectively, in the cold temperate region where their Δ values were higher than 500 ^{o}C·h. However, there was 1 city in the tropic region, 1 in the temperate region and 3 in the cold temperate region, respectively, where their Δ values were less than 300 ^{o}C·h. These suggested that incorporating the movable PESS to PTHs located in both tropic region and temperate region would lead to better indoor thermal environmental comfort than those located in cold temperate region.

Furthermore, the Δ' values in the 12 selected cities are also shown in Table 7.4. As seen, except for Abu Dhabi with a Δ' value of 7.17%, for all other cities, their Δ' values were not less than 46%. There were 4 cities, Tokyo, Incheon, Toronto and Hohhot, where their Δ' values were all over 97%. However, since their *UDH* values were all on the low side at not greater than 234 °C·h, applying movable PESS to PTHs in these cities may not be too attractive. In addition, for Abu Dhabi, although its *UDH* value was the highest, its Δ' value was only at 7.17%, suggesting the insignificant effect of applying PCM to the PTHs located there. Finally, for the remaining seven cities, i.e., Singapore, Miami, Bangkok, Chengdu, Damascus, Hanoi and Urumqi, their *UDH* values were all relatively higher at $>$ 487 °C·h, their Δ values not less than 382 °C·h, and their Δ' values greater than 46%, suggesting that the application of the movable PESS to the disaster-relief PTHs located in the seven cities can help remarkably improve their indoor thermal environment inside in the summer month of July. It should be further mentioned that six out of the seven cities were actually located in both the tropic and temperate regions. This was consistent with the earlier results when analyzing Δ values, that the application of the movable PESS to the disaster-relief PTHs located in both tropic and temperate regions would result in better indoor thermal environmental control in July, than those located in the cold temperate region.

Table 7.4 *UDH*, *UDH* ', Δ and Δ' values for PTHs located in 12 selected cities

Region	City	*UDH* (°C·h)	*UDH* ' (°C·h)	Δ (°C·h)	Δ' (%)
Tropic region	Singapore	738	226	513	69.45
	Miami	794	234	561	70.58
	Bangkok	1056	488	568	53.77
	Abu Dhabi	3085	2864	221	7.17
Temperate region	Tokyo	229	4	224	98.04
	Chengdu	487	105	382	78.37
	Damascus	1260	391	869	68.95
	Hanoi	1219	655	563	46.23
Cold temperate region	Incheon	151	4	147	97.55
	Toronto	227	3	225	98.87
	Hohhot	234	5	229	97.88
	Urumqi	513	99	415	80.77

7.4 Conclusions

This Chapter reports a further numerical study on applying the movable PESS to full-scale disaster-relief PTHs located in different climate regions in the northern hemisphere to improve their indoor thermal environment in July. 12 cities in the northern hemisphere were selected based on a comprehensive consideration of several factors. The previously developed and experimentally validated EnergyPlus based simulation model for a PTH incorporating the movable PESS used in Chapter 6 was deployed in this further numerical study.

Based on the official meteorological data for July in the typical weather year of 1989, this further numerical study results demonstrated that for the PTHs located in all the 12 selected cities in July, all the highest values in the monthly variation ranges in T_{in} were greater than those for T_{in}', and all the monthly averaged T_{in}' values were smaller than all the monthly averaged T_{in} values. It was further demonstrated that on the hottest day in July, in all the 12 cities, both the daily peak and daily averaged T_{in}' values were smaller than both the daily peak and daily averaged T_{in} values. These results demonstrated that applying the movable PESS to disaster-relief PTHs located in the 12 cities in July was functional in bringing down the air temperatures inside PTHs.

However, based on the evaluated values of *UDH*, *UDH* ', Δ and Δ' for the PTHs located in the 12 selected cities in July, it was further shown that although *UDH* ' values in the 12 selected cities were all smaller than *UDH* values, there were significant variations in Δ and Δ' values. Following a comprehensive examination of *UDH*, *UDH* ', Δ and Δ' values, it was suggested that although applying the movable PESS to disaster-relief PTHs in July was functional, for all 12 cities, it was more effective for the following seven cities of Singapore, Miami, Bangkok, Chengdu, Damascus, Hanoi and Urumqi, with six of the seven cities located in both tropic and temperate climate regions.

Chapter 8

Conclusions and future work

8.1 Conclusions

A programmed research work on firstly experimentally studying the application of PCMs to disaster-relief PTHs in summer, secondly developing and validating a numerical model for the full-scale disaster-relief PTH and numerically optimizing designs of applying PCMs at different positions relative to PTH's envelopes and analysing the impacts of the amount of PCM used on the thermal environment inside the PTH, and thirdly further numerically studying the application of the movable PESS to full-scale disaster-relief PTHs located in different climate regions in the northern hemisphere in July, has been successfully carried out and is reported in this Thesis. The conclusions of the Thesis are:

An experimental study on applying PCMs to disaster-relief PTHs for improving their internal thermal environments in summer has been carried out and the study results are reported in Chapter 5. Two different designs of applying PCMs to PTHs were examined. In Design 1, PCM was fixed to the internal surfaces of the PCM based MH, but a movable PESS was used in Design 2. The experimental results from both Designs demonstrated that the use of PCM can help improve the thermal environment inside

PTHs at daytime in summer. However, the comparison between the two Designs suggested that, since outdoor air at a lower temperature at nighttime may be the only cooling energy source available for charging the PCM, using the movable PESS shall therefore be preferred. Furthermore, to achieve a suitable balance between the cost of a PESS and the level of thermal environment improvement inside a disaster-relief PTH, the PESS must be properly sized. Finally, a practical design of applying the movable PCMs to future disaster-relief PTHs was also proposed to enable the future wider application of the PCMs to disaster-relief PTHs.

A numerical study on optimizing the designs of applying PCM to a full-scale disaster-relief PTH in order to improve its indoor thermal environment in summer is reported in Chapter 6. The numerical study included two parts: 1) optimizing designs of applying PCMs at different positions relative to PTH's envelopes for improved indoor thermal environment at daytime in summer, and 2) an analysis on the impacts of the amount of PCM used on the thermal environment inside the PTH. The study results for the first part demonstrated that in summer, D4, D7, D10, D13 and D16, among the 16 designs, can lead to a better thermal environment inside the PTH, than all the other designs, because in D4, D7, D10, D13 and D16, the PCM was placed on the indoor side of all envelope components and may be moved to outside the PTH for charging the PCM with cooling energy from both the sky radiation and low temperature outdoor air at nighttime. Based on the simulation results, D10 was identified as the most effective design among all the 16 designs, and could result in the highest number of acceptable hours at 90 hours. In the second part, the simulation results based on D10 demonstrated that increasing PCM's thickness from 0 mm to 20 mm would have noticeable improvements in the thermal environment inside the PTH, but to beyond 20 mm, would be negligible on further improving indoor thermal environment. Hence, the thickness of 20 mm for PCM was recommended as a reference design value for future practical applications.

A further numerical study on applying the movable PESS to full-scale disaster-relief PTHs located in different climate regions in the northern hemisphere to improve their indoor thermal environments in July is reported in Chapter 7. 12 cities in the northern hemisphere were selected based on a comprehensive consideration of several factors. This further numerical study results demonstrated that for the PTHs located in all the 12 selected cities in July, all the highest values in the monthly variation ranges in T_{in} were greater than those for T_{in}', and all the monthly averaged T_{in}' values were smaller than all the monthly averaged T_{in} values. It was further demonstrated that on the hottest day in July, in all the 12 cities, both the daily peak and daily averaged T_{in}' values were smaller than both the daily peak and daily averaged T_{in} values. These results demonstrated that applying the movable PESS to disaster-relief PTHs located in the 12 cities in July was functional in bringing down the air temperatures inside PTHs. Furthermore, following a comprehensive examination of *UDH*, *UDH* ', Δ and Δ' values, it was suggested that although applying the movable PESS to disaster-relief PTHs in July was functional, for all 12 cities, it was more effective for the following seven cities of Singapore, Miami, Bangkok, Chengdu, Damascus, Hanoi and Urumqi, with six of the seven cities located in both tropic and temperate climate regions.

The outcomes of the programmed research work reported in this Thesis have made significant contributions to studying the application of PCMs to disaster-relief PTHs for improving their indoor thermal environments in summer time. This would help provide the occupants living in disaster-relief PTHs where PCMs have been applied with more acceptable thermal environments in summer time by using a low-cost and effective passive method. The outcomes of the study reported in this thesis may be used to guide the future applications of PCM to disaster-relief temporary houses of various configurations, and located in different climates. The long-term significance for the programmed research work is its contribution to providing thermally acceptable temporary houses for disaster victims during a disaster-relief process.

8.2 Proposed further work

A number of future studies, following on the successful completion of the programmed research work reported in this Thesis, are proposed as follows:

- Experimental and numerical studies on applying PCMs to disaster-relief PTHs for improving their indoor thermal environments in summer time have been carried out. The thermal environments inside the disaster-relief PTHs can however also be very poor in winter. Therefore, it is suggested that the application of PCMs to disaster-relief PTHs for improving their indoor thermal environments in winter should be further examined;
- In the studies reported in this Thesis, only one passive method, i.e., applying PCM, was applied to disaster-relief PTHs for improving their indoor thermal environments. Other passive methods such as shading and ventilation can also influence the thermal environments inside disaster-relief PTHs. Therefore, it may become more effective by combining various passive methods;
- In the studies reported in this Thesis, only air temperature and internal surface temperatures of PTHs' envelopes were considered. Other parameters such as air humidity and indoor air quality can also influence the comfort level of occupants inside PTHs. Therefore, these parameters should be considered in further studies.

- In the further numerical studies reported in Chapter 7, only the applications of the movable PESS to full-scale disaster-relief PTHs located in different climate regions in the northern hemisphere were considered. Therefore, other cities in different climate regions in the southern hemisphere should be considered in further studies.

References

1. Gunawardena et al. 2014

   Gunawardena T., Ngo T., Mendis P., Aye L.and Crawford R.

   Time-Efficient Post-Disaster Housing Reconstruction with Prefabricated Modular Structures. Open House International, 39, 59-69.

2. Tang et al. 2017

   Tang A., Kwasinski A. and Yu K.

   A Longitudinal Study of Tohoku Telecommunication Network Three Years after the Great East Japan Earthquake and Tsunami. Congress on Technical Advancement 2017: Infrastructure Resilience and Energy, 135-142.

3. Aye et al. 2012

   Aye L., Ngo T., Crawford R. H., Gammampila R.and Mendis P.

   Life cycle greenhouse gas emissions and energy analysis of prefabricated reusable building modules. Energy and Buildings, 47, 159-168.

4. Tas et al. 2011

   Tas N., Tas M. and Cosgun N.

   Permanent Housing Production Process after 17 August 1999 Marmara Earthquake in Turkey. International Journal of Strategic Property Management, 15, 312-328.

5. Wang et al. 2016a

   Wang Y., Wang L., Long E. S. and Deng S. M.

An experimental study on the indoor thermal environment in prefabricated houses in the subtropics. Energy and Buildings, 127, 529-539.

6. Felix et al. 2015

Felix D., Monteiro D., Branco J. M., Bologna R. and Feio A.

The role of temporary accommodation buildings for post-disaster housing reconstruction. Journal of Housing and the Built Environment, 30, 683-699.

7. Asefi and Sirus 2012

Asefi M. and Sirus F. A.

Transformable Shelter: Evaluation and New Architectural Design Proposals. World Conference on Design, Arts and Education (Dae-2012), 51, 961-966.

8. Dikmen et al. 2012

Dikmen N., Elias-Ozkan S. T. and Davidson C.

Comparison of Post-Disaster Housing Procurement Methods in Rural Areas of Turkey. Open House International, 37, 28-39.

9. Huang et al. 2015

Huang L. H., Long E. S. and Ouyang J. L.

Measurement of the Thermal Environment in Temporary Settlements with High Building Density after 2008 Wenchuan Earthquake in China. 9th International Symposium on Heating, Ventilation and Air Conditioning (Ishvac) Joint with the 3rd International Conference on Building Energy and Environment (Cobee), 121, 95-100.

10. Zhang et al. 2017a

Zhang H. B., Liu J., Li C. N. and Lian Z. W.

Long-term investigation of moisture environment in underground civil air defence work. Indoor and Built Environment, 26, 744-757.

11. Wang et al. 2017

Wang Y., Long E. S. and Deng S. M.

Applying passive cooling measures to a temporary disaster-relief prefabricated house to improve its indoor thermal environment in summer in the subtropics. Energy and Buildings, 139, 456-464.

12. Saffari et al. 2017

Saffari M., de Gracia A., Fernandez C. and Cabeza L. F.

Simulation-based optimization of PCM melting temperature to improve the energy performance in buildings. Applied Energy, 202, 420-434.

13. Wikipedia

https://zh.wikipedia.org/zh-hans/

14. Wang et al. 2018

Wang C. X., Huang X., Deng S. M., Long E. S. and Niu J. L.

An experimental study on applying PCMs to disaster-relief prefabricated temporary houses for improving internal thermal environment in summer. Energy and Buildings, 179, 301-310.

15. Shen et al. 2005

Shen L., Cheng S. K., Gunson A. J. and Hui W.

Urbanization, sustainability and the utilization of energy and mineral resources in China. Cities, 22, 287-302.

16. Subasinghe 2013

Subasinghe C.

Spatial confrontations: abandonment of self-labor in transitional sheltering after a natural disaster. International Journal of Disaster Risk Reduction, 6, 78-86.

17. Ni and Qian 2017

Ni F. and Qian F.

Comparative study on temporary shelter planning after earthquake with the plate-houses constructio Wenchuan earthquake as an example. China City Planning Review, 26, 50-57.

18. Asfour 2019

Asfour O. S.

Learning from the past: Temporary housing criteria in conflict areas with reference to thermal comfort. International Journal of Disaster Risk Reduction, 38.

19. Belcher and Bates 1983

Belcher J. C. and Bates F. L.

Aftermath of natural disasters - coping through residential-mobility. Disasters, 7, 118-128.

20. Alexander 1984

Alexander D.

Housing crisis after natural disaster - the aftermath of the November 1980 southern Italian earthquake. Geoforum, 15, 489-516.

21. Gutierrez 2017

Gutierrez M. P.

Floods: shaping resilient emergency relief housing. Journal of Architectural and Planning Research, 34, 236-270.

22. Cao et al. 2014

Cao X. Y., Jiang X. L., Pang S., Li S. J., Cheng Y. J. and Tian L.

The prevalence and risk factors for psychological distress in older men and women affected by the Wenchuan, China earthquake. Australasian Journal on Ageing, 33, E20-E26.

23. Fussell and Lowe 2014

Fussell E. and Lowe S. R.

The impact of housing displacement on the mental health of low-income parents after Hurricane Katrina. Social Science & Medicine, 113, 137-144.

24. Tsuchiya et al. 2019

Tsuchiya M., Aida J., Watanabe T., Shinoda M., Sugawara Y., Tomata Y., Yabe Y., Sekiguchi T., Watanabe M., Osaka K., Sasaki K., Hagiwara Y. and Tsuji I.

High prevalence of toothache among Great East Japan Earthquake survivors living in temporary housing. Community Dentistry and Oral Epidemiology, 47, 119-126.

25. Sodha et al. 1986

Sodha M. S., Bansal N. K., Bansal P. K., Kumar A. and Malik M. A. S.

Solar passive building. Pergamon Press,Elmsford.

26. Davis 1978.

Davis I.

Shelter after disaster, Oxford, Oxford Polytechnic Press.

27. Tyagi et al. 2012

Tyagi V. V., Buddhi D., Kothari R. and Tyagi S. K.

Phase change material (PCM) based thermal management system for cool energy storage application in building: An experimental study. Energy and Buildings, 51, 248-254.

28. Zhou et al. 2012

Zhou D., Zhao C. Y. and Tian Y.

Review on thermal energy storage with phase change materials (PCMs) in building applications. Applied Energy, 92, 593-605.

29. Pomianowski et al. 2013

Pomianowski M., Heiselberg P. and Zhang Y. P.

Review of thermal energy storage technologies based on PCM application in buildings. Energy and Buildings, 67, 56-69.

30. Soares et al. 2013

Soares N., Costa J. J., Gaspar A. R. and Santos P.

Review of passive PCM latent heat thermal energy storage systems towards buildings' energy efficiency. Energy and Buildings, 59, 82-103.

31. Tyagi et al. 2013

Tyagi V. V., Pandey A. K., Buddhi D. and Tyagi S. K.

Exergy and energy analyses of two different types of PCM based thermal management systems for space air conditioning applications. Energy Conversion and Management, 69, 1-8.

32. Sage-Lauck. and Sailor 2014

Sage-Lauck J. S. and Sailor D. J.

Evaluation of phase change materials for improving thermal comfort in a super-insulated residential building. Energy and Buildings, 79, 32-40.

33. Figueiredo et al. 2017

Figueiredo A., Vicente R., Lapa J., Cardoso C., Rodrigues F. and Kampf J.

Indoor thermal comfort assessment using different constructive solutions incorporating PCM. Applied Energy, 208, 1208-1221.

34. Alam et al. 2017

Alam M., Sanjayan J., Zou P. X. W., Ramakrishnan S. and Wilson J.

Evaluating the passive and free cooling application methods of phase change materials in residential buildings: A comparative study. Energy and Buildings, 148, 238-256.

35. Kenisarin and Mahkamov 2016

Kenisarin M. and Mahkamov K.

Passive thermal control in residential buildings using phase change materials. Renewable and Sustainable Energy Reviews, 55, 371-398.

36. Konuklu et al. 2015

Konuklu Y., Ostry M., Paksoy H. O. and Charvat P.

Review on using microencapsulated phase change materials (PCM) in building applications. Energy and Buildings, 106, 134-155.

37. Silva and Rodrigues 2016a

Silva T., Vicente R. and Rodrigues F.

Literature review on the use of phase change materials in glazing and shading solutions. Renewable & Sustainable Energy Reviews, 53, 515-535.

38. Weinläder et al. 2016

Weinläder H., Klinker F. and Yasin M.

PCM cooling ceilings in the Energy Efficiency Center—passive cooling potential of two different system designs. Energy and Buildings, 119, 93-100.

39. Lin et al.2016

Lin W., Ma Z., Cooper P., Sohel M. I. and Yang L.

Thermal performance investigation and optimization of buildings with integrated phase change materials and solar photovoltaic thermal collectors. Energy and Buildings, 116, 562-573.

40. Song et al. 2018

Song M. J., Niu F. X., Mao N., Hu Y. X. and Deng S. M.

Review on building energy performance improvement using phase change materials. Energy and Buildings, 158, 776-793.

41. The International Disaster Database

https://www.emdat.be/

42. Ward et al. 2020

Ward P. J., Blauhut V., Bloemendaal N., Daniell J. E., de Ruiter M. C., Duncan M. J., Emberson R., Jenkins S. F., Kirschbaum D., Kunz M., Mohr S., Muis S., Riddell G. A., Schafer A., Stanley T., Veldkamp T. I. E. and Winsemius H. C.

Review article: Natural hazard risk assessments at the global scale. Natural Hazards and Earth System Sciences, 20, 1069-1096.

43. Forero-Ortiz et al. 2020

Forero-Ortiz E., Martinez-Gomariz E. and Porcuna M. C.

A review of flood impact assessment approaches for underground infrastructures in urban areas: a focus on transport systems. Hydrological Sciences Journal-Journal Des Sciences Hydrologiques, 65, 1943-1955.

44. Ngcamu and Chari 2020

Ngcamu B. S. and Chari F.

Drought Influences on Food Insecurity in Africa: A Systematic Literature Review. International Journal of Environmental Research and Public Health, 17.

45. Wang et al. 2020

Wang Y., Gardoni P., Murphy C. and Guerrier S.

Worldwide Predictions of Earthquake Casualty Rates with Seismic Intensity Measure and Socioeconomic Data: A Fragility-Based Formulation. Natural Hazards Review, 21.

46. Stahl et al. 2017

Stahl T., Clark M. K., Zekkos D., Athanasopoulos-Zekkos A., Willis M., Medwedeff W., Knoper L., Townsend K. and Jin J.

Earthquake science in resilient societies. Tectonics, 36, 749-753.

47. Karaca and Aslani 2016

Karaca E. and Aslani H.

Review of two Japan Typhoon catastrophe models for commercial and industrial properties. Natural Hazards, 83, 19-40.

48. Weiskerger and Phanikumar 2020

Weiskerger C. J. and Phanikumar M. S.

Numerical Modeling of Microbial Fate and Transport in Natural Waters: Review and Implications for Normal and Extreme Storm Events. Water, 12.

49. Wang et al. 2012

Wang J., Yang S., Ji X. J. and Ou G. Q.

The Review and Prospects of the Study on Chinese Geological Disaster. Progress in Structure, Pts 1-4, 166-169, 2597-2600.

50. Burger et al. 2020

Burger R., Gavilan E., Inzunza D., Mulet P. and Villada L. M.

Exploring a Convection-Diffusion-Reaction Model of the Propagation of Forest Fires: Computation of Risk Maps for Heterogeneous Environments. Mathematics, 8.

51. Xu et al. 2020

Xu X. Y., Jia G. S., Zhang X. Y., Riley W. J. and Xue Y.

Climate regime shift and forest loss amplify fire in Amazonian forests. Global Change Biology, 26, 5874-5885.

52. Bercak et al. 2018

Bercak R., Holusa J., Lukasova K., Hanuska Z., Agh P., Vanek J., Kula E. and Chromek I.

Forest Fires in the Czech Republic - Characteristics, Prevention and Firefighting: Review. Reports of Forestry Research-Zpravy Lesnickeho Vyzkumu, 63, 184-194.

53. Dou et al. 2018

Dou Y. Y., Huang Q. X., He C. Y., Meng S. T. and Zhang Q.

Rapid Population Growth throughout Asia's Earthquake-Prone Areas: A Multiscale Analysis. International Journal of Environmental Research and Public Health, 15.

54. Juang et al. 2019

Juang C. S., Stanley T. A. and Kirschbaum D. B.

Using citizen science to expand the global map of landslides: Introducing the Cooperative Open Online Landslide Repository (COOLR). Plos One, 14.

55. Cardona et al. 2014

Cardona O. D., Ordaz M. G., Mora M. G., Salgado-Galvez M. A., Bernal G. A., Zuloaga-Romero D., Fraume M. C. M., Yamin L. and Gonzalez D.

Global risk assessment: A fully probabilistic seismic and tropical cyclone wind risk assessment. International Journal of Disaster Risk Reduction, 10, 461-476.

56. Hong and Moller 2012

Hong L. X. and Moller B.

An economic assessment of tropical cyclone risk on offshore wind farms. Renewable Energy, 44, 180-192.

57. Trepanier et al. 2017

Trepanier J. C., Yuan J. and Jagger T. H.

The combined risk of extreme tropical cyclone winds and storm surges along the US Gulf of Mexico Coast. Journal of Geophysical Research-Atmospheres, 122, 3299-3316.

58. Vallejo et al. 2020

de Vallejo L. I. G., Hernandez-Gutierrez L. E., Miranda A. and Ferrer M.

Rockfall Hazard Assessment in Volcanic Regions Based on ISVS and IRVS Geomechanical Indices. Geosciences, 10.

59. Freire 2019

Freire S., Florczyk A. J., Pesaresi M. and Sliuzas R.

An Improved Global Analysis of Population Distribution in Proximity to Active Volcanoes, 1975-2015. Isprs International Journal of Geo-Information, 8.

60. Iimura 2020

Iimura K., Shibayama T., Takabatake T. and Esteban M.

Experimental and numerical investigation of tsunami behavior around two upright sea dikes with different heights. Coastal Engineering Journal.

61. Ali et al. 2020

Ali R., Kuriqi A. and Kisi O.

Human-Environment Natural Disasters Interconnection in China: A Review. Climate, 8.

62. Dagher et al. 2020

Dagher T. N., Al-Bayssari C., Diene S. M., Azar E. and Rolain J. M.

Bacterial infection during wars, conflicts and post-natural disasters in Asia and the Middle East: a narrative review. Expert Review of Anti-Infective Therapy, 18, 511-529.

63. Paul 2002

Paul P.

Reconstruction of climate anomalies and occurrences of natural disaster (floods, dryness, storms) in central Europe during the last 500 years. Houille Blanche-Revue Internationale De L Eau, 111-114.

64. Radovic et al. 2012

Radovic V., Vitale K. and Tchounwou P. B.

Health Facilities Safety in Natural Disasters: Experiences and Challenges from South East Europe. International Journal of Environmental Research and Public Health, 9, 1677-1686.

65. Edoun et al. 2015

Edoun E. I., Balgah R. A. and Mbohwa C.

The impact of effective management of natural disasters For Africa's development. Economic Research-Ekonomska Istrazivanja, 28, 924-938.

66. Michellier et al. 2020

Michellier C., Pigeon P., Paillet A., Trefon T., Dewitte O. and Kervyn F.

The Challenging Place of Natural Hazards in Disaster Risk Reduction Conceptual Models: Insights from Central Africa and the European Alps. International Journal of Disaster Risk Science, 11, 316-332.

67. Alcantara-Ayala 2010

Alcantara-Ayala I.

Disasters in Mexico and Central America: A Little Bit More Than a Century of Natural Hazards. Natural Hazards and Human-Exacerbated Disasters in Latin America: Special Volumes of Geomorphology, 13, 75-97.

68. Ishizawa and Miranda 2019

Ishizawa O. A. and Miranda J. J.

Weathering Storms: Understanding the Impact of Natural Disasters in Central America. Environmental & Resource Economics, 73, 181-211.

69. Forbes et al. 2018

Forbes D., Bryant R., Molyneaux R. and O'Donnell M.

Recent developments in research into the incidence and treatment of psychosocial problems following natural disasters in Australia. Australian Psychologist, 53, 70-71.

70. Wisetjindawat et al. 2017

Wisetjindawat W., Burke M. I. and Fujita M.

Analysing impacts of natural disasters on logistics activities: flood risks and petroleum fuels in Queensland, Australia. World Conference on Transport Research - Wctr 2016, 25, 1198-1212.

71. Carrasco-Ochoa and Martinez-Trinidad 2004

Carrasco-Ochoa J. A. and Martinez-Trinidad J. F.

Feature selection for natural disaster texts classification using testors. Intelligent Data Engineering and Automated Learning Ideal 2004, Proceedings, 3177, 424-429.

72. Chan et al. 2019

Chan E. Y. Y., Man A. Y. T. and Lam H. C. Y.

Scientific evidence on natural disasters and health emergency and disaster risk management in Asian rural-based area. British Medical Bulletin, 129, 91-105.

73. Nascimento and Alencar 2016

Nascimento K. R. D. and Alencar M. H.

Management of risks in natural disasters: A systematic review of the literature on NATECH events. Journal of Loss Prevention in the Process Industries, 44, 347-359.

74. Rinaldi and Bergamini 2020

Rinaldi A. and Bergamini K.

Inclusion of learning about management of natural disasters risk in territorial planning instruments (2005-2015). Revista De Geografia Norte Grande, 103-130.

75. Li et al. 2016

Li M. Y., Wang J. and Sun X. J.

Scenario-based risk framework selection and assessment model development for natural disasters: a case study of typhoon storm surges. Natural Hazards, 80, 2037-2054.

76. Rus et al. 2018

Rus K., Kilar V. and Koren D.

Resilience assessment of complex urban systems to natural disasters: A new literature review. International Journal of Disaster Risk Reduction, 31, 311-330.

77. Kreibich et al. 2014

Kreibich H., Bubeck P., Kunz M., Mahlke H., Parolai S., Khazai B., Daniell J., Lakes T. and Schroter K.

A review of multiple natural hazards and risks in Germany. Natural Hazards, 74, 2279-2304.

78. Jahangiri et al. 2017

Jahangiri K., Eivazi M. R. and Mofazali A. S.

The role of Foresight in avoiding systematic failure of natural disaster risk management. International Journal of Disaster Risk Reduction, 21, 303-311.

79. Bashawri et al. 2014

Bashawri A., Garrity S. and Moodley K.

An Overview of the Design of Disaster Relief Shelters. 4th International Conference on Building Resilience, Incorporating the 3rd Annual Conference of the Android Disaster Resilience Network, 18, 924-931.

80. Wang et al. 2016b

Wang Y., Wang L., Long E. and Deng S.

An experimental study on the indoor thermal environment in prefabricated houses in the subtropics. Energy and Buildings, 127, 529-539.

81. Felix et al. 2013

Felix D., Branco J. M. and Feio A.

Temporary housing after disasters: A state of the art survey. Habitat International, 40, 136-141.

82. Atmaca 2017

Atmaca N.

Life-cycle assessment of post-disaster temporary housing. Building Research and Information, 45, 524-538.

83. Song et al. 2016

Song Y. M., Mithraratne N. and Zhang H.

Life-time performance of post-disaster temporary housing: A case study in Nanjing. Energy and Buildings, 128, 394-404.

84. Shinohara et al.2013

Shinohara N., Tokumura M., Kazama M., Yoshino H., Ochiai S. and Mizukoshi A.

Indoor air quality, air exchange rates, and radioactivity in new built temporary houses following the Great East Japan Earthquake in Minamisoma, Fukushima. Indoor Air, 23, 332-341.

85. Iwasa et al. 2012

Iwasa A., Hasegawa T., Shinkai S., Shinozaki M., Yasutake A. and Kobayashi K.

A Practical Approach to Temporary Housing for Disaster Victims. Journal of Asian Architecture and Building Engineering, 11, 33-38.

86. Basile 2020

Basile A. L.

Disaster relief shelter experience during Hurricane Sandy: A preliminary phenomenological inquiry. International Journal of Disaster Risk Reduction, 45.

87. Arslan 2007

Arslan H.

Re-design, re-use and recycle of temporary houses. Building and Environment, 42, 400-406.

88. Cena et al. 2003

Cena K., Davey N. and Erlandson T.

Thermal comfort and clothing insulation of resting tent occupants at high altitude. Applied Ergonomics, 34, 543-550.

89. Jiang and Chen 2019

Jiang Y. N. and Chen X. X.

An experimental study on the improvement of indoor thermal environment of tents by shading in summer. 2018 International Seminar on Computer Science and Engineering Technology (Scset 2018), 1176.

90. Easton 2008

Easton P.

Disaster relief that comes in a tent. Mechanical Engineering, 130, 21-21.

91. Wang et al. 2015

Wang S. F., So E. and Smith P.

Detecting tents to estimate the displaced populations for post-disaster relief using high resolution satellite imagery. International Journal of Applied Earth Observation and Geoinformation, 36, 87-93.

92. Liu et al. 2016

Liu J. B., Jiang Y. N., Gong Z. G. and Yang H.

Experiment Research on Shading to Improve the Thermal Environment of Tents. International Seminar on Applied Physics, Optoelectronics and Photonics (Apop 2016), 61.

93. Naylor et al. 2018

Naylor A., Walker J. F. and Suppasri A.

Suitability of the early warning systems and temporary housing for the elderly population in the immediacy and transitional recovery phase of the 2011 Great East Japan Earthquake and Tsunami. International Journal of Disaster Risk Reduction, 31, 302-310.

94. Shinohara et al. 2014

Shinohara N., Tokumura M., Kazama M., Yonemoto Y., Yoshioka M., Kagi N., Hasegawa K., Yoshino H. and Yanagi U.

Indoor air quality and thermal comfort in temporary houses occupied after the Great East Japan Earthquake. Indoor Air, 24, 425-437.

95. Cornaro et al. 2015

Cornaro C., Sapori D., Bucci F., Pierro M. and Giammanco C.

Thermal performance analysis of an emergency shelter using dynamic building simulation. Energy and Buildings, 88, 122-134.

96. Kim et al. 2015

Kim J. G., Lee J., Ahn B. L., Shin H., Yoo S., Jang C. Y., Song D. and Kim J.

Indoor Thermal Environment of Temporary Mobile Energy Shelter Houses (MeSHs) in South Korea. Energies, 8, 11139-11152.

97. Hirmiz et al. 2019

Hirmiz R., Teamah H. M., Lightstone M. F. and Cotton J. S.

Performance of heat pump integrated phase change material thermal storage for electric load shifting in building demand side management. Energy and Buildings, 190, 103-118.

98. Mourid et al. 2018

Mourid A., El Alami M. and Kuznik F.

Experimental investigation on thermal behavior and reduction of energy consumption in a real scale building by using phase change materials on its envelope. Sustainable Cities and Society, 41, 35-43.

99. Sun et al. 2018

Sun X. Q., Medina M. A., Lee K. O. and Jin X.

Laboratory assessment of residential building walls containing pipe-encapsulated phase change materials for thermal management. Energy, 163, 383-391.

100. Sun et al. 2020a

Sun H., Li Y. J., Yan X. Y., Wang Z. Y. and Liu W. Q.

CaO/CaCO3 thermochemical heat storage performance of CaO-based micrometre-sized tubular composite. Energy Conversion and Management, 222.

101. Yan et al. 2019a

Yan J., Zhao C. Y., Xia B. Q. and Wang T.

The effect of dehydration temperatures on the performance of the CaO/Ca(OH)(2) thermochemical heat storage system. Energy, 186.

102. Umair et al. 2019

Umair M. M., Zhang Y., Iqbal K., Zhang S. F. and Tang B. T.

Novel strategies and supporting materials applied to shape-stabilize organic phase change materials for thermal energy storage-A review. Applied Energy, 235, 846-873.

103. Cai et al. 2015

Cai Y. B., Liu M. M., Song X. F., Zhang J., Wei Q. F. and Zhang L. F.

A form-stable phase change material made with a cellulose acetate nanofibrous mat from bicomponent electrospinning and incorporated capric-myristic-stearic acid ternary eutectic mixture for thermal energy storage/retrieval. Rsc Advances, 5, 84245-84251.

104. Zhang et al. 2014a

Zhang N., Yuan Y. P., Du Y. X., Cao X. L. and Yuan Y. G.

Preparation and properties of palmitic-stearic acid eutectic mixture/expanded graphite composite as phase change material for energy storage. Energy, 78, 950-956.

105. Zhang et al. 2014b

Zhang N., Yuan Y. P., Yuan Y. G., Cao X. L. and Yang X. J.

Effect of carbon nanotubes on the thermal behavior of palmitic-stearic acid eutectic mixtures as phase change materials for energy storage. Solar Energy, 110, 64-70.

106. Choi et al. 2019

Choi J., Yoshie K., Moteki T. and Ogura M.

Theoretical Evaluation of an Organic Phase Change Material (PCM)-Inserted Dual-Functional Adsorbent for the Recovery of Heat of Adsorption. Industrial & Engineering Chemistry Research, 58, 10114-10118.

107. Wang et al. 2019a

Wang F. X., Gao S. Y., Pan J. C., Li X. M. and Liu J.

Short-Chain Modified SiO2 with High Absorption of Organic PCM for Thermal Protection. Nanomaterials, 9.

108. Xie et al. 2019

Xie M., Huang J. C., Ling Z. Y., Fang X. M. and Zhang Z. G.

Improving the heat storage/release rate and photo-thermal conversion performance of an organic PCM/expanded graphite composite block. Solar Energy Materials and Solar Cells, 201.

109. Mohseni et al. 2020

Mohseni E., Tang W. C., Khayat K. H. and Cui H. Z.

Thermal performance and corrosion resistance of structural-functional concrete made with inorganic PCM. Construction and Building Materials, 249.

110. Peng et al. 2019

Peng S. Q., Huang J., Wang T. Y. and Zhu P. P.

Effect of fumed silica additive on supercooling, thermal reliability and thermal stability of Na2HPO4 center dot 12H(2)O as inorganic PCM. Thermochimica Acta, 675, 1-8.

111. Sun et al. 2020b

Sun W. C., Zhang Y. X., Ling Z. Y., Fang X. M. and Zhang Z. G.

Experimental investigation on the thermal performance of double-layer PCM radiant floor system containing two types of inorganic composite PCMs. Energy and Buildings, 211.

112. Cunha and Aguiar 2020

Cunha S. R. L. and Aguiar J. L. B.

Phase change materials and energy efficiency of buildings: A review of knowledge. Journal of Energy Storage, 27.

113. Qu et al. 2020

Qu Y., Wang S., Zhou D. and Tian Y.

Experimental study on thermal conductivity of paraffin-based shape-stabilized phase change material with hybrid carbon nano-additives. Renewable Energy, 146, 2637-2645.

114. Vasu et al. 2019

Vasu A., Hagos F. Y., Mamat R., Kaur J. and Noor M. M.

The effect of thermal cyclic variation on the thermophysical property degradation of paraffin as a phase changing energy storage material. Applied Thermal Engineering, 149, 22-33.

115. Yao and Wu 2020

Yao Y. P. and Wu H. Y.

Thermal transport process of metal foam/paraffin composite (MFPC) with solid-liquid phase change: An experimental study. Applied Thermal Engineering, 179.

116. Kou et al. 2019

Kou Y., Wang S. Y., Luo J. P., Sun K. Y., Zhang J., Tan Z. C. and Shi Q.

Thermal analysis and heat capacity study of polyethylene glycol (PEG) phase change materials for thermal energy storage applications. Journal of Chemical Thermodynamics, 128, 259-274.

117. Wijesena et al. 2020

Wijesena R. N., Tissera N. D., Rathnayaka V. W. S. G., Rajapakse H. D., de Silva R. M. and de Silva K. M. N.

Shape-stabilization of polyethylene glycol phase change materials with chitin nanofibers for applications in "smart" windows. Carbohydrate Polymers, 237.

118. Kalnaes and Jelle 2015

Kalnaes S. E. and Jelle B. P.

Phase change materials and products for building applications: A state-of-the-art review and future research opportunities. Energy and Buildings, 94, 150-176.

119. Lin et al. 2018

Lin Y. X., Alva G. and Fang G. Y.

Review on thermal performances and applications of thermal energy storage systems with inorganic phase change materials. Energy, 165, 685-708.

120. Oliver et al. 2012

Oliver A., Neila F. J. and Garcia-Santos A.

PCM choosing and classification according to their characteristics for their application for thermal energy storage systems. Materiales De Construccion, 62, 131-140.

121. Hasnain 1998a

Hasnain S. M.

Review on sustainable thermal energy storage technologies, part I: Heat storage materials and techniques. Energy Conversion and Management, 39, 1127-1138.

122. Hasnain 1998b

Hasnain S. M.

Review on sustainable thermal energy storage technologies, part II: Cool thermal storage. Energy Conversion and Management, 39, 1139-1153.

123. Lv et al. 2016

Lv P. Z., Liu C. Z. and Rao Z. H.

Experiment study on the thermal properties of paraffin/kaolin thermal energy storage form-stable phase change materials. Applied Energy, 182, 475-487.

124. da Cunha and Eames 2016

da Cunha J. P. and Eames P.

Thermal energy storage for low and medium temperature applications using phase change materials - A review. Applied Energy, 177, 227-238.

125. Tyagi and Buddhi 2008

Tyagi V. V. and Buddhi D.

Thermal cycle testing of calcium chloride hexahydrate as a possible PCM for latent heat storage. Solar Energy Materials and Solar Cells, 92, 891-899.

126. Campos-Celador et al. 2014

Campos-Celador A., Diarce G., Zubiaga J. T., Bandos T. V., Garcia-Romero A. M., Lopez L. M. and Sala J. M.

Design of a finned plate latent heat thermal energy storage system for domestic applications. Proceedings of the 2nd International Conference on Solar Heating and Cooling for Buildings and Industry (Shc 2013), 48, 300-308.

127. Rezaei et al. 2013

Rezaei M., Anisur M. R., Mahfuz M. H., Kibria M. A., Saidur R. and Metselaar I. H. S. C.

Performance and cost analysis of phase change materials with different melting temperatures in heating systems. Energy, 53, 173-178.

128. Sharma et al. 2009

Sharma A., Tyagi V. V., Chen C. R. and Buddhi D.

Review on thermal energy storage with phase change materials and applications. Renewable & Sustainable Energy Reviews, 13, 318-345.

129. Yun et al. 2019

Yun H. D., Ahn K. L., Jang S. J., Khil B. S., Park W. S. and Kim S. W.

Thermal and Mechanical Behaviors of Concrete with Incorporation of Strontium-Based Phase Change Material (PCM). International Journal of Concrete Structures and Materials, 13.

130. Bahrar et al. 2018

Bahrar M., Djamai Z. I., El Mankibi M., Larbi A. S. and Salvia M.

Numerical and experimental study on the use of microencapsulated phase change materials (PCMs) in textile reinforced concrete panels for energy storage. Sustainable Cities and Society, 41, 455-468.

131. Cabeza et al. 2020

Cabeza L. F., Navarro L., Pisello A. L., Olivieri L., Bartolome C., Sanchez J., Alvarez S. and Tenorio J. A.

Behaviour of a concrete wall containing micro-encapsulated PCM after a decade of its construction. Solar Energy, 200, 108-113.

132. Raj et al. 2019

Raj A. K., Srinivas M. and Jayaraj S.

A cost-effective method to improve the performance of solar air heaters using discrete macro-encapsulated PCM capsules for drying applications. Applied Thermal Engineering, 146, 910-920.

133. Yan et al. 2020

Yan W. M., Ho C. J., Tseng Y. T., Qin C. Y. and Rashidi S.

Numerical study on convective heat transfer of nanofluid in a minichannel heat sink with micro-encapsulated PCM-cooled ceiling. International Journal of Heat and Mass Transfer, 153.

134. Aziz et al. 2018

Aziz S., Amin N. A. M., Majid M. S. A., Bruno F. and Belusko M.

Effectiveness-NTU correlation for a TES tank comprising a PCM encapsulated in a sphere with heat transfer enhancement. Applied Thermal Engineering, 143, 1003-1010.

135. Yan et al. 2019b

Yan T., Gao J. J., Xu X. H., Xu T., Ling Z. Y. and Yu J. H.

Dynamic simplified PCM models for the pipe-encapsulated PCM wall system for self-activated heat removal. International Journal of Thermal Sciences, 144, 27-41.

136. Uthaichotirat et al. 2020

Uthaichotirat P., Sukontasukkul P., Jitsangiam P., Suksiripattanapong C., Sata V. and Chindaprasirt P.

Thermal and sound properties of concrete mixed with high porous aggregates from manufacturing waste impregnated with phase change material. Journal of Building Engineering, 29.

137. Qian and Li 2018

Qian T. T. and Li J. H.

Octadecane/C-decorated diatomite composite phase change material with enhanced thermal conductivity as aggregate for developing structural-functional integrated cement for thermal energy storage. Energy, 142, 234-249.

138. Zhu et al. 2018

Zhu N., Li S. S., Hu P. F., Wei S., Deng R. J. and Lei F.

A review on applications of shape-stabilized phase change materials embedded in building enclosure in recent ten years. Sustainable Cities and Society, 43, 251-264.

139. Tao and He 2018

Tao Y. B. and He Y. L.

A review of phase change material and performance enhancement method for latent heat storage system. Renewable & Sustainable Energy Reviews, 93, 245-259.

140. Dardir et al. 2019

Dardir M., Panchabikesan K., Haghighat F., El Mankibi M. and Yuan Y. P.

Opportunities and challenges of PCM-to-air heat exchangers (PAHXs) for building free cooling applications-A comprehensive review. Journal of Energy Storage, 22, 157-175.

141. Rao et al. 2018

Rao V. V., Parameshwaran R. and Ram V. V.

PCM-mortar based construction materials for energy efficient buildings: A review on research trends. Energy and Buildings, 158, 95-122.

142. Rathore and Shukla 2019

Rathore P. K. S. and Shukla S. K.

Potential of macroencapsulated PCM for thermal energy storage in buildings: A comprehensive review. Construction and Building Materials, 225, 723-744.

143. Cabeza et al. 2007

Cabeza L. F., Castellón C., Nogués M., Medrano M., Leppers R. and Zubillaga O.

Use of microencapsulated PCM in concrete walls for energy savings. Energy and Buildings, 39, 113-119.

144. Zhao et al. 2019

Zhao J., Yuan Y. P., Haghighat F., Lu J. and Feng G. H.

Investigation of energy performance and operational schemes of a Tibet-focused PCM-integrated solar heating system employing a dynamic energy simulation model. Energy, 172, 141-154.

145. Lu et al. 2020

Lu S. L., Xu B. W. and Tang X. L.

Experimental study on double pipe PCM floor heating system under different operation strategies. Renewable Energy, 145, 1280-1291.

146. Park and Kim 2019

Park J. and Kim T.

Analysis of the Thermal Storage Performance of a Radiant Floor Heating System with a PCM. Molecules, 24.

147. Lu 2017

Lu S. L., Zhao Y. Q., Fang K., Li Y. R. and Sun P. C.

Establishment and experimental verification of TRNSYS model for PCM floor coupled with solar water heating system. Energy and Buildings, 140, 245-260.

148. Kuznik 2016

Kuznik F., Johannes K., Franquet E., Zalewski L., Gibout S., Tittelein P., Dumas J. P., David D., Bedecarrats J. P. and Lassue S.

Impact of the enthalpy function on the simulation of a building with phase change material wall. Energy and Buildings, 126, 220-229.

149. Imani 2019

Imani G.

Lattice Boltzmann simulation of melting of a phase change material confined within a cylindrical annulus with a conductive inner wall using a body-fitted non-uniform mesh. International Journal of Thermal Sciences, 136, 549-561.

150. Kolaitis and Founti 2017

Kolaitis D. I. and Founti M. A.

Solar wall enhanced with phase-change materials: a detailed numerical simulation study. Advances in Building Energy Research, 11, 87-103.

151. Wang 2016c

Wang H., Zhou X. Y., Long B., Yang J. and Liu H. Z.

Thermal properties of closed-cell aluminum foams prepared by melt foaming technology. Transactions of Nonferrous Metals Society of China, 26, 3147-3153.

152. Zhang 2017b

Zhang Y., Long E., Li Y. and Li P.

Solar radiation reflective coating material on building envelopes: Heat transfer analysis and cooling energy saving. Energy Exploration & Exploitation, 35, 748-766.

153. Costanzo et al. 2016

Costanzo V., Evola G. and Marletta L.

Energy savings in buildings or UHI mitigation:Comparison between green roofs and cool roofs. Energy and Buildings, 114, 247-255.

154. Morakinyo et al. 2017

Morakinyo T. E., Dahanayake K. W. D. K. C., Ng E. and Chow C. L.

Temperature and cooling demand reduction by green-roof types in different climates and urban densities: A co-simulation parametric study. Energy and Buildings, 145, 226-237.

155. Karachaliou et al. 2016

Karachaliou P., Santamouris M. and Pangalou H.

Experimental and numerical analysis of the energy performance of a large scale intensive green roof system installed on an office building in Athens. Energy and Buildings, 114, 256-264.

156. Foustalieraki et al. 2017

Foustalieraki M., Assimakopoulos M. N., Santamouris M. and Pangalou H.

Energy performance of a medium scale green roof system installed on a commercial building using numerical and experimental data recorded during the cold period of the year. Energy and Buildings, 135, 33-38.

157. Silva et al. 2016b

Silva C. M., Gomes M. G. and Silva M.

Green roofs energy performance in Mediterranean climate. Energy and Buildings, 116, 318-325.

158. Zeng et al. 2017

Zeng C., Bai X. L., Sun L. X., Zhang Y. Z. and Yuan Y. P.

Optimal parameters of green roofs in representative cities of four climate zones in China: A simulation study. Energy and Buildings, 150, 118-131.

159. Inman et al. 2013

Inman R. H., Pedro H. T. C. and Coimbra C. F. M.

Solar forecasting methods for renewable energy integration. Progress in Energy and Combustion Science, 39, 535-576.

160. ASHRAE, 2001

ASHRAE

International Weather for Energy Calculations. IWEC Weather Files Atlanta.

161. ASHRAE, 2013a

ASHRAE

ASHRAE Handbook Fundamentals. American Society of Heating.

162. ASHRAE, 2013b

ASHRAE

ANSI/ASHRAE standard 55-2013. Thermal Environmental Conditions for Human Occupancy.

163. Wang et al. 2019b

Wang C. X., Deng S. M., Niu J. L. and Long E. S.

A numerical study on optimizing the designs of applying PCMs to a disaster-relief prefabricated temporary-house (PTH) to improve its summer daytime indoor thermal environment. Energy, 181, 239-249.

164. Kottek et al. 2006

Kottek M., Grieser J., Beck C., Rudolf B. and Rubel F.

World map of Köppen-Geiger climate classification uptdated. Meteorol Z., 259–263

165. Wang 2020.

Wang C. X.

Applying turnable-PCM composited wall to disaster-relief prefabricated temporary-house to improve its summer indoor thermal environment. Sichuan University.

166. Wang et al. 2019c

Wang C. X., Deng S. M., Niu J. L. and Long E. S.

A numerical study on optimizing the designs of applying PCMs to a disaster-relief prefabricated temporary-house (PTH) to improve its summer daytime indoor thermal environment. Energy, 181, 239-249.